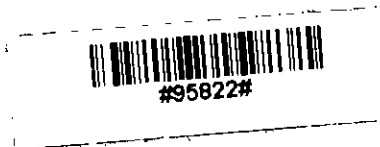# MODELLING OF CONSOLIDATION BEHAVIOUR OF SOIL
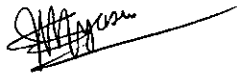
MD. HABIBULLAH

DEPARTMENT OF CIVIL ENGINEERING
BUET, DHAKA

MODELLING OF CONSOLIDATION BEHAVIOUR OF SOIL
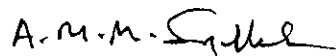
A Project Report
by
Md. Habibullah

Approved as to style and content by:

(Dr. Sarwar Jahan Md. Yasin)   Chairman
Associate Professor,
Dept. of Civil Engineering,
BUET, Dhaka.

(Dr. A. M. M. Safiullah)   Member
Professor,
Dept. of Civil Engineering,
BUET, Dhaka.

(Dr. Md. Zoynul Abedin)   Member
Professor,
Dept. of Civil Engineering,
BUET, Dhaka.

September 2001

MODELLING OF CONSOLIDATION BEHAVIOUR OF SOIL

A Project report

by

MD. HABIBULLAH

Submitted to the Department of Civil Engineering
Bangladesh University of Engineering & Technology, Dhaka
in partial fulfillment of the requirements for the degree
of

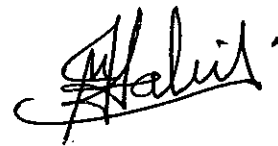**MASTER OF ENGINEERING IN CIVIL ENGINEERING**

September 2001

(i)

Dedicated

to

my brother

MD. NAZRUL ISLAM

DECLARATION

I hereby declare that the project work presented herewith has been performed by me and that this work has not been submitted for any other degree previously.

(MD. HABIBULLAH)

ACKNOWLEDGEMENTS

(All praises to Almighty Allah)

The author expresses his heartiest appreciation to his supervisor, Dr. Sarwar Jahan Md. Yasin Associate professor, Department of Civil Engineering, BUET, Dhaka, for his continued encouragement and guidance in the research. His keen interest in this topic and valuable suggestions, constructive criticisms and advice at every stage made this research possible.

The author also expresses his profound gratitude to Dr. A. M. M. Safiullah and Dr. Md. Zoynul Abedin both Professors of the Department of Civil Engineering, BUET, Dhaka, for their time and effort in reading this report and making valuable suggestions.

Sincere appreciation goes to colleagues and friends for their help and suggestions at different stage of the work.

Assistance provided by Mr. Habibur Rahman and Md. Alimuddin, both staffs of the Geotechnical Engineering Laboratory, is duly acknowledged.

Finally, the author expresses his gratitude and appreciation to his parents, brothers and relatives for their inspiration and encouragement.

ABSTRACT

Routine laboratory consolidation test, though simple in procedure, involves a long time (about a week) and hence cost. Also, the determination of parameters for estimation of settlement and rate of settlement is tedious. After involving such time and effort, the amount of total settlement and rate of settlement estimated from test data vary significantly from field observations. It was, therefore, envisaged that use of the one-dimensional test with a pressure increment ratio larger than that used in conventional tests (thereby reducing the load steps, and time) together with a suitable mathematical model may produce the settlement information of a soil layer for a lesser time and effort. The model will also facilitate implementation of computational methods such as finite element method in settlement estimation. With these objectives, a simple mathematical function is proposed that can represent the void ratio ~ time relations (or dial reading ~ time relations) observed in a one dimensional consolidation test on clay soil. The model consists of three parameters. The role and physical significance of each parameter is explained.

To verify the effectiveness of the model, consolidation tests were performed on specimens from soil cakes reconstituted in the laboratory under two different vertical pressures (50 kPa and 100 kPa). Tests were performed with pressure increment ratios of 2 (used in conventional tests) and 4. The nature and amount of variation of the model parameters were determined from these tests. Comparison of e~t, e~σ' relations from test data and that back calculated using the model showed reasonably good agreement testifying the effectiveness of the model.

It was observed that there is virtually no effect of using a pressure increment ratio of 4 instead 2 on the model parameters. Therefore, it is suggested that routine consolidation tests may be performed with a larger pressure increment ratio, especially in cases where the range of pressure to be investigated is large, together with the model without sacrificing accuracy. The values of c_v at intermediate pressure levels can be obtained from the model.

CONTENTS

Chapter-3 Equipment and test material

Chapter-4 Laboratory Investigation and test results

Chapter-5 A model for one dimensional consolidation

Chapter-6 Conclusion & recommendation for future study

LIST OF FIGURES

(xii)

LIST OF TABLE

LIST OF SYMBOL

σ = Total stress

σ' = Effective stress

e = Void ratio

S_c = Consolidation settlement

C_c = Compression index

w_n = Natural moisture content

LL = Liquid limit

PI = Plasticity index

U_v = Degree of consolidation

T_v = Non dimensional time factor

K = Coefficient of permeability

i = Hydraulic gradient

Reconstituted = Term for a clay soil which has been remoulded at a water content of between one and one and half time the liquid, without air or oven drying and then consolidated under one-dimensional consolidation.

Remoulded = Term for a clay soil which has been remoulded without changing its moisture contend.

Chapter 1

INTRODUCTION
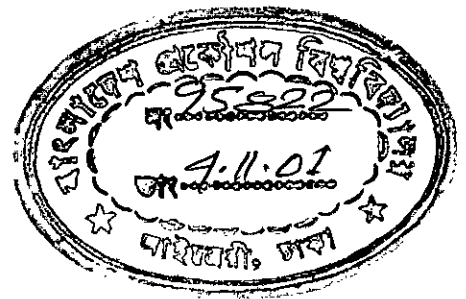
1.1 Introduction

All soils are compressible, in that they undergo volume changes when they are subjected to changes in the stresses applied to them. The resulting compression is relatively large when drainage is allowed. However, the magnitude of settlement is of engineering significance when reference is made to the tolerable settlement for the structure concerned. Since the introduction of Terzaghi's consolidartion theory, a great number of contributions have been made for predicting the magnitude and rate of settlement by introducing more refined soil models and less restricted assumptions on the parameters describing these models. In spite of all these improvements, prediction of settlement has remained more an art than a routine procedure. While it is possible today to predict the magnitude of total settlement within 10 to 20% in many cases, the capability of predicting time settlement relationships has remained rather poor (Balasubramanium, 1981). It is therefore not surprising that Terzaghi's one-dimensional consolidation theory and one-dimensional consolidation test is widely used by practicing engineers, even in case where the loading conditions are far from one-dimensional.

1.2 Objectives of the present study

The one-dimensional consolidation test, though simple is lengthy and the calculation for obtaining parameters is also tedious. So, it was conceived that if a mathematical model could be established for the time dial reading curves under any load increment and the magnitude and trend of variation of the model parameters for different test conditions could be known then a consolidation test using one or two load increment might be used. Thus, savings in both time and cost could be made without sacrificing much accuracy. With this view, the following objectives were set for the present study:

1

(1) To find the effect(s) of initial pressure, load increment ratio, pre-consolidation pressure etc. on

      (a) $e \sim \sigma'$ and $e \sim \log(\sigma')$ relations

      (b) Compression index, C_c

      (c) Coefficient of consolidation, C_v

(2) To search for a suitable mathematical function (a mathematical model) which can be used to represent dial reading vs. time (or void ratio vs. time) relations as obtained in a consolidation test for a certain pressure.

(3) To provide physical and meaningful interpretation of the parameters.

(4) To determine model parameters for different pressure increment and thus to establish correlations between these parameters and pressure or pressure increment ratio so that $e \sim \sigma'$ and $e \sim \log(\sigma')$ plots can be obtained.

(5) To find the effect(s) of initial pressure, load increment ratio, pre-consolidation pressure etc. on the model parameters.

1.3 The test program

Reconstituted sample was prepared from clay slurry under overburden pressures of 50 and 100 kPa. The purpose of using reconstituted soil is to obtain a homogeneous soil layer with a known stress history. The clay was obtained from an excavation in Dhaka city from a depth of about 10m. One dimensional compression test was then performed on these specimens to reveal the effects of several factors such as load increment ratio, initial pressure etc. on pre-consolidation pressure σ'_c, compression index C_c, coefficient of consolidation c_v etc. The data is also used to find the variation of the three parameters of a proposed model from which the void ratio $\sim$ time plots and void ratio $\sim$ pressure plots can be generated and thus be useful for settlement analysis using numerical techniques of finite element.

Chapter 2

LITERATURE REVIEW

2.1 Introduction

A settlement analysis usually consists of (1) an assessment of the stress increment in the compressible layer by the imposed load, and (2) the evaluation of the settlement caused by the stress increment using an appropriate stress-strain relationship of the soil. Settlements are classified as immediate, consolidation and creep settlement. Of these three types of settlements, consolidation settlement is usually the major contributor to total settlement. Consolidation is an important fundamental phenomenon causing ground settlement and must be understood to solve geotechnical problems. Although numerical methods, such as finite element, has enabled three dimensional analysis of soil medium, the theory of one dimensional consolidation and parameters from one dimensional consolidation test (oedometer test) is still largely used to estimate total consolidation settlement and the rate of settlement. In this chapter, the process of consolidation, the one-dimensional theory of consolidation, the laboratory test, determination of the related parameters and their variation etc. are discussed.

2.2 The process of consolidation

All soils undergo compression when they are subjected to increase in the stresses applied to them. If the soil is initially saturated then the stress increase causes instantaneous increase in the pore-water pressure and initially the added load is carried entirely by the water medium. Due to the excess-pore pressure, the pore water tends to escape through the drainage paths and with time the load is transferred from the water to the soil skeleton. This process of dissipation of excess pore-water pressure accompanied by gradual transfer of load from the pore fluid to the soil skeleton is termed as consolidation. According to Terzaghi (1943) " a decrease of water content of a saturated soil without replacement of the water by air is called a process of consolidation".
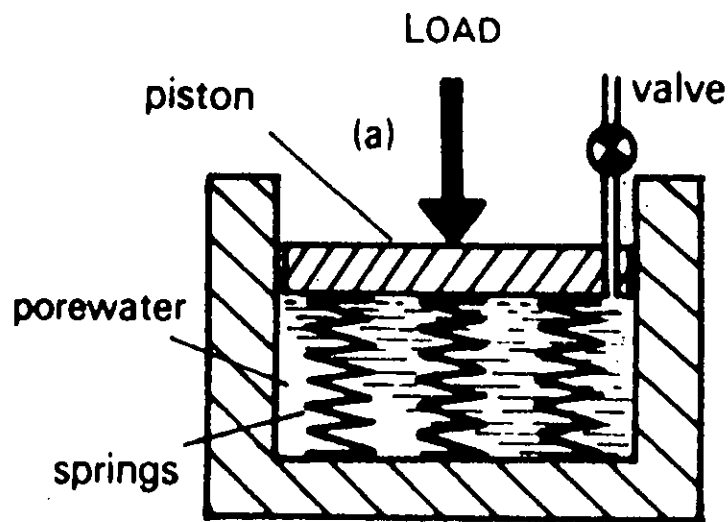
Fig.2.1   Terzaghi's one-dimensional consolidation model
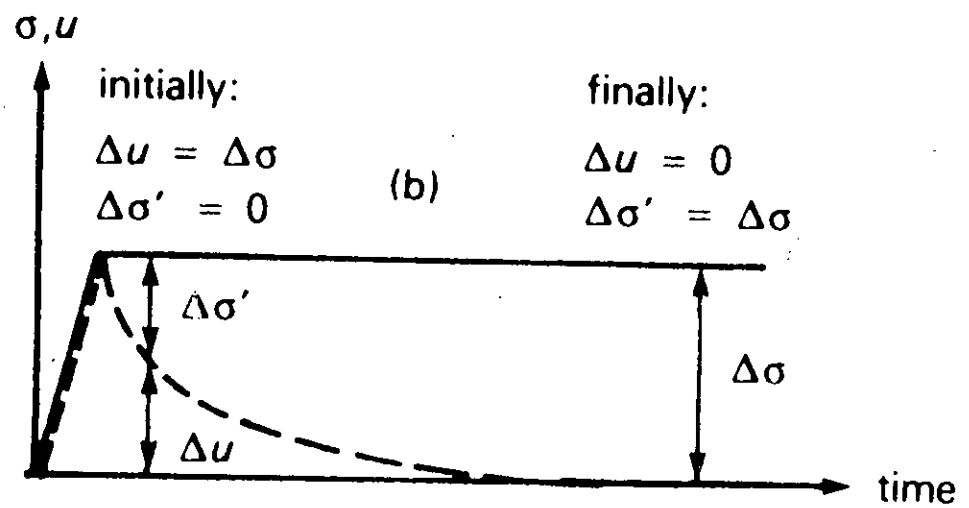
Fig.2.2   Stress~Time curve

Terzaghi (1943) suggested the model shown in Fig.2.1 to illustrate the process of consolidation. Here the steel springs represent the soil. It is assumed that the frictionless piston is supported by the springs and the cylinder is filled with water. If a load is applied to the piston with the valve closed, the length of the springs remain unchanged since water is incompressible (assumed). If the load induces an increase in total stress of $\Delta\sigma$, then the whole of this must be taken up by an equal increase in pore water pressure (Fig.2.2). When the valve is opened, the excess pore water pressure causes the water to flow out, the pore water pressure decreases and the piston sinks as the springs are compressed. Thus, the load is gradually transferred to the springs, causing them to shorten, until it is all carried by the springs. At the final stage, therefore, the increase in effective stress is equal to the increase in total stress and the excess pore water pressure reduces to zero. The rate of compression obviously depends on the extent to which the valve is opened; this is analogous to the permeability of the soil.

2.3 The one-dimensional consolidation test and its interpretation

The compressibility characteristics of a soil layer, in terms of the amount and rate of settlement, are usually determined from the one-dimensional consolidation test. This test is detailed in ASTM D-2435 (ASTM, 1986).

The apparatus used is called an oedometer (Fig.2.3). A soil specimen in the form of a disc [63.5 mm diameter (2.5 inch) and 25.4 mm (1 inch) thickness in standard test] is cut out from a soil cake. The specimen, enclosed in a metal ring, is sandwiched between two porous stone discs. There may be two types of assembly of the metal ring, soil specimen and porous discs;

(1) Floating ring type: Both the top and bottom porous stone discs are slightly smaller than the metal ring (Fig.2.3a). Both the top and bottom porous stones provide vertical and lateral drainage. Compression takes place from both the faces of the soil specimen.

5
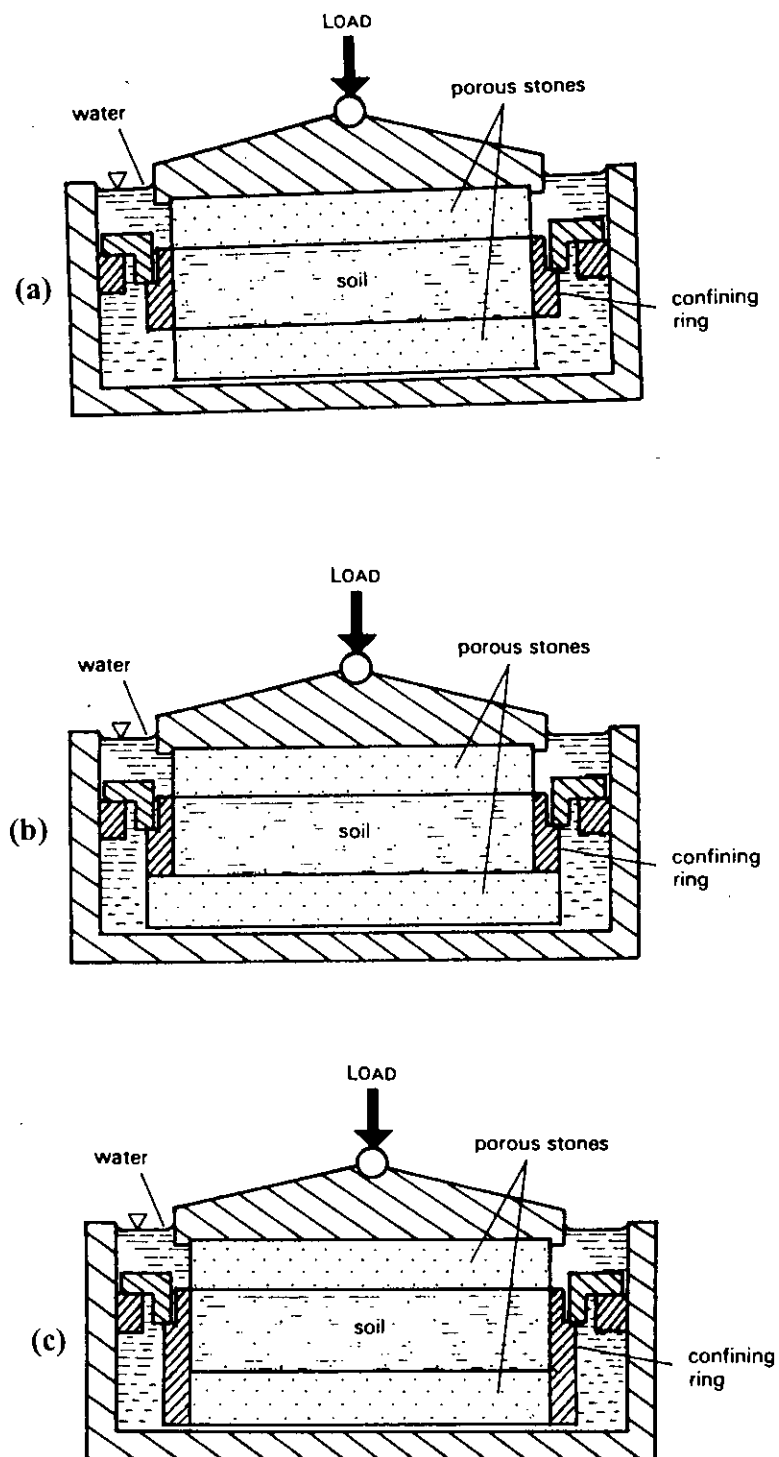
Fig.2.3   The oedometer cell (a) Floating ring (b) & (c) Fixed ring

(2) Fixed ring type: The top porous disc is slightly smaller than the metal ring. The bottom porous stone may be either smaller or larger than the metal ring. If the bottom porous stone is larger than the metal ring then the metal ring rests on the bottom porous disc (Fig.2.3b). In case the bottom porous stone is slightly smaller than the metal ring, then the metal ring touches the bottom of the container (Fig.2.3c). Soil specimen is compressed from the top face only.

The metal ring, specimen and porous stone assembly is placed in the cell (a container with the top open), which is then filled with water. A vertical static load is then applied through a lever system. The porous stones allow the excess pore pressure, due to load increment, to freely escape as the soil voids are compressed. The change in thickness of the sample is recorded by means of a dial gauge or LVDT (linear variable displacement transducer). Readings are recorded at certain intervals of time and continued until the specimen is fully consolidated under the current load increment. Bowels (1984) suggests that this may be taken as the time when the dial reading has remained relatively unchanged for three successive readings, where the elapsed time of each reading is approximately double that of the previous reading. In conventional laboratory tests, loads are changed every 24 hour, which is generally satisfactory for samples of 2 to 3 cm thickness. The pressure applied at the first stage is normally equal to the in-situ vertical stress at the depth from which the sample was obtained, except for soft and very soft clays, when a lower value must be used. Further pressure increments are then applied each being double the previous increment producing a ratio of $\Delta\sigma/\sigma'=1$ (Leonards,1962). A typical sequence is 25, 50, 100, 200, 400, 800, 1600, 3200 kPa or 0.25, 0.5, 1, 2, 4, 8, 16 tsf. There is evidence (Leonards, 1962) that if the initial pressure increment is too low, the excess pore pressure may not be sufficient to initiate pore water flow in some clay soils. It is reported (Bowels,1984) that initial pressure of the order of 25 kPa appear adequate to avoid it. The value of final pressure depends on the type of soil and on the magnitude of stress anticipated on site. The specimen is kept under water throughout the test.

After full consolidation is reached under the final load, the load is removed either in one or in several stages.

2.3.1 e versus σ' curve

The data collected from a consolidation test enable to relate the change in void ratio to the change in effective stress. Usually the void ratio is plotted against the effective stress as shown in Fig.2.4. This curve provides the most direct method of computing the consolidation settlement for a known stress increment.

Suppose a stratum of clay of thickness H_0 is subjected to a change in effective stress from σ'_0 to σ'_1. From e versus σ' curve the corresponding values of void ratio, e_0 and e_1 are obtained and then the consolidation settlement is calculated as :

$$\text{Consolidation settlement, } S_c = \Delta H = \frac{e_0 - e_1}{1 + e_0} . H_0 \tag{2.1}$$

2.3.2 Prediction of pre-consolidation pressure

If a soil layer has been subjected, some times in the past in its loading history, to a magnitude of effective stress greater than that now exists, then that soil layer is said to be over consolidated and the past maximum effective stress is said to be its pre-consolidation pressure, σ'_c. Otherwise the soil is said to be normally consolidated. σ'_c enables an assessment of the degree of over consolidation expressed in terms of over consolidation ratio (OCR).

$$\text{OCR} = \frac{\sigma'_c}{\sigma'_0} = \frac{\text{Previous maxium effective stress}}{\text{Present effective stress}}$$

The significance of σ'_c for an over consolidated clay is that, if stresses are kept below this value, settlement can be expected to be small. However, if the applied stresses due to loading exceed σ'_c, then large settlement will occur. The OCR has also significant influence on different parameters (such as shear strength) for most soils.

Casagrande (1936) suggested a graphical method based on e~log(σ)' curve to determine the pre-consolidation pressure (Fig.2.5). The steps are as follows:

1. The point P that has the maximum curvature on the upper curved portion of the e~ log(σ') is located by visual estimation.
2. A horizontal line PQ is drawn at P.
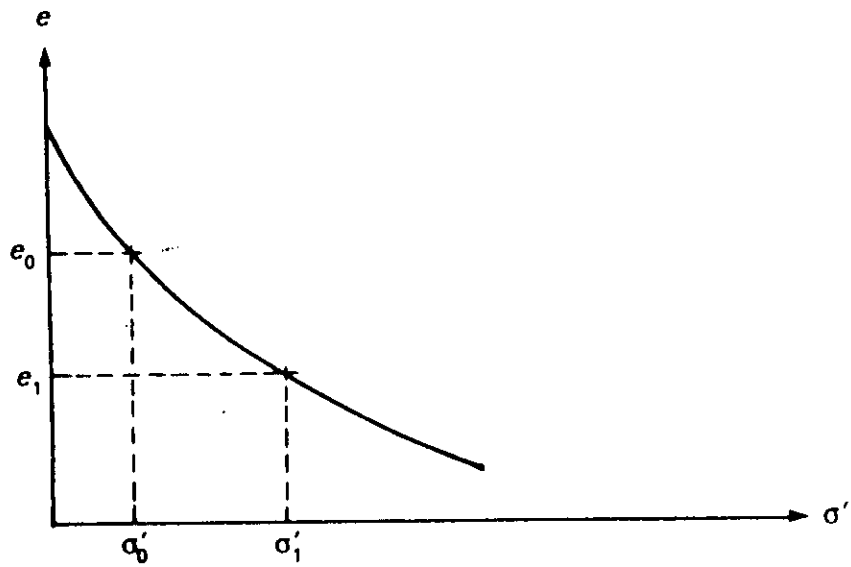
Fig.2.4 Void ratio vs. effective stress curve
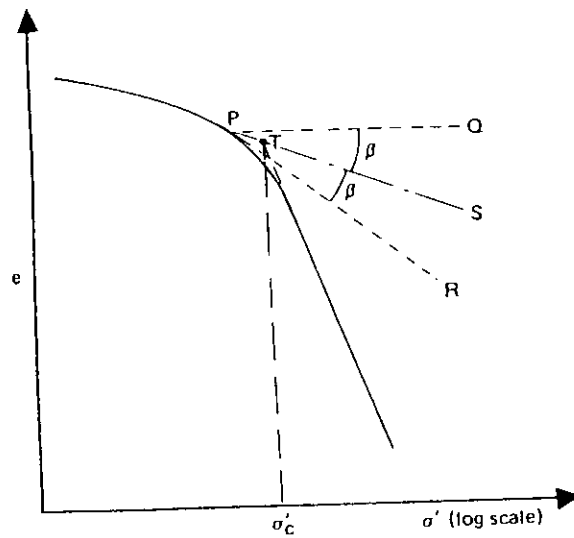
Fig.2.5 Procedure for determination of preconsolidation pressure by Casagrande's method

3. A tangent line PR is drawn at P.

4. A line PS is drawn at P that bisects the angle QPR.

5. The bottom straight line portion of the e~log(σ') plot is extended backward to intersect the bisector PS at T.

6. The effective pressure corresponding to point T is the pre-consolidation pressure σ'_c.

2.3.3 The compression index, C_c

The slope of the e~log(σ') plot for normally consolidated soil is referred to as the compression index C_c. From Fig.2.6.

$$C_c = \frac{\Delta e}{\Delta[\log(\sigma')]} = \frac{e_0 - e_1}{\log(\sigma'_1) - \log(\sigma'_0)} = \frac{e_0 - e_1}{\log(\frac{\sigma'_1}{\sigma'_0})} \qquad (2.2)$$

The void ratio for a given change in effective stress may, therefore, be obtained as

$$e_1 = e_0 - C_c \log(\frac{\sigma'_1}{\sigma'_0}) \qquad (2.3)$$

If the soil acts as a normally consolidated clay due to the change of effective stress then settlement can be obtained by using C_c. From equation 2.3 :

$$\Delta e = e_0 - e_1 = C_c \log(\frac{\sigma'_1}{\sigma'_0}) \qquad (2.4)$$

Substituting Δe from equation 2.4 into equation 2.1,

$$\text{Consolidation settlement, } S_c = \frac{C_c}{1 + e_0} \cdot \log(\frac{\sigma'_1}{\sigma'_0}).H_0 \qquad (2.5)$$

Several correlations exist in literature for the value of C_c. Terzaghi and Peck (1967) gave a correlation for the compression index as

$$C_c = 0.009(LL-10) \qquad (2.6)$$

where LL is the liquid limit. This relation is reported to have a reliability in the range of ±30% and should not be used for clays with sensitivity ratios greater than 4.

For remoulded clay Terzaghi and Peck (1967) suggested the following relation

$$C_c = 0.007(LL-10) \qquad (2.7)$$

10

$$\text{Slope} = C_c = \frac{e_0 - e_1}{\log(\frac{\sigma_1'}{\sigma_0'})}$$
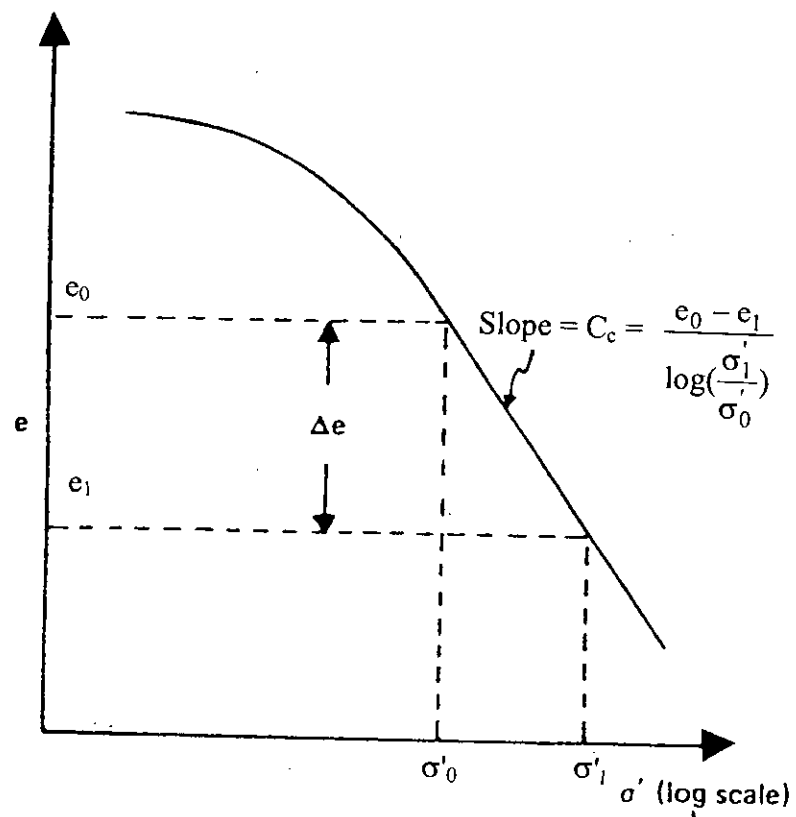
Fig.2.6   Compression index C_c

Azzouz et al. (1976) has correlated compression index with basic soil properties for different types of clays which are presented in Table 2.1 here from Das(1983).

Table 2.1 Empirical equations for C_c.

Equation	Regions of applicability
$C_c = 0.01 w_n$	Chicago clay
$C_c = 0.0046(LL-9)$	Brazilian Clay
$C_c = 1.21 + 1.055(e_0 - 1.87)$	Motley clays from Sao Paulo city
$C_c = 0.208 e_0 + 0.0083$	Chicago clays
$C_c = 0.0115 w_n$	Organic soil, peats
$C_c = 0.02 + 0.014(PI)$	Natural deep ocean soil samples from the North Atlantic (Nacci et al. (1975)

w_n = natural moisture content (%) , e_0 = in situ void ratio,
LL =Liquid limit, Pl = Plasticity index.

2.3.4 Coefficient of volume compressibility, m_v

The coefficient of volume compressibility (m_v) is defined as the amount of change in unit volume of soil that results from a unit increase in effective stress. The value of m_v is not constant for a given soil but varies with the level of effective stress i.e.

$$m_v = \frac{\varepsilon_{vol}}{\Delta\sigma'} = \frac{\Delta V}{V_0}.\Delta\sigma' \qquad (2.8)$$

In a one-dimensional consolidation test it may be reasonably assumed (if the consolidation ring is thick enough) that no change in lateral dimension takes place and there is only a change in thickness of the specimen. The change in volume ΔV of the specimen which results from an increase in effective stress ($\Delta\sigma'$) may, therefore, be represented by either the change in thickness (ΔH) or the change in void ratio (Δe). The volumetric strain of a layer initially H_0 thick can be expressed as

$$\frac{\Delta V}{V_0} = \frac{\Delta H}{H_0} = \frac{\Delta e}{1+e_0} \qquad (2.9)$$

Combining 2.8 and 2.9

$$m_v = \frac{\Delta H}{H_0}.\frac{1}{\Delta\sigma'} = \frac{\Delta e}{\Delta\sigma'}.\frac{1}{1+e_0} \qquad (2.10)$$

where $\Delta e/\Delta \sigma'$ is the slope of the e vs. σ' curve.

Now the consolidation settlement can be obtained as (from equation 2.10)

$$S_c = \Delta H = m_v.\Delta\sigma'.H_0 \qquad (2.11)$$

m_v may also be considered as the reciprocal of constrained modulus, E'_0 :

$$m_v = \frac{1}{\Delta\sigma' / \varepsilon_{vol}} = \frac{1}{E'_0} \qquad (2.12)$$

2.3.5 Time rate of consolidation : Co-efficient of consolidation c_v

It is important to estimate the rate of settlement of a structure so that if the total estimated settlement ΔH is large, an estimate of the time span over which significant portion of the settlement will take place can be anticipated. However, if the total settlement is small, its rate is usually of little importance. The settlement rate can be estimated using the coefficient of consolidation, c_v. Determination of the coefficient of consolidation is based on the theory of one-dimensional consolidation proposed by Terzaghi (1925, 1943). The theory considers the rate at which water is squeezed out of an element of soil and can be used to determine the rates of:

 a) volume change of the soil with time

 b) settlement of the soil with time

 c) pore pressure dissipation with time

The underlying assumptions in the derivation of the mathematical equations are as follows:

1. The clay layer is homogeneous

2. The clay layer is saturated

3. Both water and soil particles are incompressible.

4. Deformation of the soil layer and flow of fluid is one-dimensional and in the direction of the applied stress.

5. The change in volume and thus void ratio is due to the squeezing out of the pore water only.

6. Darcy's law of water flow applies.

7. The load is applied instantaneously and over the whole of the soil layer.

13

In Fig.2.7 a layer of clay is shown to be subjected to a sudden increase in total vertical stress $\Delta\sigma_1$ which is distributed over a semi-infinite area. The layer is located between two highly permeable sand layers. Now, let us consider an elemental layer, within the clay stratum, of thickness dz, in which at time t, the excess pore water pressure is u. If a hypothetical standpipe is introduced (as shown in Fig.2.7) it can be seen that the fall in pore water pressure across the element is dh.

Fig.2.8 shows a prismatic portion of the elemental layer having dimentions dx, dy and dz. The drainage across the sample is one dimensional in the z direction, with a hydraulic gradient of $\dfrac{\partial h}{\partial z}$. According to Darcy's law the flow condition will be :

Flow in : $q_z = vA = kiA = k\dfrac{\partial h}{\partial z}\,dx\,dy$ $\hspace{2cm}$ (2.13)

Flow out : $q_{out} = k\,(i + di)\,dx\,dy$

$$= k\,.(\frac{\partial h}{\partial z} + \frac{\partial^2 h}{\partial z^2}\,dz)\,.dx\,dy \hspace{2cm} (2.14)$$

where k = coefficient of permeability and i = hydraulic gradient.

Net rate of flow out of the element is therefore : $q_{out} - q_{in} = k.\,\dfrac{\partial^2 h}{\partial z^2}\,dx\,dy\,dz$ $\hspace{1cm}$ (2.15)

Volume of void in the soil element is $V_v = eV_s$ $\hspace{3cm}$ (2.16)

Therefore, rate of change of volume of void is

$$\frac{\partial V_v}{\partial t} = V_s\,\frac{\partial e}{\partial t} = \frac{V}{1+e}.\frac{\partial e}{\partial t} = \frac{dx\,dy\,dz}{1+e}.\frac{\partial e}{\partial t} \hspace{2cm} (2.17)$$

Now the rate of flow out of the element must be equal to the change of volume of voids :

Therefore : $k.\,\dfrac{\partial^2 h}{\partial z^2}\,dx\,dy\,dz = \dfrac{dx\,dy\,dz}{1+e}.\dfrac{\partial e}{\partial t}$

i.e. $k.\,\dfrac{\partial^2 h}{\partial z^2} = \dfrac{1}{1+e}.\dfrac{\partial e}{\partial t}$ $\hspace{3cm}$ (2.18)

But, $h = \dfrac{u}{\gamma_w}$

$\therefore\ \dfrac{k}{\gamma_w}.\dfrac{\partial^2 u}{\partial z^2} = \dfrac{1}{1+e}.\dfrac{\partial e}{\partial t}$ $\hspace{3cm}$ (2.19)
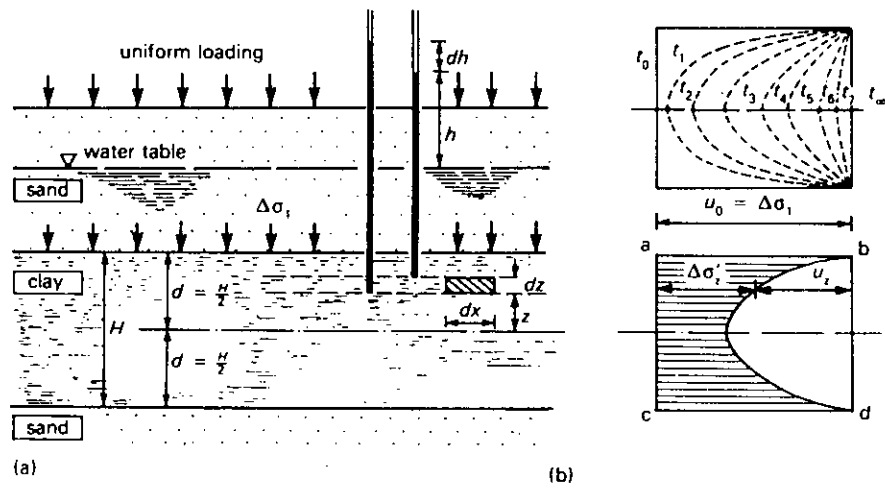
Fig.2.7 Distribution of excess pore pressure in a clay layer subject to a uniform increase in vertical stress (a) Sectional elevation (b) Excess pore pressure distribution

flow out $= k\left\{-\frac{\delta h}{\delta z} + \frac{\delta}{\delta z}\left(-\frac{\delta h}{\delta z}\right)dz\right\}dy\ dx$

flow in $= k\left(-\frac{\delta h}{\delta z}\right)dy\ dx$
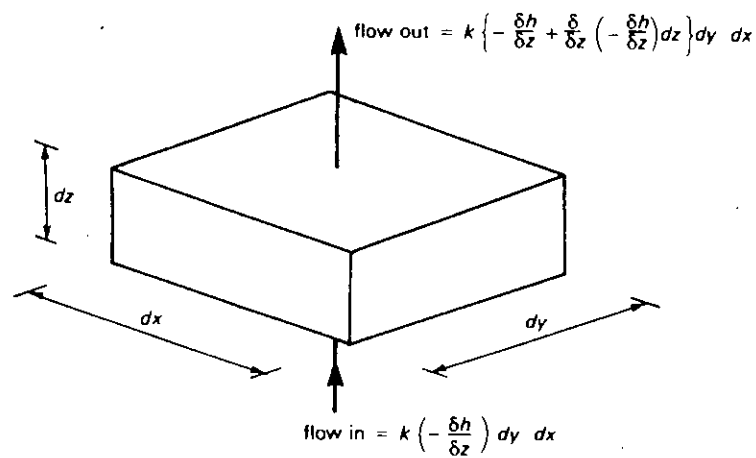
Fig.2.8 One dimensional flow through a prismatic element.

15

The change in void ratio ∂e is due to the increase in effective stress; assuming that these are linearly related, then

$$\partial e = - a_v \, \partial \sigma'$$

(2.20)

where a_v is the coefficient of compressibility. The negative sign in equation 2.20 implies that if σ' increase, void ratio decreases.

Again total stress σ remain constant and $\sigma' = \sigma - u$; so that $\partial \sigma' = - \partial u$

(2.21)

From equations 2.20 and 2.21

$$\partial e = a_v \, \partial u$$

(2.22)

Substituting 2.22 into 2.19

$$\frac{k}{\gamma_w} \cdot \frac{\partial^2 u}{\partial z^2} = \frac{a_v}{1+e} \cdot \frac{\partial u}{\partial t}$$

(2.23)

Again $m_v = \dfrac{\partial e}{\partial \sigma'} \cdot \dfrac{1}{1+e}$ [from equation 2.10]

$$= \frac{a_v}{1+e}$$

(2.24)

m_v = coefficient of volume compressibility

$$\therefore \quad \frac{k}{\gamma_w} \cdot \frac{\partial^2 u}{\partial z^2} = m_v \cdot \frac{\partial u}{\partial t}$$

or $\quad \dfrac{\partial u}{\partial t} = \dfrac{k}{m_v \, \gamma_w} \cdot \dfrac{\partial^2 u}{\partial z^2}$

(2.25)

where c_v = coefficient of consolidation $= \dfrac{k}{m_v \, \gamma_w}$

(2.26)

Equation 2.25 is the basic differential equation of Terzaghi's consolidation theory. In order to obtain a solution to equation 2.25 the following non-dimensional factors are substituted

Degree of consolidation, $U_v = \dfrac{e_0 - e}{e_0 - e_f} = \dfrac{u_0 - u}{u_0}$

(2.27)

Time factor $T_v = \dfrac{c_v t}{d^2}$

(2.28)

Drainage path ratio $Z = \dfrac{z}{d}$

(2.29)

where e_0 = initial void ratio

     e = void ratio after time t

     e_f = final void ratio

u_0 = initial excess pore water pressure

u = excess porewater pressure after time t

d = length of drainage path

Substituting the above non-dimensional factors the one dimensional consolidation equation becomes

$$\frac{\partial^2 U_v}{\partial Z^2} = \frac{\partial U_v}{\partial T_v} \qquad (2.30)$$

The solution to the above equation is obtained as

$$U_v = 1 - \sum_{m=0}^{\infty} \frac{2}{M} \mathrm{Sin}(MZ) e^{-M^2 T_v} \qquad (2.31)$$

where $M = \dfrac{\pi}{2}(2m+1)$ $\qquad$ m = 0, 1, 2 ..... etc

Equation 2.31 merely relates the three parameters U_v, Z and T_v and these are conveniently represented as a graph of U_v versus Z for different T_v values (Fig.2.9). The curved lines refer to constant values of time (or T_v) and so are called isochrones.

The value of coefficient of consolidation c_v for a particular pressure increment in the consolidation test is determined by comparing the characteristics of time vs. dial reading plot. (from test data) and that for U_v vs. T_v (theoretical curve), the process being known as curve fitting. There are two curve fitting methods: (1) Square-root of time method (2) Logarithm-of-time method.

Square-root of time method

Taylor (1942) showed that the Terzaghi theory of one dimensional consolidation gave a straight line when U_v was plotted against the square root of T_v, at least up to U_v=60% , and that at U_v=90% the theoretical curve occurred at 1.15 times the extrapolated straight line portion. The experimental curve consists of three parts (Fig.2.10b) :

(a) Initial compression : indicated by a short curved line. It results from bedding of the porous stones, compression of air or gas bubbles that may be present or slight particle reorientation; it is assumed that air, and not water is expelled during this stage.

17
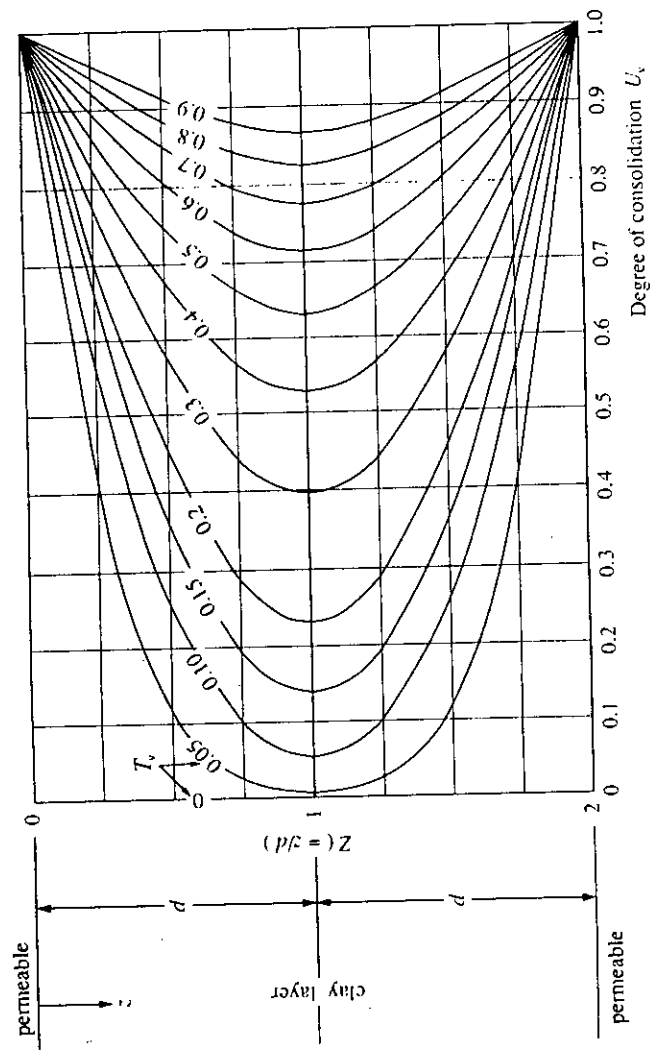
Fig.2.9 One dimensional consolidation isochrones.

18

(b) Primary compression : commences as soon as water is squeezed out of the soil and is represented by the portion of the curve starting from zero percent consolidation to hundred percent consolidation.

(c) Secondary compression : indicated by the final curved portion of the curve, is the compression that takes place after the excess pore water pressure has reached zero and is thought to be caused by delayed reorientation of the particles due to high viscosity of the adsorbed water layers.

In order to apply the consolidation theory to the laboratory test result the 'root-time curve fitting method' is used as follows (Fig.2.10c) :

1. On the dial gauge reading versus square root of time plot, draw a best fit straight line R_0P through the initial portion and extrapolate back to a corrected origin R_0 to eliminate the initial compression.

2. Draw a straight line R_0R from R_0 with a slope of 1.15 times the slope of the straight portion R_0P of the experimental plot. This can be easily done by locating point R such that OR=1.15 X OQ.

3. The point S (i.e. the intersection of R_0R and the experimental curve) is considered to be the point corresponding to 90% consolidation. The abscissa of this point give $\sqrt{(t_{90})}$ from which t_{90} is calculated.

4. Now c_v is obtained as : $c_v=(T_{v90}d^2)/t_{90}$ where d is the average length of the drainage path, for the load increment and T_{v90} refers to the value of T_v for U_v =90%. From theoretical curve T_{v90} =0.848.

Logarithm of time method

This method was proposed by Casagrande and Fedum (1940). They observed that the curve U_v vs. $\log(T_v)$ had three parts (Fig.2.11) :

1. An initial portion with a shape very similar to a parabola and comprises the initial compression.

2. A middle straight line portion attributed to primary consolidation.

3. A lower straight line portion representing secondary compression.

(a) 0

U_v

straight line passing through origin

theoretical curve

at $U_v = 90\%$

90   A   B   C   length AC = 1.15 × length AB

100

$\sqrt{T_v}$

(b) initial compression

Gauge readings

experimental curve

primary consolidation

secondary compression

$\sqrt{\text{time}}$

(c) R_0

Gauge readings

$\sqrt{t}$ line

Curve fitting method

$1.15 \times \sqrt{t}$ line

P

R_{90}

S

O   Q $\sqrt{t_{90}}$ R $\sqrt{\text{time}}$
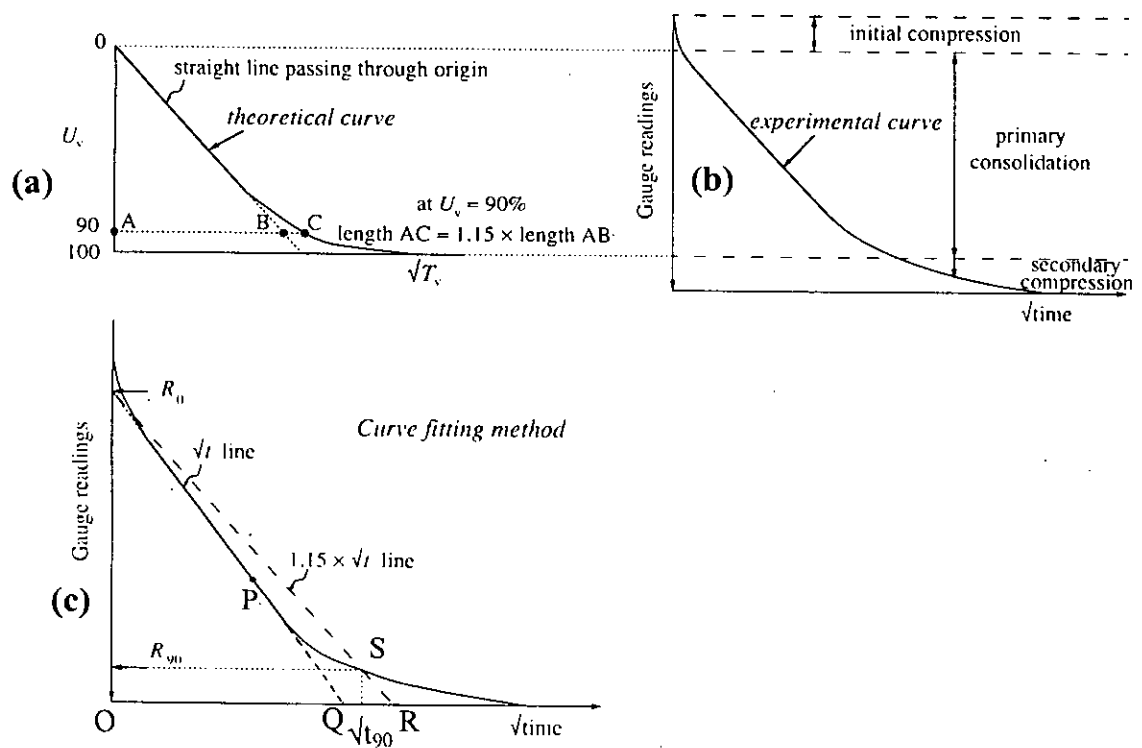
Fig.2.10   Square root of time curve fitting method.
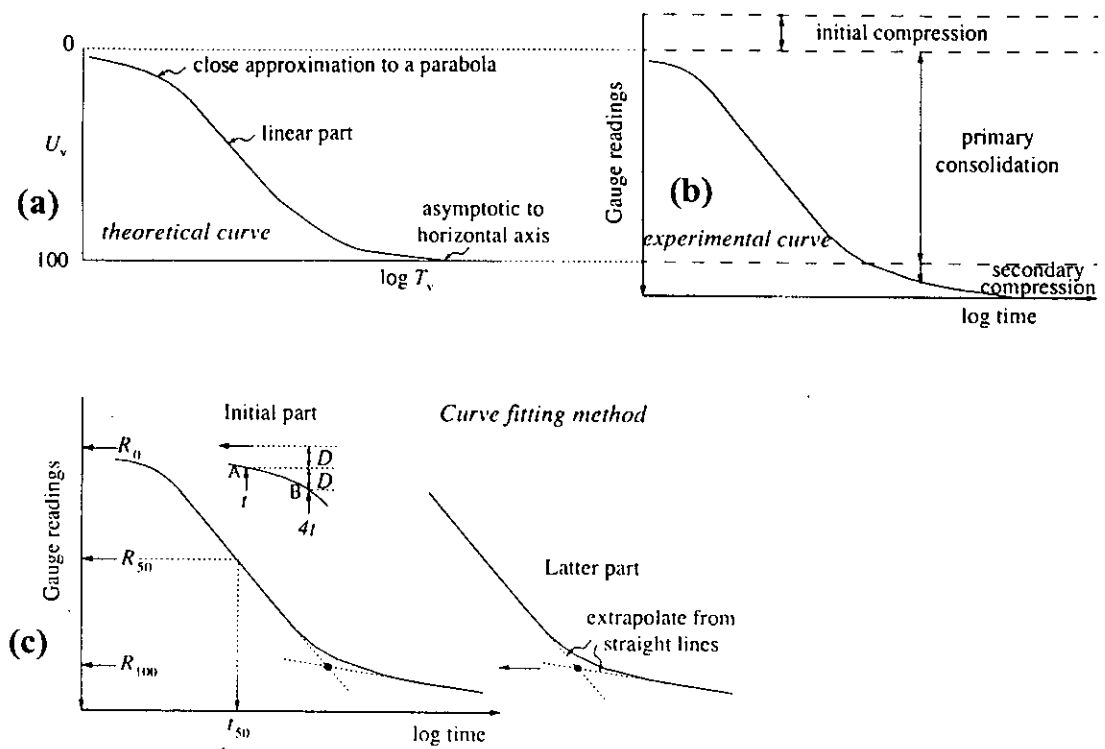
Fig.2.11 Log of time curve fitting method

Calculation of c_v from dial reading vs log(time) plot, the steps followed are :

1. On the initial part of the curve two points A and B are marked at values of time t in the ratio 1:4. The vertical distance between these points D is marked above point A to give the initial reading R_0 for primary consolidation.

2. For soils displaying secondary compression, it is commonly found that compression continue in a straight line on the log graph. So this line is extrapolated back to meet the extrapolated straight middle portion. Where these lines intersect is the final reading for primary consolidation R_{100}. For soils which display very little secondary compression, such as heavily over consolidated clays, the final part of the experimental curve will be a horizontal line which will then define the end reading for primary consolidation R_{100}.

3. R_{50} corresponding to 50% consolidation is then located mid-way between R_0 and R_{100}.

4. The value of t_{50} is noted from the plot corresponding to R_{50}. Next c_v is determined from $c_v = T_{v50}d/t_{50}$ where T_{v50} refers to the value of T_v at $U_v=50\%$. From theoretical curve $T_{v50} = 0.197$.

The root-time method requires readings over a much shorter time period and less judgement is required.

The conventional units of c_v are m^2/year. The value of c_v varies from increment to increment and is different for loading and unloading. It may vary considerably among specimens of same soil. Actual rate of settlement has been observed to be 2 to 4 times faster than the rate predicted on the basis of c_v (Singh, 1992). Typical values of c_v (in m^2/year) for undisturbed clays (mont-morillonite) varying with plasticity index are as follows (Lambe and Whitman, 1979; Head, 1982) :

(i) $I_p > 25$, $c_v = 0.1$-1; (ii) $I_p = 25$ to 5 ; $c_v = 1 - 10$; (iii) $I_p \Omega 5$, $c_v = 10 - 100$

For silts $c_v > 100$. Disturbed values are about 25-0% of undisturbed values.

2.4 Effect of several factors on the e~σ' relationship and deformation ~ time relationship

2.4.1 Effect of sample disturbance

Soil samples collected from the field are somewhat disturbed. Specially, disturbance is inevitable for normally consolidated soil. Sampling disturbance alters and partially destroys the stable arrangement of soil particles and the force or bonds acting between them. Sample disturbance may be the result of combination of a number of factors, mentioned below, in varying degrees (Whitlow, 1995).

Sampler effects :
- (a) Stress relief due to removal of overburden stress.
- (b) Shear strain in the soil beneath the tube or piston.
- (c) Change in moisture content during sampling: decrease due to pressure on driving, increase due to suction on withdrawal.
- (d) Internal vertical shear in soil near to inner face of tube.
- (e) Smearing along sides of sample.
- (f) Changes in density: increase due to driving pressure, decreases due to lateral expansion at clearance diameter.

Transport and storage effects:
- (a) Ineffective sealing producing change in moisture content.
- (b) Mechanical, vibratory or shock damage.
- (c) Lateral and vertical moisture movement.
- (d) Oxidation and ion transfer from steel tubes.
- (e) Crystallization of salts or other compounds that exist in ground water tables.

Sample preparation :
- (a) Density and moisture content changes due to extrusion from sample tube.
- (b) Smearing or plucking damage to drainage faces affecting boundary flow.
- (c) Shrinkage or swelling.

2.4.2 Effect of past loading history

Normally consolidated clay

Fig.2.12 shows e~log(σ') curves that a normally consolidated soil would exhibit in the field (i.e. in situ state), at disturbed state and at remoulded state. If the soil skeleton is disturbed, a relatively flat 'void ratio-effective stress' plot is obtained (Barnes, 1995; Das, 1983). In other words, for a given σ' the recorded value of e is reduced with the increase in sample disturbance. From Fig.2.12 it can be inferred that e vs. log(σ') relationship for in situ condition, usually termed as 'virgin compression curve', will lie to the right of the curve for laboratory tested least disturbed soil. Schmertmann (1955) found that irrespective of degree of disturbance all curves coincide at a void ratio of about 0.4e_0. He proposed the following method to construct the in situ e~log(σ') curve from the curve obtained from laboratory test (Fig.2.13).

1. A consolidation test is carried out with pressures applied which reduce the void ratio to 0.4e_0 or at least sufficient values to enable extrapolation to 0.4e_0.

2. The present void ratio e_0 and effective stress σ'_0 are determine and this point A is marked on the graph.

3. The point B at 0.4e_0 on the virgin compression curve is marked.

4. The in situ curve is then plotted as the line A-B.

Overconsolidated clay

Fig.2.14 shows the nature of field consolidation curve of an over-consolidated clay. The in situ reloading curve commences at the point A(e_0,σ'_0) and it will have a flatter portion up to σ_c' (point D), followed by a steeper portion when the soil returns to being normally consolidated. After careful testing, Schmertmann (1953) concluded that the field re-compression branch (AD in Fig.2.14) has approximately the same slope as the laboratory unload/reload branch. To plot the in situ void ratio versus log(σ') curve, it is necessary to carry out a consolidation test to produce a reloading curve with pressures applied beyond the pre-consolidation pressure σ'_c, followed by an unload/reload loop (BC on Fig.2.14). Further pressure is then applied which reduce
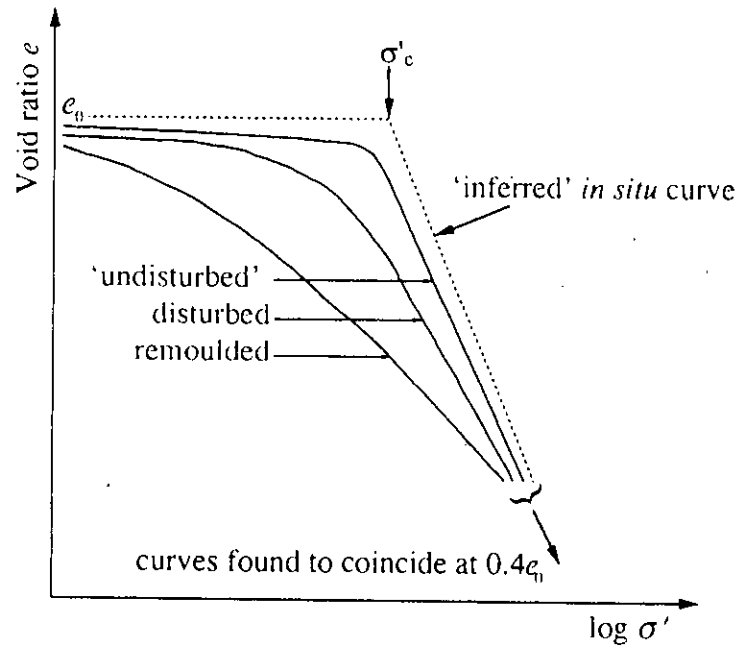
Fig.2.12 Effect of sampling disturbance on normally
consolidated clay (After Barnes, 1995)
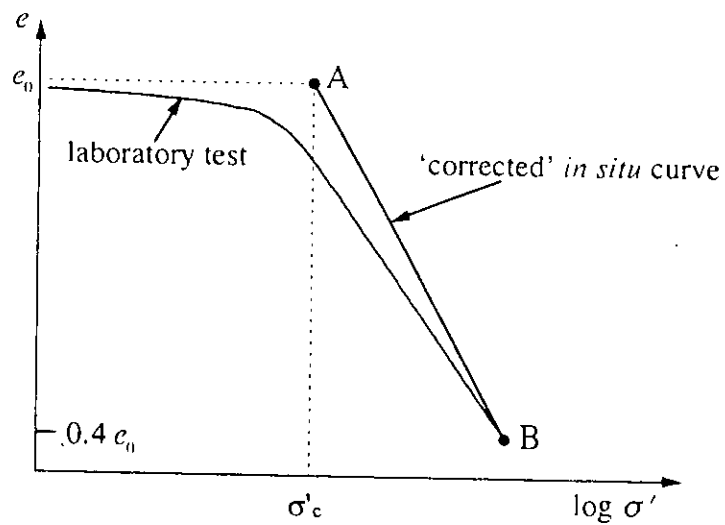
Fig.2.13 In situ curve -normally consolidated clay.
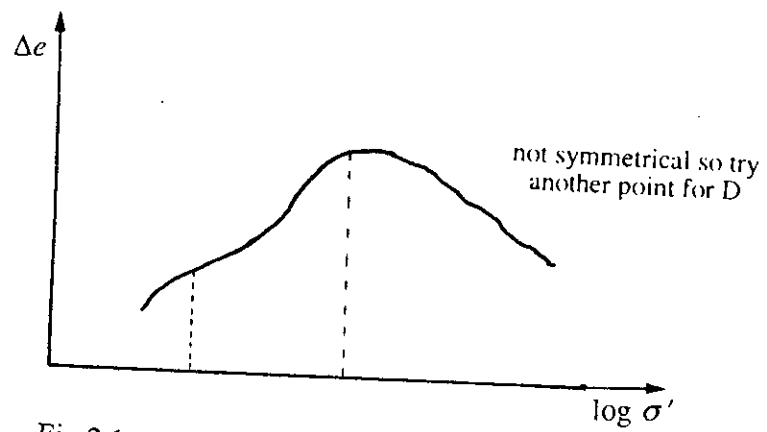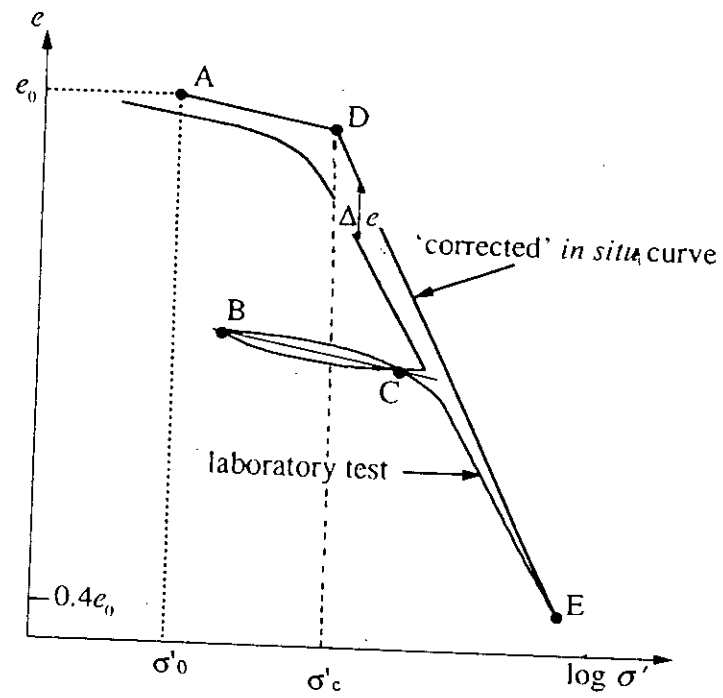
Fig.2.14 In situ curve - over consolidated clay.

the void ratio to $0.4e_0$ or at least sufficient values to enable extrapolation to $0.4e_0$. The in situ curve is then constructed as follows:

1. Point A having coordinate (e_0,σ'_0) is located first. From A, a line is drawn parallel to the average unload/reload loop BC up to point D. σ'_c may be obtained from the Casagrande construction.

2. The point E at $0.4e_0$ on the normal compression line is marked. Line DE is drawn to complete the two limbs AD and DE of the in situ curve.

Barnes (1995) proposed an alternative method if σ'_c cannot be determined very accurately. A point D is chosen and lines AD and DE are drawn. Then, Δe the difference between the trial line and the laboratory test result is plotted against $\log(\sigma')$. When Δe-$\log(\sigma')$ curve is symmetrical it is considered that the point D represent the most likely value of σ'_c.

2.4.3 Effect of magnitude of load increment

Leonards and Altschaeffl (1964) reported striking changes in the shape of the compression time curves for one-dimensional compression tests if the load increment ratio is reduced to a substantially low value. Fig.2.15 shows the shape of dial reading vs. time curves for undisturbed Mexico City clay. Curve I is for $\Delta\sigma/\sigma'=1$. Curve II and III are for load increment ratios of 0.25 and 0.22, respectively. The position of the end of primary consolidation - i.e. zero excess pore water pressure in curves II and III is somewhat difficult to resolve.

The load increment ratio is reported to have influence on the consolidation of clay (Das, 1983). Fig.2.16 shows the nature of the e vs. $\log(\sigma')$ curve for various values of $\Delta\sigma/\sigma'$. If $\Delta\sigma/\sigma'$ is small, the ability of individual clay particles to readjust to their positions of equilibrium is small, which results in a smaller compression as compared to that for a large $\Delta\sigma/\sigma'$. The e~$\log(\sigma')$ relationship become more distinct when smaller load increments are applied, especially for normally consolidated clays. This is very important when pre-consolidation pressure and in situ curve is to be determined for lightly over consolidated clays.

27
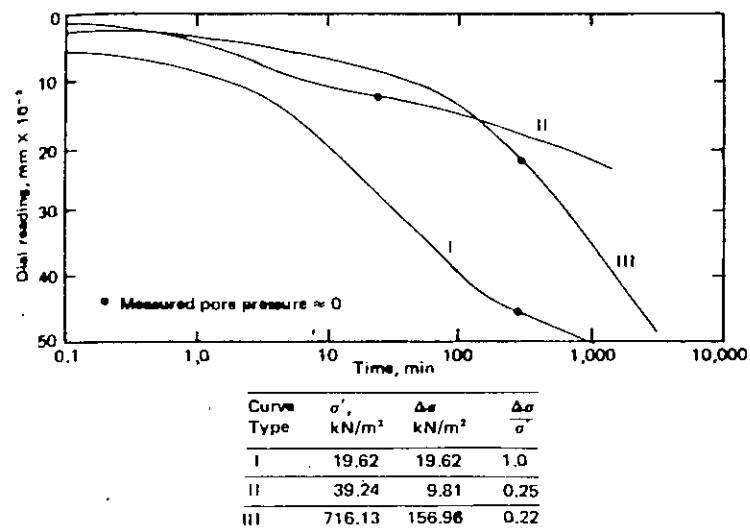
Fig.2.15 Effect of $\Delta\sigma/\sigma'$ on consolidation curves for Mexico city clay. (After Leonards and Altschaeffl, 1964).

Curve Type	σ', kN/m²	$\Delta\sigma$ kN/m²	$\frac{\Delta\sigma}{\sigma'}$
I	19.62	19.62	1.0
II	39.24	9.81	0.25
III	716.13	156.96	0.22
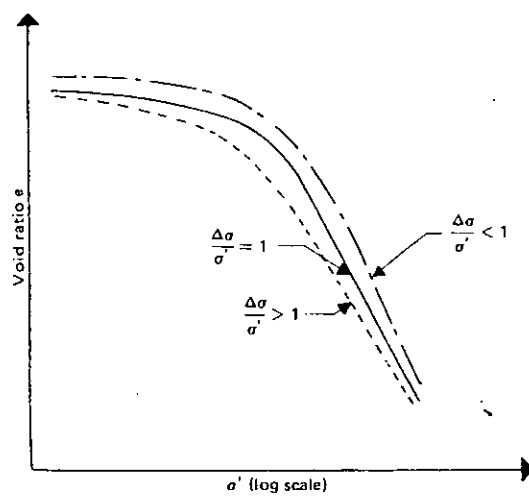
Fig.2.16 Effect of load increment ratio on void ratio vs. logσ' curve (Das, 1983).

28

2.4.4 Effect of sample thickness

Das (1983) pointed out that for similar load increment ratios, the ratio of secondary to primary compression increases with the decrease of sample thickness (Fig.2.17). Also the ratio of secondary to primary compression increases with decrease of $\Delta\sigma/\sigma'$.

2.4.5 Effect of load duration

In conventional testing, the soil specimen is left under a given load for about a day (24 hour) and then the next load increment is added. In this case certain amount of secondary consolidation takes place before the next load increment is added. If the specimen is left under a given load for more than a day, additional secondary consolidation settlement will occur. This additional amount of secondary consolidation will have an effect on the $e\sim\log(\sigma')$ curve as shown in Fig.2.18.
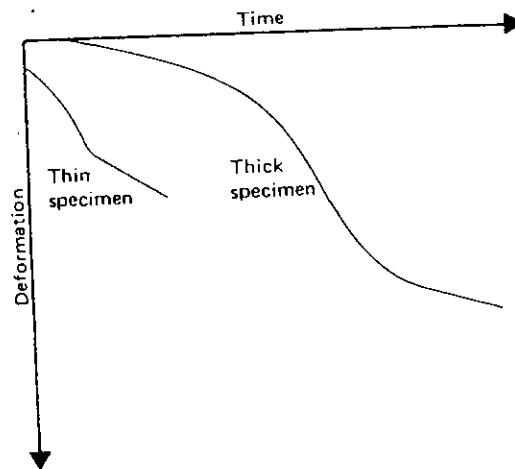
Fig.2.17 Effect of similar load increment ratio, $\Delta\sigma/\sigma'$ on sample thickness (Das, 1983).
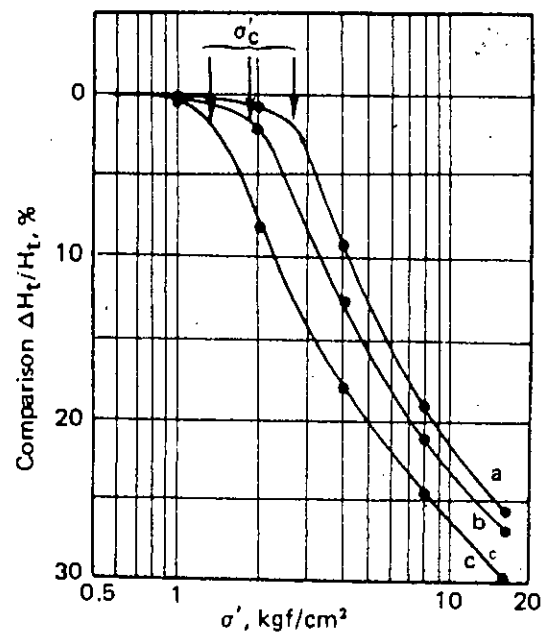
Curve a: at the end of primary
Curve b: at the end of one day
Curve c: at the end of one week

Fig.2.18 Compression vs. $\log\sigma'$ curve for normal and long term incremental loading on Leda clay (After Crawford, 1964)

Chapter 3

EQUIPMENT AND TEST MATERIAL

3.1 Introduction

Reconstituted soils are those which are prepared by breaking down natural soils, mixing them as slurry and reconsolidating them. Reconstituted soils are different from both remoulded and resedimented soils. Soils that are mixed as a suspension and allowed to settle from that state are called resedimented soils. Jardine (1985) discussed the difficulties of implementing detailed investigations of general stress-strain and strength properties using intact samples and it was found that the most comprehensive studies invariably employed reconstituted soil. Reconstituted soil enables a general pattern of behavior to be established. Also comparisons with the response of intact samples may be used to identify any special features associated with fabric, stress history or bonding. The major advantages of using data from reconstituted soil are that the ambiguous and substantial effects of sampling of natural soils and inhomogeneity can be eliminated, while the essential history and composition of in-situ soils can be represented. The disadvantages are that the important effect of post-depositional process, such as ageing, heaving, etc. and of variations of composition and fabric are not included.

3.2 Test material

Sample collection and preparation for making slurry

Natural clay deposit was collected from the site of Bangabandhu Sheikh Mujibur Rahman Novotheatre Project at Bijoy Sarani, Dhaka which was under construction at the time of sample collection. A large area was excavated for the construction of the basement of the project and the samples were collected from the foundation level of the north east quadrant of the dome area (which is at a depth of about 30 ft from the nearby road surface). The colour of the clay is grey and in the in situ state it was identified as medium to stiff clay. After bringing in the laboratory, the clay was dried

in the sun. Next it was powdered by using a wooden mallet. The powdered clay was then sieved through a No.100 sieve and stored for preparation of slurry.

Physical / Index properties of the clay used for slurry

Grain size distribution : The grain size distribution of the clay used for slurry is shown in Fig.3.1. More than 98% of the material is finer than No.200 sieve (0.075 mm). According to MIT soil classification majority of the particles are of silt size.

Atterberg limits : Liquid and Plastic limits of the clay used for slurry were determined. The liquid limit (LL) of the clay was found to be 49.8%. The plastic limit (PL) was found to be 27.2%. The plasticity index (PI) was 22.5%. On the plasticity chart used by Unified Soil Classification (USC) system (originally proposed by Wagner,1957), the value of PI for the soil used plots on the intersection of A line (which is the border line between silt and clay) and LL=50 line. Thus, the soil lies on the borderline of CL, CH, ML and MH (Fig.3.2).

3.3 Preparation of soil slurry

Clay slurry with an initial water content well beyond the liquid limit has been commonly used as an initial state for sample preparation (Siddique,1990; Hopper,1992). Higher initial water content provides higher degree of saturation and higher freedom of particle orientation but require larger initial volume and longer consolidation period. Since it was planned to prepare several consolidation specimens from the same soil cake obtained from consolidation of slurry, it was essential to use such an initial water content so as to be was just sufficient to yield a uniform and homogeneous slurry. It also was required to reduce the consolidation time required for the preparation of the soil cake.

Around 6.5 kg of air-dry clay powder was mixed with 3500 cc of water for preparation of soil cake with 50 kPa and 100 kPa consolidation pressure. The water added is more than the liquid limit of the clay. The soil and water were thoroughly mixed by hand kneading to form a slurry ensuring full saturation. The slurry was then

MIT soil classification

	Sand		Silt			Clay
Medium	Fine	Coarse	Medium	Fine		
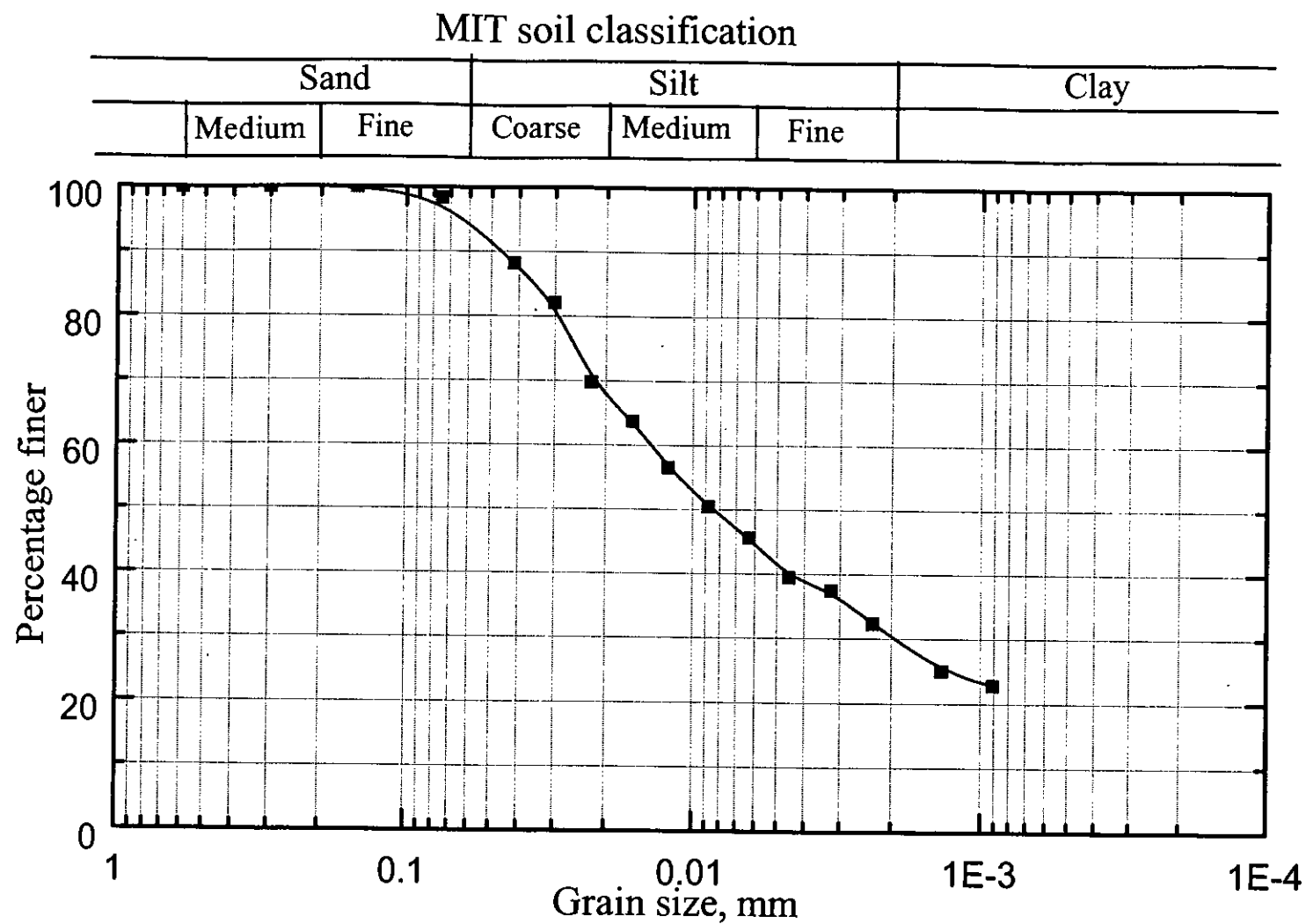
Fig.3.1 Grain size distribution of soil used.
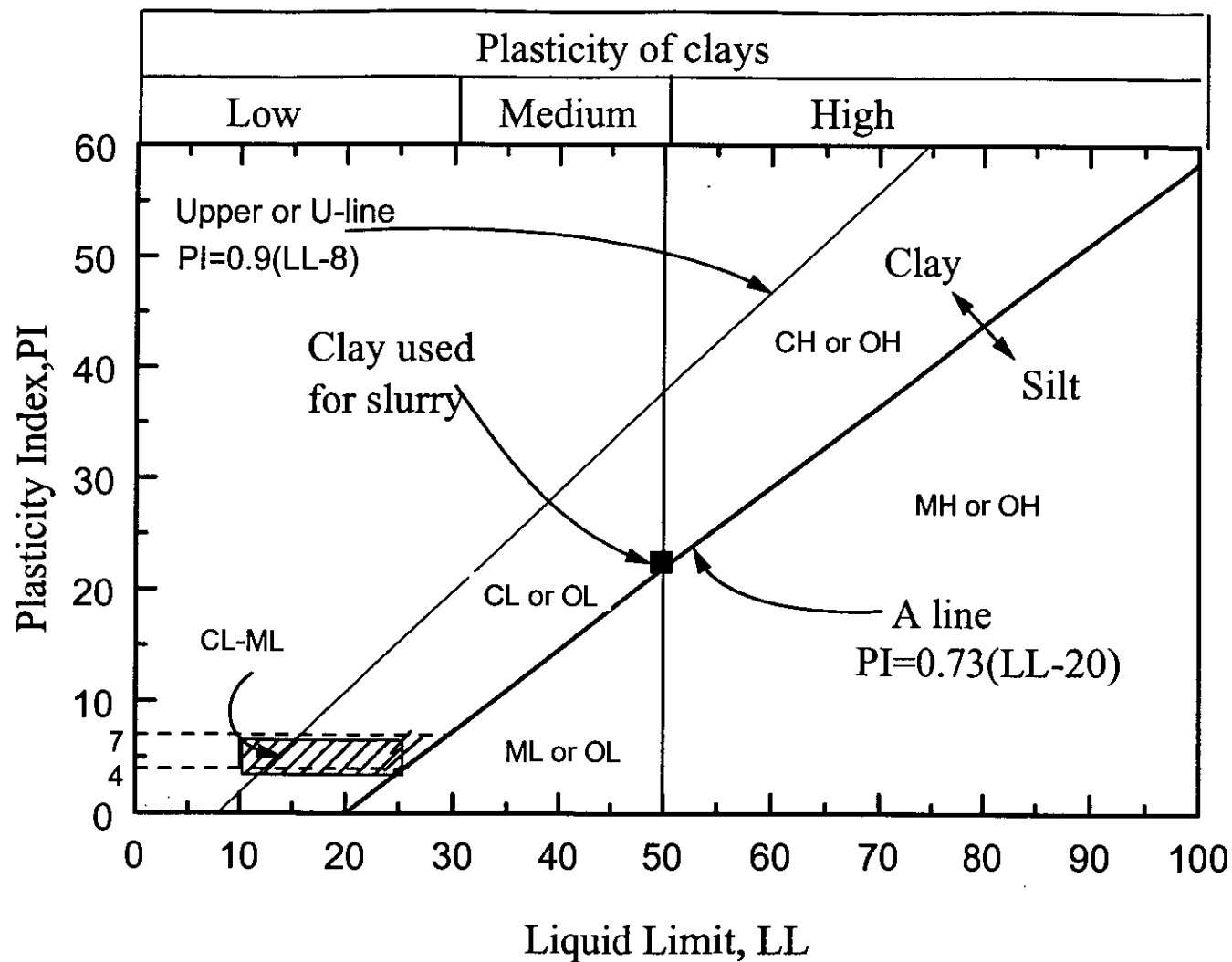
Fig.3.2   Plasticity chart used by Unified classification system

mixed, by using a rotary laboratory mixer machine, for about 30 minutes. Farooq (1995) has mentioned the process of slurry preparation in detail.

3.4 The Rotary Laboratory Mixer

A Hobart mixer machine was used for making soil slurry. The rotary blades of this machine ensured proper mixing of soil particles with water over a short period of time at the required moisture content. The mixer machine used has a dimension of 738 mm x 406 mm x 489 mm and includes a three speed gear box driven by a fully enclosed and ventilated motor. The shift handle is mechanically interlocked with the switch, giving definite gear location and making it necessary to switch off the motor before changing gear. The beater shaft is carried on ball bearings. The bowl locks at the top and bottom of lift travel, which is controlled by convenient hand lever. The speed used for preparing slurry was 113 revolutions/min for attachment and 198 revolution/min for beater. The mixing time was approximately 30 minutes. A photograph of the rotary mixer machine is shown in Fig.3.3 shows photographs of the attachment and bowl of the mixer machine.

3.5 Apparatus for consolidation of slurry

The apparatus consists of a K_0-consolidation cell with a loading frame arrangement. The consolidation cell was prepared from a segment of a steel pipe. Its internal diameter is 203 mm (8 inch) and height 305 mm (10 inch). Two different cells were used. For preparation of soil cakes with 50 kPa and 100 kPa a cell of 260 mm internal diameter and 305 mm (12 inch) high was used. A metal tray was required on which the K_o–consolidation cell (containing the soil slurry) was placed.

3.6 Consolidation of slurry

A geotextile filter and a 6 mm thick perforated steel disc were placed at the bottom of the K_0- consolidation cell. The wall of the cell was coated with a thin layer of silicon
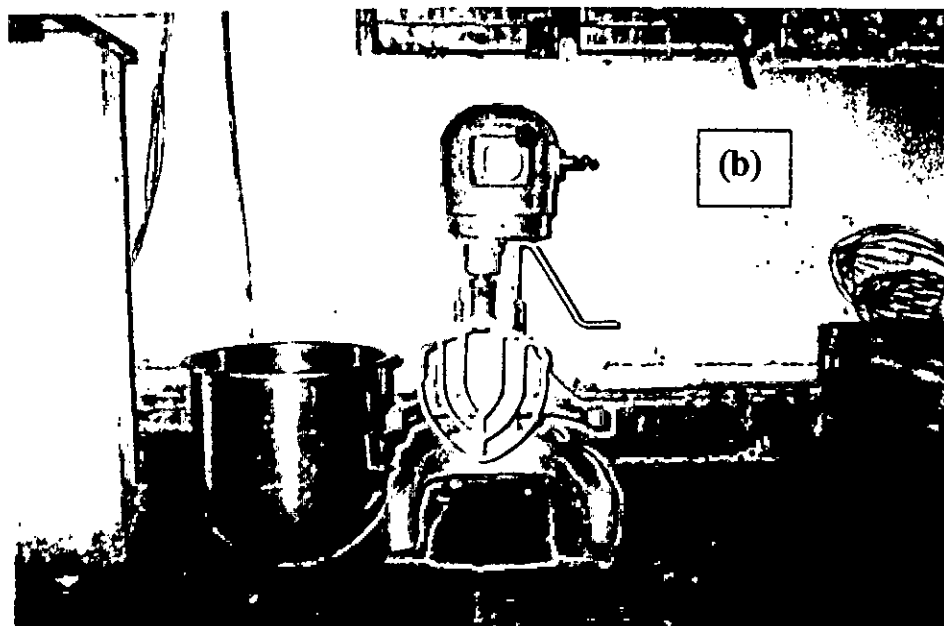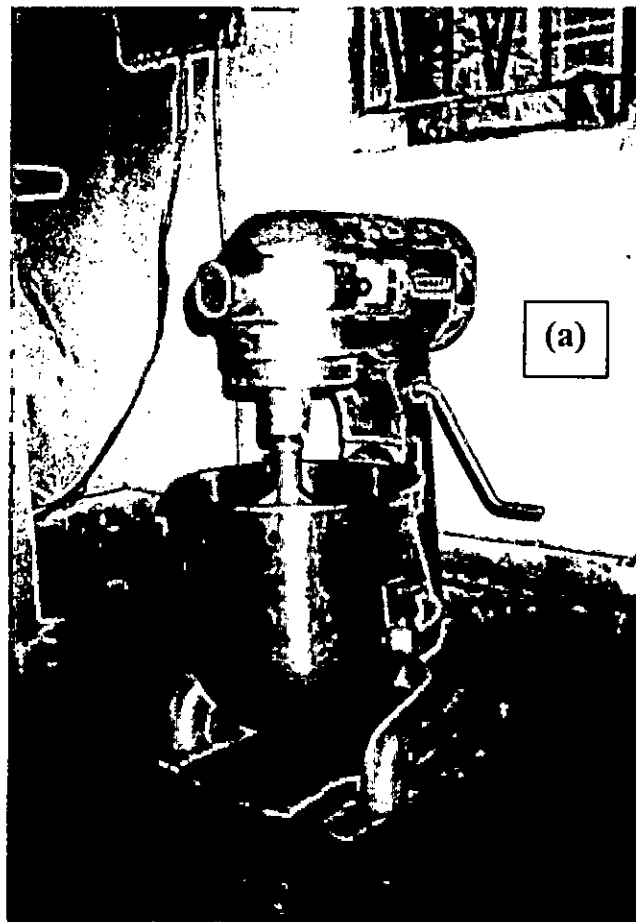
Fig.3.3   The Hobert laboratory mixer machine (a) Complete set up
(b) Bowel and attachment

grease to minimize side friction. A geotextile filter was placed over the disc at the bottom of the cell. The slurry was then poured into the K_o-consolidation cell. Next the slurry was stirred with a steel rod to remove the entrapped air. After removing air bubbles, the top surface of the soil slurry was leveled properly by light tamping on the side of the consolidation cell using a wooden hammer. At the top of the slurry, one geotextile filter followed by one perforated disc was placed to permit drainage. A clearance of a few millimeters in between the perforated discs and inside edge of the cell was provided to eliminate side friction. Fig.3.4 shows a schematic diagram of the arrangements for preparation of reconstituted sample in K_o-consolidation cell.

The required axial pressure (50 kPa or 100 kPa) was gradually applied to the sample using a loading frame. At first, the sample was subjected to consolidate by the self-weight of the sample and the weight of the top porous disc for about 24 hours. Then a pressure of 14 kPa was applied to the sample for the next 24 hour. The vertical pressure was increased gradually to the ultimate value of 50 kPa and100 kPa each time nearly doubling the previous pressure. The pressure was maintained until the end of primary consolidation, which was indicated by the constant reading of a compression dial gauge. It took about nine to ten days for the completion of primary consolidation. Rate of compression was very fast at initial stage of consolidation and gradually it decreased with time. After the completion of consolidation, the top and bottom parts of the cell were separated and the soil cake was extruded by using a mechanical extruder. A soil cake of about 140 mm to 165 mm (5.5 to 6.5 inch) thickness was obtained by the above mentioned procedure for preconsolidation pressures of 50 kPa and 100 kPa.

3.7 Test program

Standard one dimensional consolidation tests were performed on specimens (2.5 inch diameter and 1 inch height) cut from the reconstituted soil cakes. Fig.3.5 shows a photograph of the apparatus used. The bottom porous stone was slightly larger than the outside diameter of the consolidation ring and thus the tests performed can be termed as of fixed ring type. The porous stones were boiled with water and kept under water till setting of the specimen to avoid intrusion of air bubbles. Table 3.1 shows the
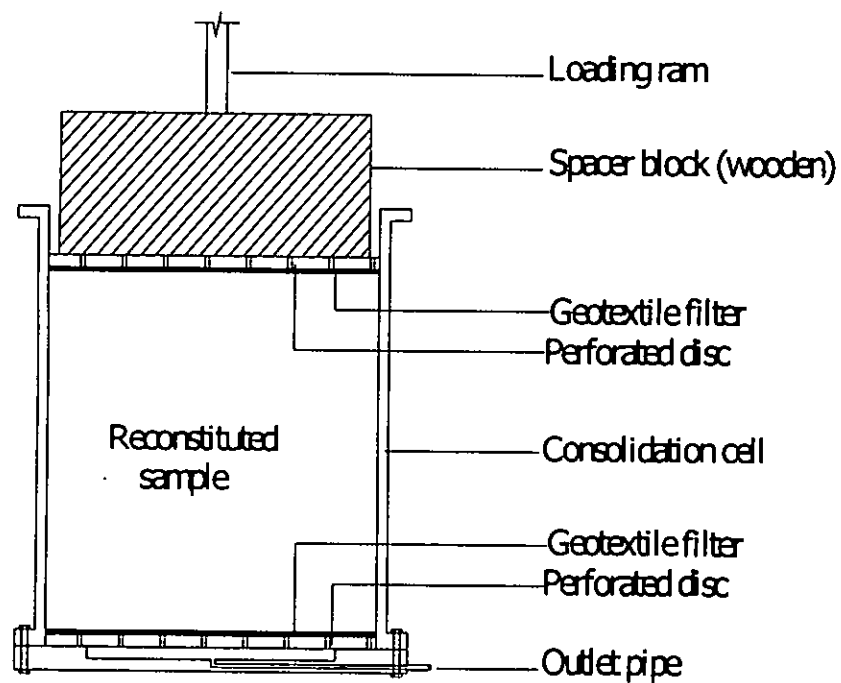
Fig.3.4 Schematic diagram of the assembly of K_0
consolidation cell and other components.
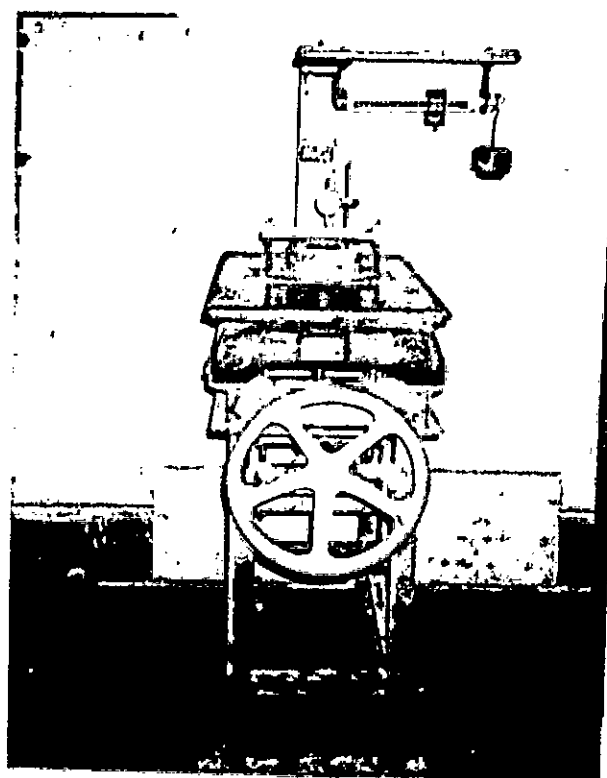
Fig.3.5   Photograph of the consolidation cell used

initial pressure, pressure increment ratio, final pressure etc. of consolidation tests performed on specimens having different pre-consolidation pressure. The maximum pre-consolidation pressure employed (100 kPa) was restricted by the available static weights and from consideration not to damage the floor of the laboratory.

Table : 3.1   Consolidation tests performed on samples with various preconsolidation pressure, initial pressure, pressure increment ratio etc.

Test designation	Pre-consolidation pressure kPa	Initial Void ratio, e_0	P_{i+1}/P_i	Initial ΔP kPa	Final P kPa
P100T01	100	0.9220	2	12.5	1600
P100T02	100	0.8669	2	12.5	800
P100T03	100	0.8823	2	50	1600
P100T04	100	0.8541	2	25	1600
P100T05	100	0.8439	4	12.5	800
P100T06	100	0.7685	4	12.5	800
P100T07	100	0.7893	4 / 2	25	800
P100T08	100	0.8271	4 / 2	25	800
P100T09	100	0.8657	2	25	800
P50T01	50	1.0282	2	12.5	800
P50T02	50	1.0873	2	12.5	800
P50T03	50	0.9396	4	12.5	800
P50T04	50	1.0112	2.5 / 1.5 / 2	25	800
P50T05	50	0.9226	2	25	800
P50T06	50	0.9008	2	50	800
P50T07	50	0.9568	2	25	800
P50T08	50	0.8498	2	50	800
P50T09	50	0.9386	4	12.5	800

P_i represent ith pressure increment

Chapter 4

LABORATORY INVESTIGATION AND TEST RESULT

4.1 Introduction

The results of the laboratory tests performed are presented in this chapter. Effect of variation of stress increment ratio on the nature of $e \sim \sigma'$ relations, and values of compression index C_c, coefficient of consolidation c_v are presented. Also the range of variation of pre-consolidation pressure estimated by Casagrande's method shown.

4.2 $e \sim \sigma'$ relations

In Figs. 4.1a through 4.2b, the void ratio e at the end of consolidation for each pressure σ' in a consolidation test is plotted in various forms (such as arithmetic, semi-log and log-log) to identify any effect of stress increment ratio and to find any trend. As seen from these figures the $e \sim \sigma'$ relationship varied for different specimens. Although all the specimens (presented in Fig.4.1) were cut from the same soil cake prepared under 100 kPa normal stress, the initial void ratio among specimens varied which was unexpected. Potential sources could be errors in weight measurements, but carefully obtained measurements for the second series of tests on specimens cut from the soil cake prepared under 50 kPa normal stress also showed similar variations (Fig.4.3). There may be another potential cause that all specimens from the same soil cake prepared under 100 kPa (or 50 kPa) normal stress, were not tested at the same time because of non-availability of consolidation apparatus. The specimens, though kept in dessicator, dried to some extent reducing the initial void ratio. However, all the curves either for specimens with σ'_c=100 kPa or 50 kPa are nearly parallel indicating vary little or no effect of stress increment ratio on the shape of $e \sim \log(\sigma')$ or $e \sim \sigma'$ curves at least for the range of stress increment ratio employed in this study. In figures 4.1a and b, curves for different stress increment ratio are made identical (i.e. light/deep/dotted line) to easily distinguish them.

Normalized plots (normalizing e and σ' by e_0 and σ'_c respectively) of e and σ' has been presented in Figs.4.3a through 4.4c which were made as an attempt to offset the effect of difference in initial void ratio.

4.3 Compression index, C_c

The compression index, C_c calculated from the bottom straight line portion of e~log(σ') plots from different tests are presented in Table 4.1. The values of C_c obtained ranges from 0.293 to 0.368 and may be considered to be within usual scatter of test data. Therefore, pre-consolidation pressure σ'_c (of a soil layer) up to 100 kPa or stress increment ratio σ'_{i+1}/σ'_i (in a consolidation test) up to 4 appear to have no effect on the value of C_c for a natural clay deposit.

Table 4.1 : Values of compression index C_c from the tests performed.

Test desig-nation	Actual σ'_c Kpa	Stress increment ratio	C_c	Test name	Actual σ'_c kPa	Stress increment ratio	C_c
P100T01	100	2	0.301	P50T01	50	2	0.350
P100T02	100	2	0.293	P50T02	50	2	0.349
P100T03	100	2	0.335	P50T03	50	4	0.368
P100T04	100	2	0.321	P50T04	50	2.5 / 1.5 / 2	0.317
P100T05	100	4	0.358	P50T05	50	2	0.326
P100T06	100	4	0.336	P50T06	50	2	0.342
P100T07	100	4 / 2	0.356	P50T07	50	2	0.366
P100T08	100	4 / 2	0.330	P50T08	50	2	0.326
P100T09	100	2	0.330	P50T09	50	4	0.335

4.4 Pre-consolidation pressure, σ'_c

Pre-consolidation pressure, σ'_c were determined from the test data by Casagrande method to have an idea about the level of accuracy of this method. The method is somewhat subjective in locating the point of maximum curvature. The values of σ'_c obtained by Casagrande method is compared in Table 4.2. For tests on specimens prepared with σ'_c =100 kPa the values from Casagrande's method showed widespread

variations ranging from 65% to actual; all the predicted values being on the lower side. For tests on specimens prepared with σ'_c =50 kPa the values from Casagrande's method ranged between 80% to 120% of actual.

Table 4.2 Comparison among values of actual σ'_c of the soil cake and those estimated by Casagrande's method from consolidation test data.

Test name	Actual σ'_c kPa	Stress increment ratio	Estimated σ'_c KPa	Test name	Actual σ'_c kPa	Stress increment ratio	Estimated σ'_c kPa
P100T01	100	2	80	P50T01	50	2	60
P100T02	100	2	70	P50T02	50	2	40
P100T03	100	2	80	P50T03	50	4	55
P100T04	100	2	90	P50T04	50	2.5 / 1.5 / 2	--
P100T05	100	4	65	P50T05	50	2	60
P100T06	100	4	70	P50T06	50	2	--
P100T07	100	4 / 2	100	P50T07	50	2	70
P100T08	100	4 / 2	90	P50T08	50	2	--
P100T09	100	2	90	P50T09	50	4	60

4.5 Coefficient of consolidation, c_v

It has been observed that for normal stresses below the pre-consolidation pressure the dial reading~log(time) or e~log(time) curves do not resemble to the theoretical curve of U~log(T_v) (U is the degree of consolidation and T_v is the time factor.). In such cases, determination of void ratio corresponding to 0% and 100% consolidation and thus T_{50} cannot be made in most cases and even when managed to be made may lead to large error. It may me inferred that, log time method of fitting for determination of c_v is not suitable for stress levels below the pre-consolidation pressure of an over-consolidated soil.

The values of coefficient of consolidation determined from test data are presented in Fig.4.5 (for specimens with σ'_c =100 kPa) and Fig.4.6 (For specimens with σ'_c =50 kPa). Note that the curves for tests with different stress increment ratio are plotted with different colour density (light / deep) for ease of distinguishing. There is not any discernible difference between the c_v values obtained from tests with stress increment ratios in the range of 2 to 4.

Fig. 4.1a   Void ratio versus effective stress plot in arithmetic scale for tests on specimens
prepared under 100 kPa normal stress
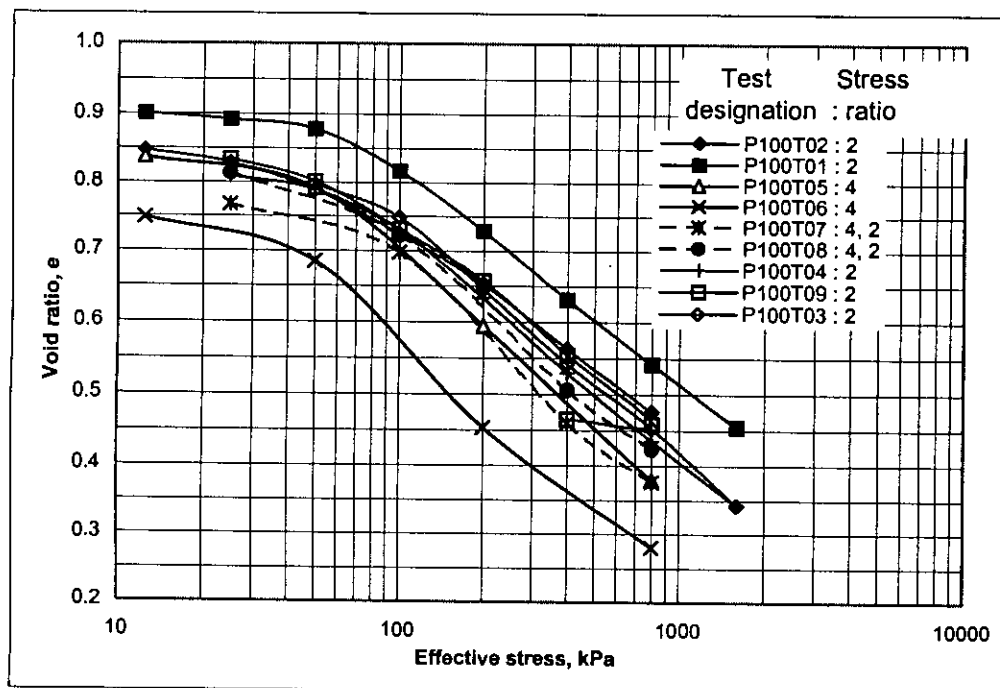
Fig. 4.1b   Void ratio versus log of effective stress plot for tests on specimens prepared
under 100 kPa normal stress

44
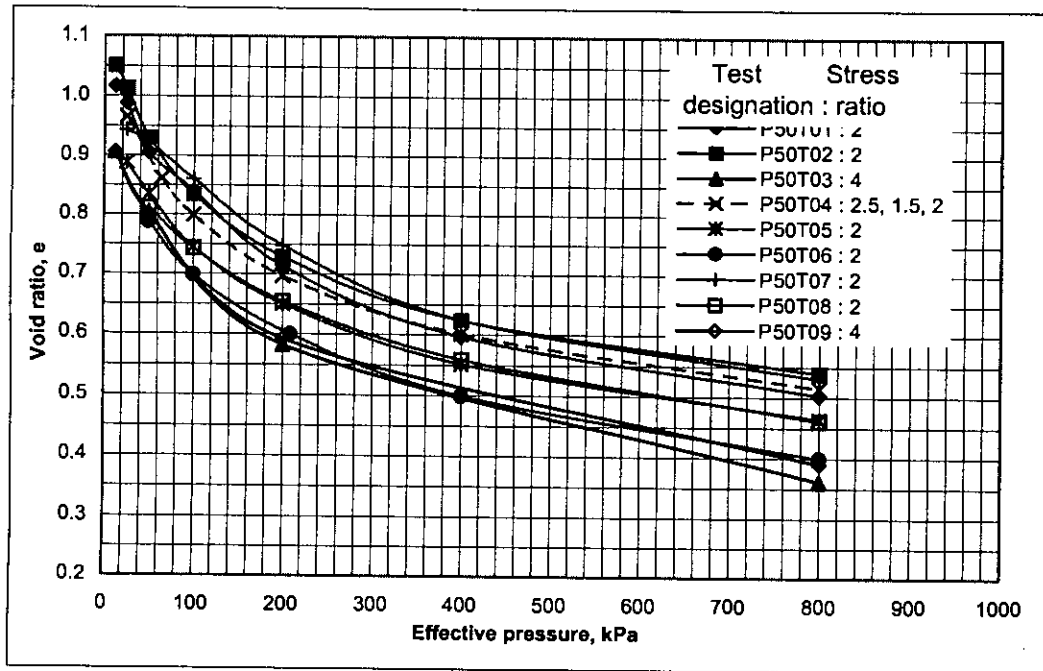
Fig. 4.2a   Void ratio versus effective stress plot in arithmetic scale for tests on specimens prepared under 50 kPa normal stress.
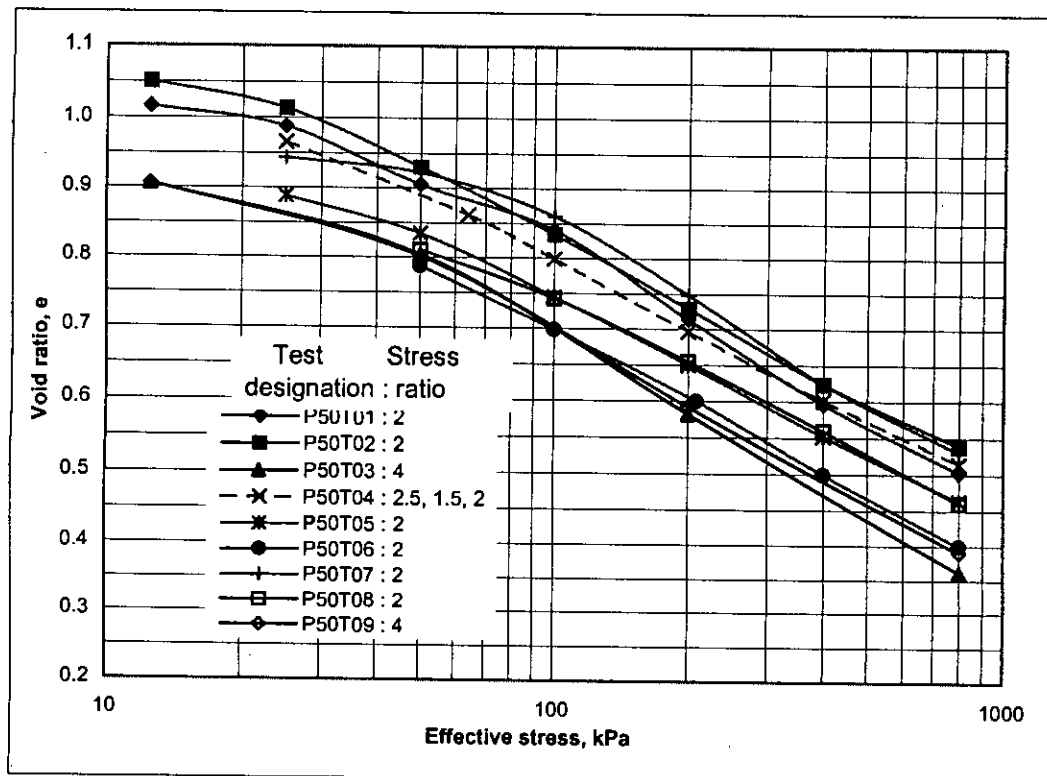
Fig. 4.2b   Void ratio versus log of effective stress plot for tests on specimens prepared specimens prepared under 50 kPa normal stress

45
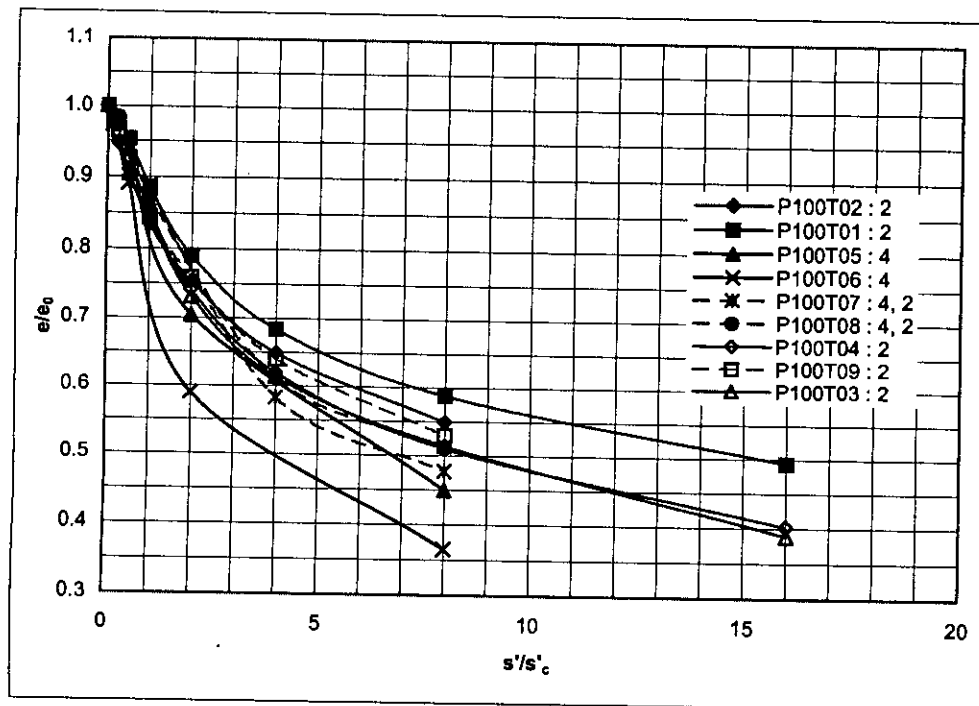
Fig. 4.3a   Normalized plot of Void ratio against effective stress in arithmetic scale for
tests on specimens prepared under 100 kPa normal stress.
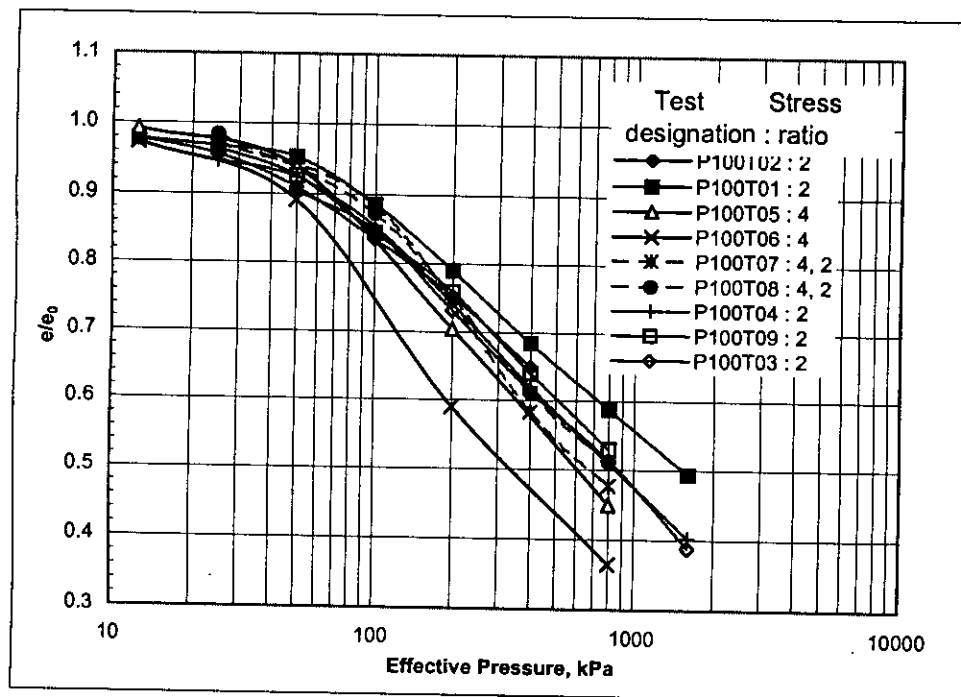
Fig. 4.3b   Normalized semilog plot of void ratio against effective stress for tests on
specimens prepared under 100 kPa normal stress

46

combined_data_p100
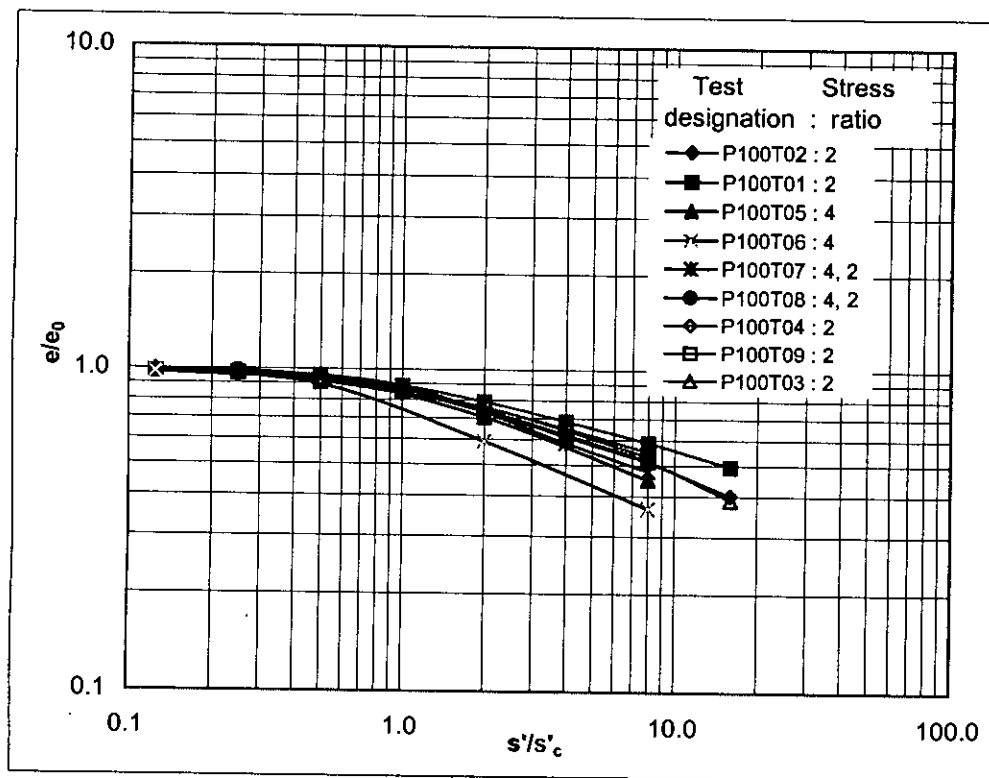
Fig. 4.3c   Normalized log-log plot of void ratio against effective stress for tests on
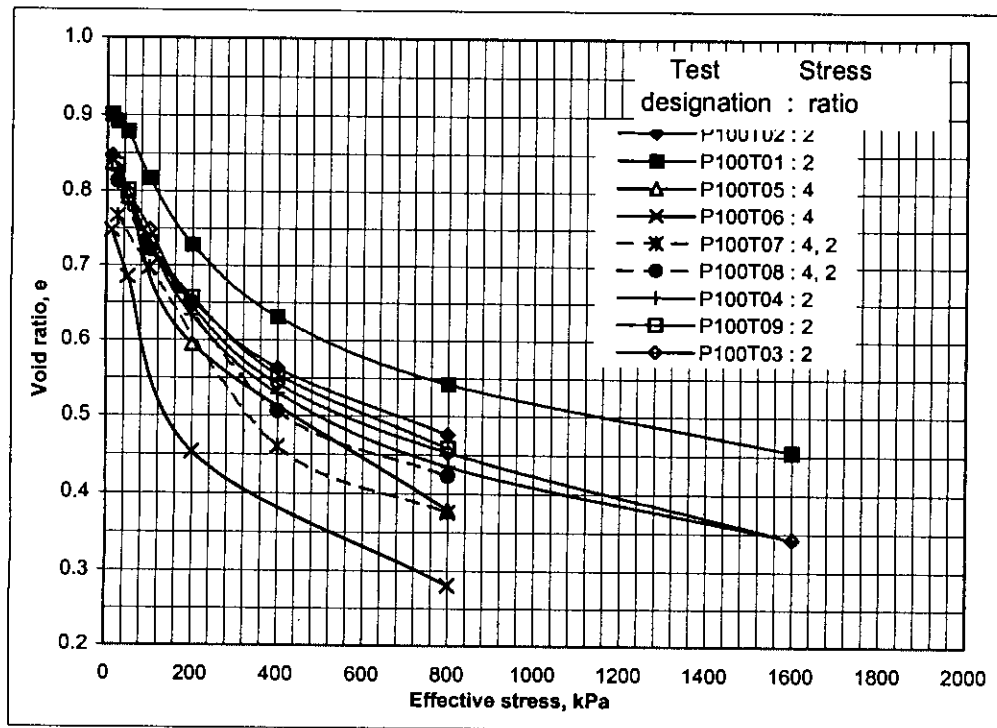for tests on specimens prepared under 100 kPa normal stress
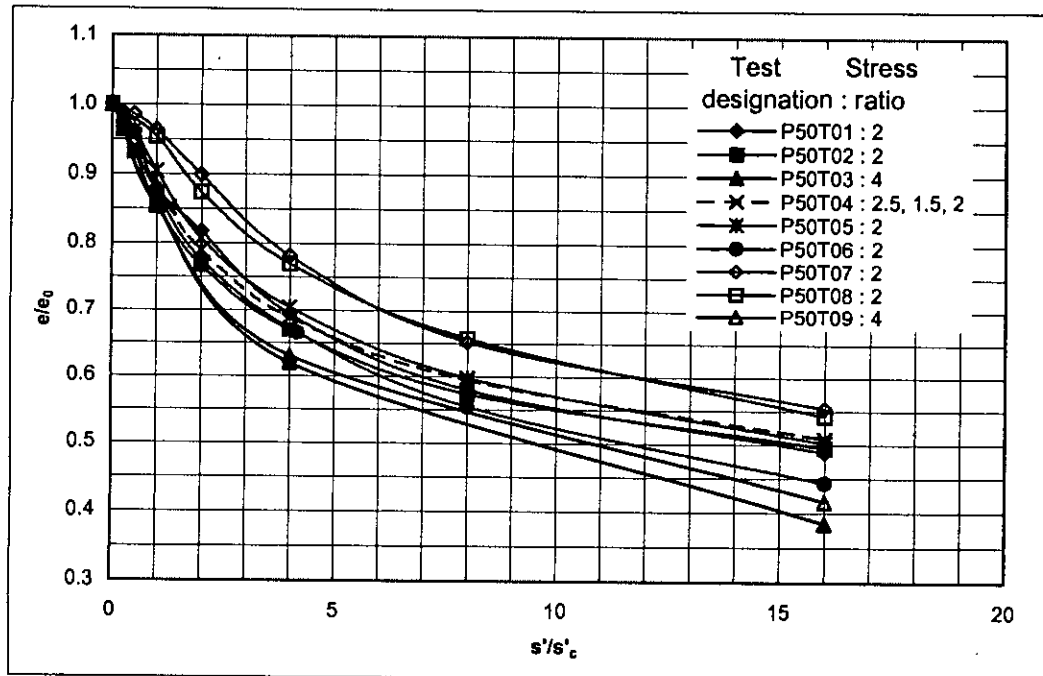
Fig. 4.4a   Normalized plot of Void ratio against effective stress in arithmetic scale for tests on specimens prepared under 50 kPa normal stress.
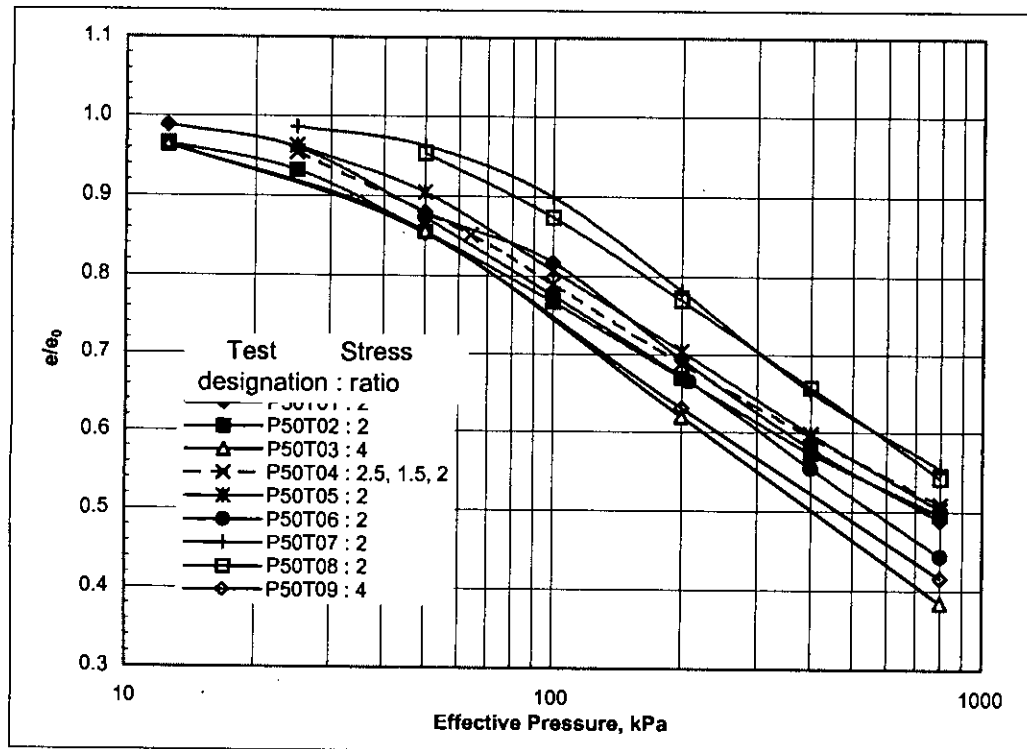
Fig. 4.4b   Normalized semilog plot of void ratio against effective stress for tests on specimens prepared under 50 kPa normal stress.

48
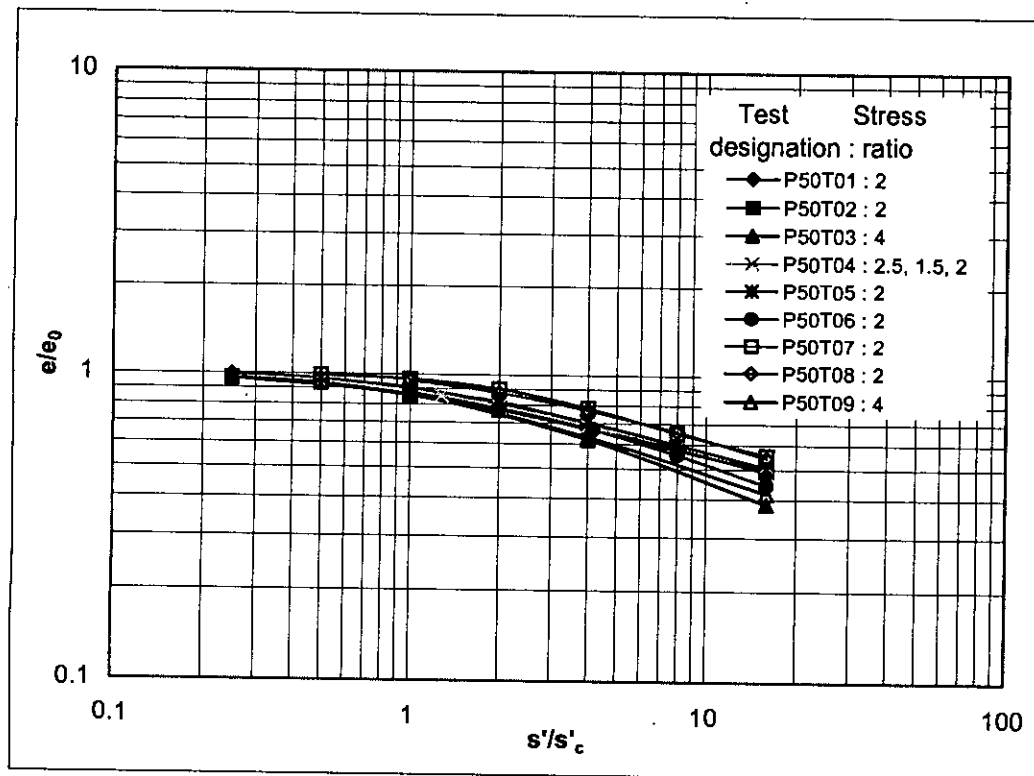
Fig. 4.4c   Normalized log-log plot of void ratio against effective stress for tests on
specimens prepared under 50 kPa normal stress.
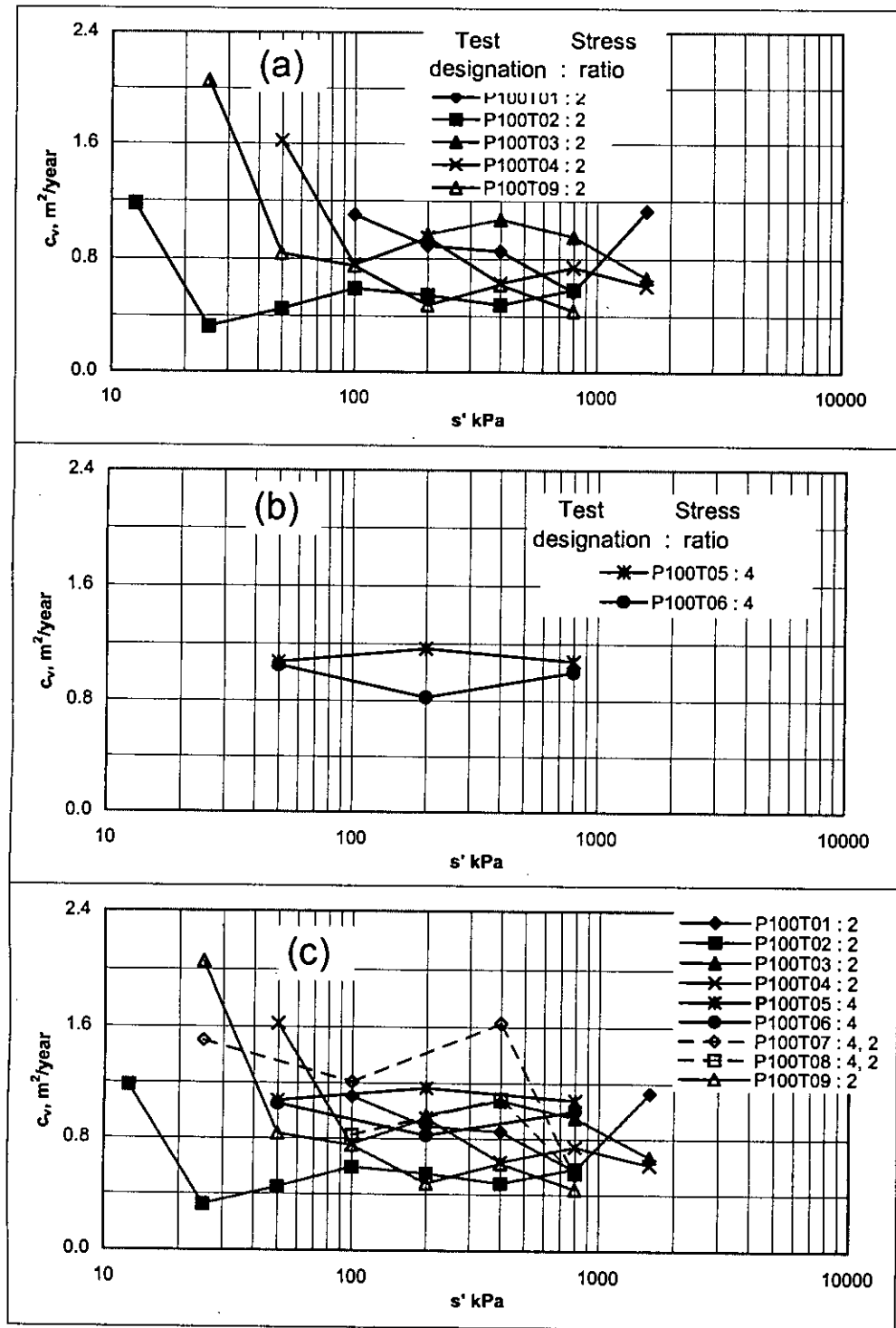
Fig.4.5   Variation of c_v with effective stress for samples prepared under 100 kPa normal stress (a) stress ratio 2 (b) stress ratio 4 (c) mixed stress ratio

50
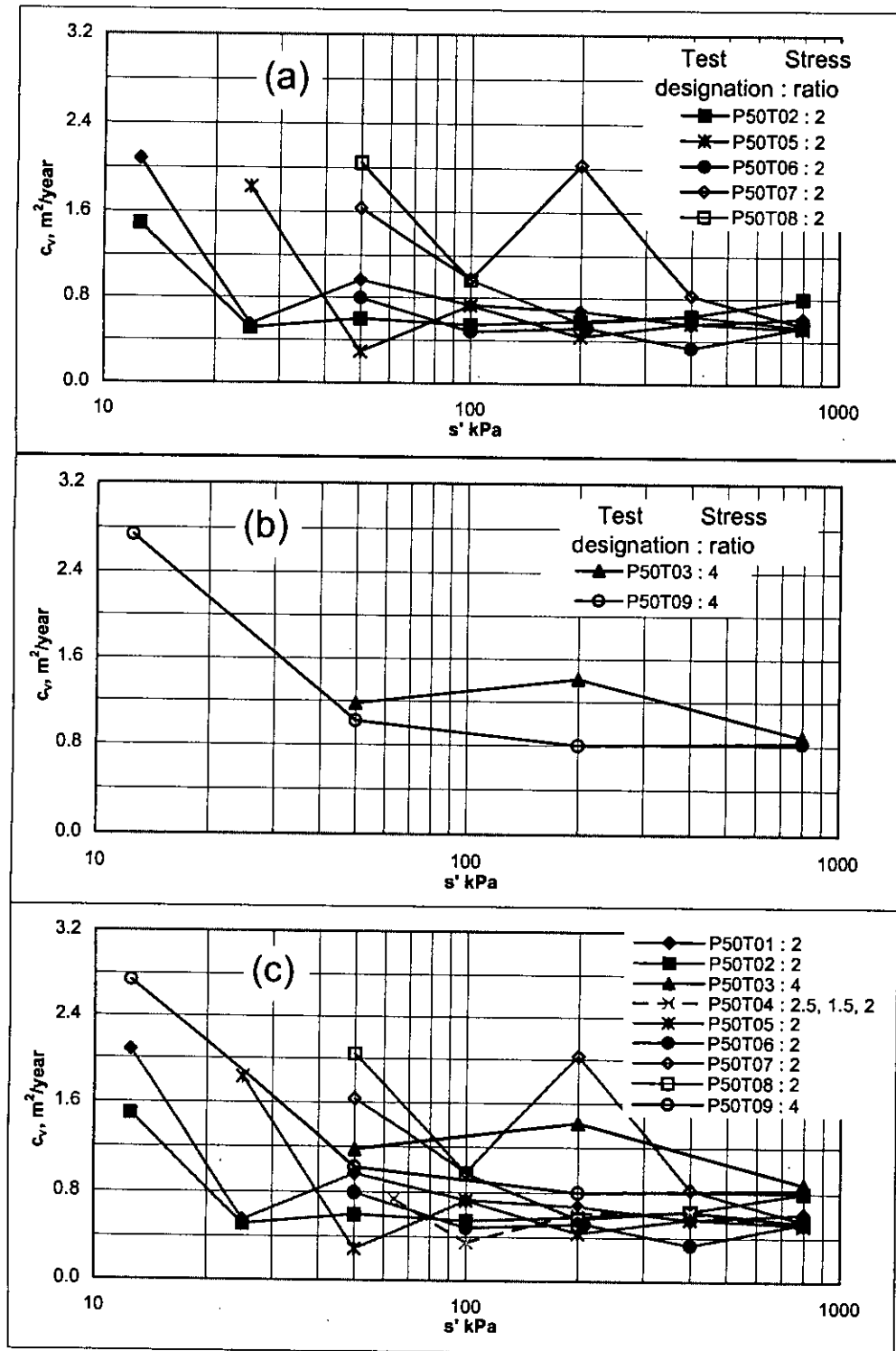
Fig.4.6 Variation of c_v with effective stress for samples prepared under 50 kPa normal stress (a) stress ratio 2 (b) stress ratio 4 (c) mixed stress ratio

51

Chapter 5

A MODEL FOR ONE DIMENSIONAL CONSOLIDATION

5.1 Introduction

A mathematical model that can simulate the series of deformation ~ time response under different pressure, as observed in a one-dimensional consolidation test, is presented in this chapter. The role or significance of the model parameters in representing a particular e~log(time) response are explained. e~log(t) and e~(σ) plots obtained from test and those back calculated using the model are compared. Also effect of variation in test conditions on model parameters are presented.

5.2 Proposed model for one-dimensional consolidation and its background

Kondner (1963) first showed that nonlinear stress~strain curves of both sand and clay may be approximated by the following hyperbolic equation

$$\sigma_1 - \sigma_3 = \frac{\varepsilon}{a + b\varepsilon} \tag{5.1}$$

Where σ_1 = major and minor principal stress,

σ_3 = minor principal stress,

ε = the axial strain ,

a and b =constants whose values may be determined experimentally

The constants a and b have readily visualized physical meaning. As shown in Fig.5.1 and Fig.5.2, a is the reciprocal of the initial tangent modulus E_i and b is the reciprocal of the asymptotic value of stress difference which the stress-strain curve approaches at infinite strain $(\sigma_1-\sigma_3)_{ult}$
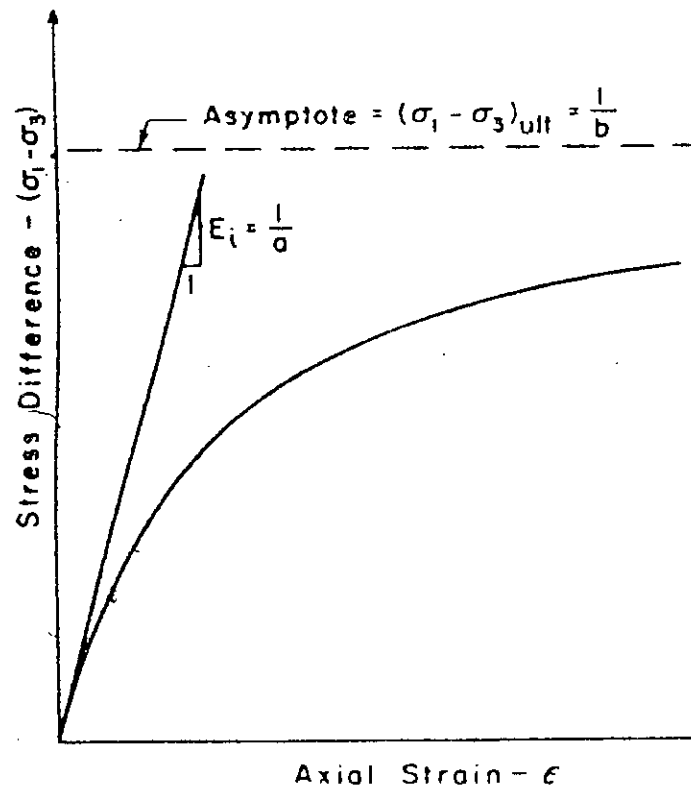
Fig.5.1   Hyperbolic stress-strain curve.
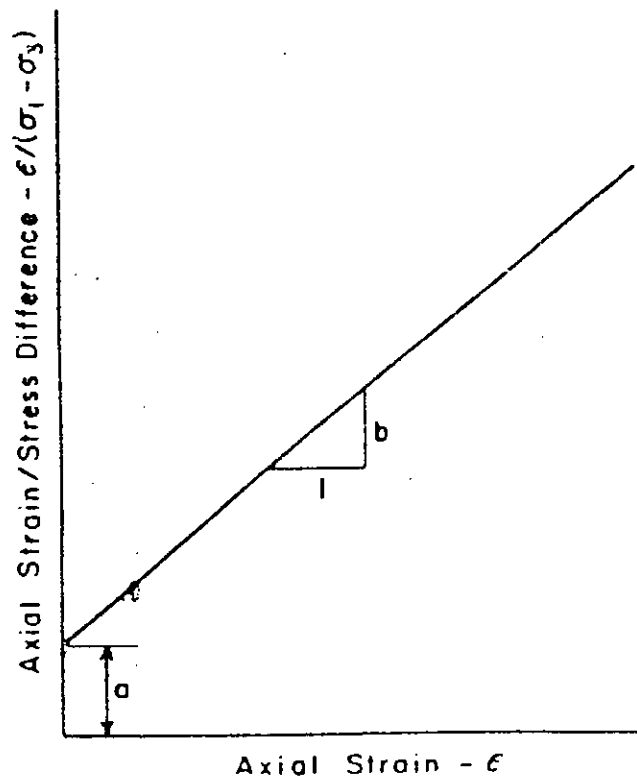
Fig.5.2 . Transformed hyperbolic stress-strain curve.
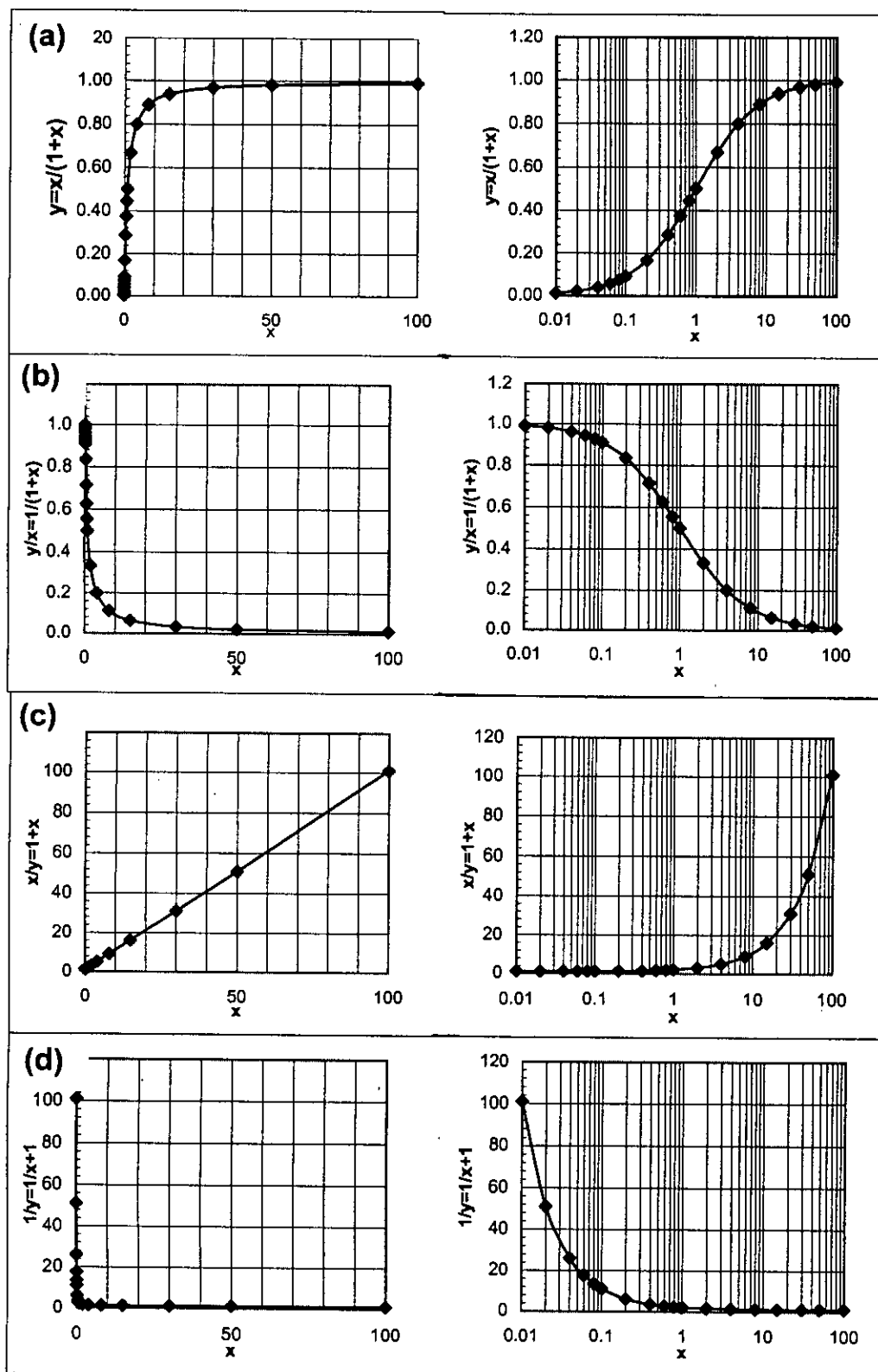
Fig. 5.3 Graphical representation of various functions presented in
equations 5.2a through 5.2d.

When a $=1/E_{max}$ and $b=1/q_{max}$ are used equation 5.1 can be rewritten by using normalized stress and strain; $y=q/q_{max}$ and $x=\varepsilon/\varepsilon_r$ where $\varepsilon_r=q_{max}/E_{max}$ as

$$y = \frac{x}{1+x} = 1 - \frac{1}{1+x} \tag{5.2a}$$

$$\frac{y}{x} = \frac{E_{sec}}{E_{max}} = \frac{1}{1+x} = 1-y \tag{5.2b}$$

$$\frac{x}{y} = 1+x \tag{5.2c}$$

$$\frac{1}{y} = \frac{1}{x} + 1 \tag{5.2d}$$

The shapes of the curves represented by the various functional representations of x and y can be seen from Fig. 5.3.

While the method of obtaining the values of a and b from linear regression analysis of measured stress~strain data has been widely in use (Duncan & Chang, 1970), it has been pointed out (Kondner, 1963) that the initial maximum modulus measured at truly very small strains is greater than the fitted value of 1/a. Also the asymptotic value of $q=\sigma_1-\sigma_3$ is larger than the measured strength of the soil by a small amount. This would be expected, because the hyperbola remains below the asymptote at all finite values of strain. Thus the hyperbolic equation as stress~strain model can be modified by introducing correction factors $c_1=1/(a.E_{max})$ and $c_2=1/(b.q_{max})$ that is

$$y = \frac{x}{\dfrac{1}{c_1} + \dfrac{x}{c_2}}$$

The above equation with constant coefficient of corrections (i.e. c_1 and c_2 being same for all values of x) can not model the stress~strain relationship for the entire range of strain upto peak and specially at small strain as has been shown by Tatsuoka and Shibuiya (1991). Tatsuoka and Shibuiya (1991, 1992) proposed a general type of hyperbolic equation, which is able to model a given stress~strain relation from very small strains to around peak stress which in a simplified form is

$$y = \frac{x}{\dfrac{1}{c_1(x)} + \dfrac{x}{c_2(x)}} \tag{5.3}$$

where $y=$normalized shear stress$=\tau/\tau_{max}$,

55

τ =shear stress= $(\sigma_1-\sigma_3)/2$

τ_{max}=shear strength

x=normalized shear strain=γ/γ_{ref}

γ=shear strain=ε_1-ε_3

G_{max}=maximum shear modulus

and $c_1(x)$ and $c_2(x)$ are correction factors which vary with strain level.

The hyperbolic relationships discussed above when plotted as y/x~log(x) shows the shape of a typical e~log(t) relations from a one dimensional consolidation test. Therefore, it was stipulated that the change in void ratio for any particular stress increment can be modelled using the relationship

$$e - C_3 = \frac{1}{\dfrac{1}{C_1} + \dfrac{t}{C_2}} \qquad (5.4)$$

However a new constant C_3 is needed to be introduced here. The necessity of this parameter is explained in section 5.3.

5.3 Interpretation of model parameters

The model has three parameters here designated as C_1, C_2 and C_3. The significance of these parameters can be understood from Fig.5.4 to Fig.5.5.

Equation 5.4 can be rearranged as follows :

$$\frac{1}{e - C_3} = \frac{1}{C_1} + \frac{t}{C_2} \qquad (5.5)$$

Equation 5.5 represents a straight line in $1/(e-C_3)$ vs t space (Fig.5.4). On such a plot the quantity $1/C_1$ can be readily visualized as the intercept on the $1/(e-C_3)$ axis at t=0. Also, the parameter C_2 represents the inverse of the slope of the fitted straight line.

Referring to equation 5.5 as t approaches 0 (zero) C_1 approaches e_0-C_3. Also, from equation 5.4, as t tends to infinity e approaches C_3 i.e. C_3 represent the end void ratio under a particular load increment (See Fig.5.5). Thus for a particular load increment
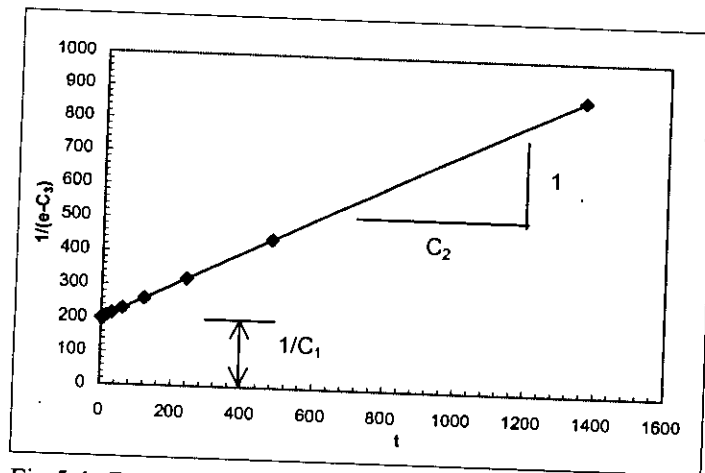
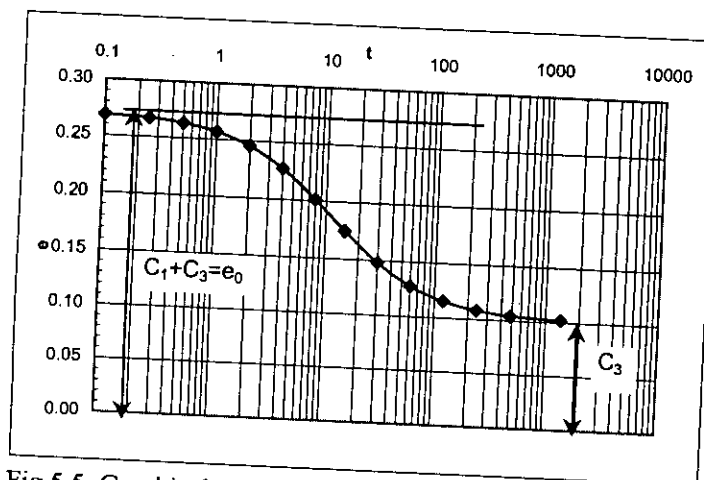Fig.5.4 Graphical representation of equation 5.4
as $1/(e-C_3)=1/C_1+t/C_2$ vs. t

Fig.5.5 Graphical representation of equation 5.4
as $e-C_3=1/(1/C_1+t/C_2)$ vs. log(t)

Model

C_1 represents the decrease in void ratio from t=0 to the time up to which consolidation continued under that load increment. Mathematically C_1 and C_3 are related as $C_1=e_0-C_3$. In general the initial and final void ratios are controlled by the parameters C_1 and C_3.

Figures 5.6, 5.7 and 5.8 show the effect of variation of C_1, C_2 and C_3 on the quantities e-C_3 and e. The series of curves on these figures have some similarity with the e~log(t) curves (or dial reading~log(t) curves) for successive load increments in a one-dimensional consolidation test.

If, in a one dimensional consolidation test, magnitudes of successive load increments are kept same, then the net change in void ratio for the same amount of elapsed time is expected to be less than that for the previous load increments. This feature is well represented in Fig.5.6b. Note that in this figure values of C_1 and C_3 is gradually decreased and C_2 is gradually increased. It is thus expected that with proper values of the model constants the entire series of e~log(t) curves and thus e~p relations, c_v, C_c etc. can be obtained.

Fig.5.7 and 5.8 are presented to demonstrate the effects of individual parameter on the resulting e-C_3 vs. log(t) and e vs. log(t) curves. In Fig.5.7a and 5.8a, C_1 is varied while C_2 and C_3 are kept constant. Note that, since C_3 is same for successive curves, values of e-C_3 at the final time for each curve coincided at e-C_3=0.0 and values of e at the final time for each curve coincided at e=0.8 (which was the value of C_3 for each of these curves). Also note that decrease in value of C_1 for successive curve caused the starting point of that curve to shift downward.

In Fig.5.7b and Fig.5.8b, for all the curves, C_1=0.17 and C_3=0.8 is used but C_2 is varied from 0.85 to 3.5. The effect is that the starting and the end points of these curves are same (because values of C_1 are same and values of C_3 are same). It is clear that the parameter C_2 controls the shape of the curve in between the two end points. For any value of t, the curve that has higher value of C_2 corresponds to a lower value of e (Fig.5.8b).

All of C_1, C_2 & C_3 varying			
	C_1	C_2	C_3
Curve -1	0.17	0.85	0.80
Curve -2	0.15	1.50	0.65
Curve -3	0.10	2.00	0.50
Curve -4	0.08	2.50	0.40
Curve -5	0.05	3.00	0.25
Cutve -6	0.01	3.50	0.15
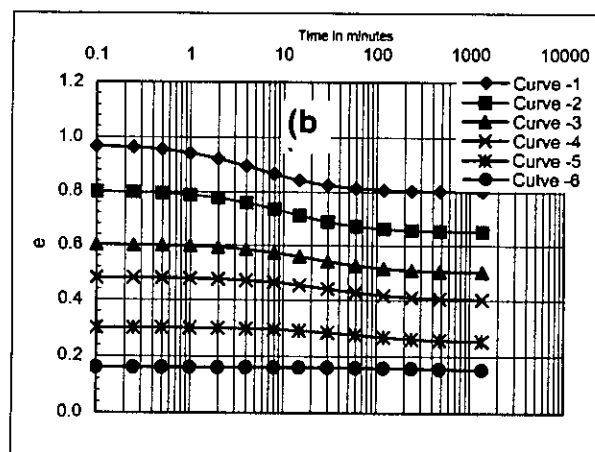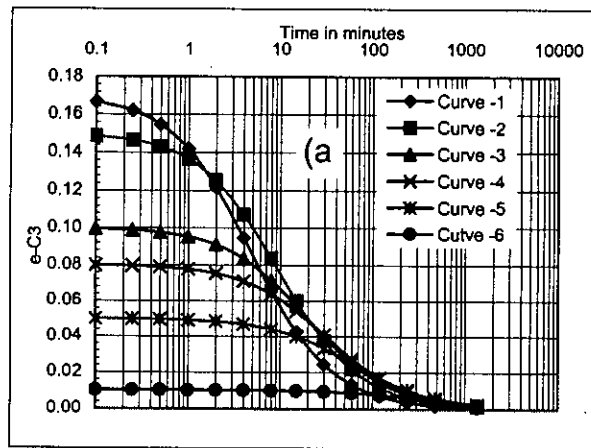
Fig.5.6 Figure showing the effect on (a) $e\text{-}C_3$ and (b) e due to variation of all the three parameters of the model.

C_2 & C_3 constant; C_1 varying

	C_1	C_2	C_3
Curve -1	0.17	0.85	0.80
Curve -2	0.15	0.85	0.80
Curve -3	0.10	0.85	0.80
Curve -4	0.08	0.85	0.80
Curve -5	0.05	0.85	0.80
Cutve -6	0.01	0.85	0.80

C_1 & C_3 constant, C_2 varying

	C_1	C_2	C_3
Curve -1	0.17	0.85	0.80
Curve -2	0.17	1.50	0.80
Curve -3	0.17	2.00	0.80
Curve -4	0.17	2.50	0.80
Curve -5	0.17	3.00	0.80
Cutve -6	0.17	3.50	0.80

C_1 & C_2 constant C_3 varying; C3 controls the vertical shifting of successive curves

	C_1	C_2	C_3
Curve -1	0.17	2.00	0.80
Curve -2	0.17	2.00	0.65
Curve -3	0.17	2.00	0.50
Curve -4	0.17	2.00	0.40
Curve -5	0.17	2.00	0.25
Cutve -6	0.17	2.00	0.15

Fig.5.7 Plots showing the effect of variation of a single parameter on the quantit
(a) C_2 & C_3 constant, C_1 varying (b) C_1 & C_3 constant, C_2 varying varyin;
(c) C_1 & C_2 constant, C_3 varying.

60

Model

C_2 & C_3 constant; C_1 varying

	C1	C2	C3
Curve -1	0.17	0.85	0.80
Curve -2	0.15	0.85	0.80
Curve -3	0.10	0.85	0.80
Curve -4	0.08	0.85	0.80
Curve -5	0.05	0.85	0.80
Cutve -6	0.01	0.85	0.80

C_1 & C_3 constant, C_2 varying

	C_1	C_2	C_3
Curve -1	0.17	0.85	0.80
Curve -2	0.17	1.50	0.80
Curve -3	0.17	2.00	0.80
Curve -4	0.17	2.50	0.80
Curve -5	0.17	3.00	0.80
Cutve -6	0.17	3.50	0.80

C_1 & C_2 constant C_3 varying; C_3 controls the vertical shifting of successive curves

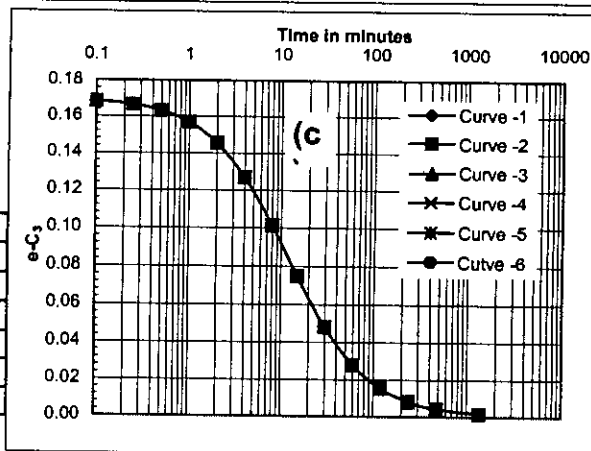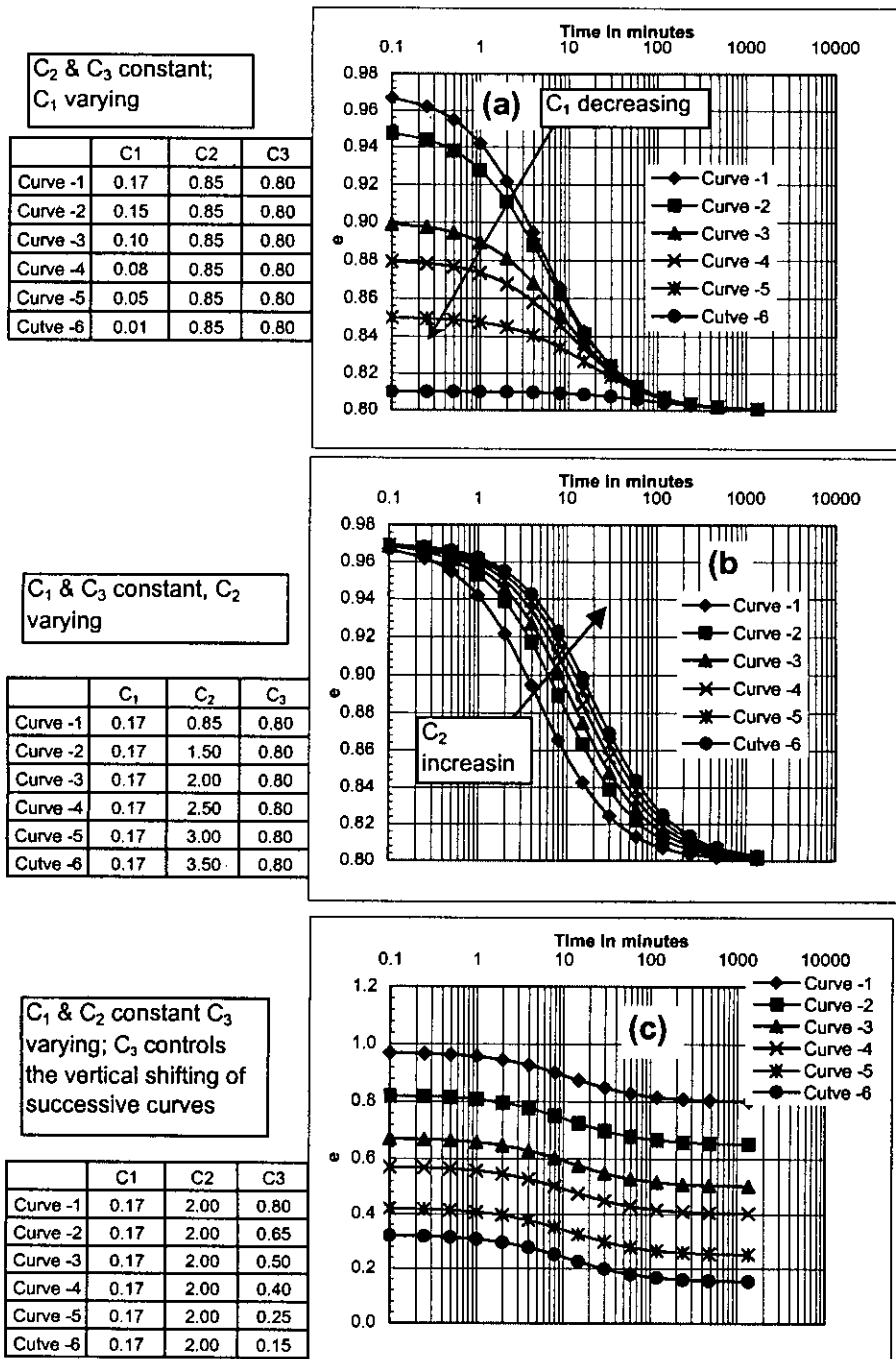|	C1	C2	C3
Curve -1	0.17	2.00	0.80
Curve -2	0.17	2.00	0.65
Curve -3	0.17	2.00	0.50
Curve -4	0.17	2.00	0.40
Curve -5	0.17	2.00	0.25
Cutve -6	0.17	2.00	0.15

Fig.5.8 Plots showing the effect of variation of a single parameter on e~log(t) rel
(a) C_2& C_3 constant, C_1 varying (b) C_1 & C_3 constant, C_2 varying varyin
(c) C_1 & C_2 constant, C_3 varying.

61

In Fig.5.7c and Fig.5.8c curves parameter $C_1=0.17$ and $C_2=2$ for all the curves whereas C_3 is varied from 0.8 to 1.5. As can be found from equation 5.4 e-C_3 ($=1/(1/C_1+t/C_2)$) is same for any t what ever is the value of C_3. Therefore, the curves e-C_3 vs log(t) coincides for different values of C_3 (Fig.5.7c). The effect on the successive e~log(t) curves is that they are identical in shape and shifted downward in parallel by the amount of C_3 (Fig.5.8c).

5.4 Determination of the model parameters

The model parameters C_1, C_2 and C_3 for any load increment may be determined in any of the three ways described below:

(1) First determine C_3 as the final void ratio at a load increment. Plot $1/(e-C_3)$ vs. t and draw a best-fit straight line. Find the intercept on the ordinate (say m_1). Now compute $C_1=1/m_1$. Determine the slope (say m_2) of the fitted straight line. Now compute $C_2 =1/m_2$.

(2) Determine C_3 as mentioned in (1). Determine C_1 and C_2 by any software with function fitting option (such as in ORIGIN or EXCEL).

(3) From test data plot e-C_3~log(t). Assume certain C_1 and C_2 and calculate e-$C_3=1/(1/C_1+t/C_2)$ and plot it on the same graph. Vary C_1 and C_2 and compare the two curves until a visual best fit is obtained.

In the present analysis the parameters C_1 and C_2 were determined by the 3rd method. The values of the parameters determined for different tests are summarized in Table 5.1 and 5.2 for specimens with 100 kPa and 50 kPa pre-consolidation pressure respectively.

5.5 Steps for numerical implementation of the model

The may be two ways for numerical implementation of the model when the parameters are known. These are :

(a) C_1, C_2 and C_3 known for each load increment. Its implementation is straight forward as individual curves can be obtained by putting the parameters in the desired equation (Eqn.5.4). In this case e~t relations for any pressure (for which C_1, C_2 and C_3 are known) can be obtained without any need of the relationship for the previous load increments. The problem with this method is that the final void ratio on a e~t relation for a particular pressure and the initial void ratio on the e~t relation for the next pressure may not be exactly same. However, this method should reproduce a particular e~t relation and the end void ratio with a greater accuracy. Comparison of

(b) Initial void ratio e_0 known. C_1 and C_2 known for different pressure or as a function of pressure.

(1) For the first load increment compute $(C_3)_{\sigma'1} = e_0 - (C_1)_{\sigma'1}$; here $(C_3)_{\sigma'1}$ and $(C_1)_{\sigma'1}$ refer to the values of C_3 and C_1 for pressure σ'_1.

(2) Obtain e for different values of t and plot e~log(t) for pressure σ'_1

(3) Determine $(e_f)_{\sigma'1} = 1 / [1/(C_1)_{\sigma'1} + t_f/(C_1)_{\sigma'1}] + (C_3)_{\sigma'1}$

(4) To obtain the e~t plots for the next pressure σ'_2 take $(e_0)_{\sigma'2} = (e_f)_{\sigma'1}$ and repeat steps (1) to (3).

Ideally the value of t_f in step 3 should be infinity. However, for practical purposes a large value may be used. In this approach the problem of method (a) is eliminated and the final void ratio for any pressure is same to the initial void ratio for the next pressure. However, in this approach errors accumulate and the deviations from test data increases for higher pressure level.

5.6 Comparison between test data and back calculation using model

e~log(t) relations

Figs.5.9 is provided to show comparison of e vs. log(t) relations from test data (test designation P100T06) and that calculated using the model and the parameters mentioned in Tables 5.1 and 5.2. In these figures the approach used for back calculation using the model is the one mentioned in step (a) in article 5.5. Fig.5.10 shows similar comparison using approach (b) stated in article 5.5. Plots for similar

comparisons between test data and back calculated data using model approach (a) and (b) (article 5.5) for all tests are given in Appendix.A.

The e~log(t) curves obtained by approach (a) shows excellent matching with the test data (Figs.5.9). However, for approach (b) the curves from the model underestimate the void ratio at any particular time and this error is cumulative as explained in article 5.5. Therefore, deviations from test data increased for e~log(t) curves of lower σ' to higher σ' for approach (b) (Fig.5.10).

e~log(σ') relations

Comparison of e~log(σ') relations from test data (test designation P100T02) and those obtained from model is made in Figs.5.11 and 5.12 for model approach (a) and (b) respectively. In these figures also, it is observed that model approach (a) has reproduced the e~log(σ') relations with great accuracy (Fig.5.11). The nature of deviation from test data for approach (b) (Fig.5.12) is the same as mentioned for e~log(t) relations above.

5.7 Variation of model parameters

Attempt has been made to reveal the trend, if any exists, of variation of the model parameters with pressure level and pressure increment ratio so that the parameters can be expressed as functions of effective pressure σ' i.e. $C_1=C_1 f(\sigma')$, $C_2=C_2 f(\sigma')$ and $C_3=C_3 f(\sigma')$. Typical variation of parameters C_1, C_2 and C_3 with σ' are shown in Fig.5.13a, Fig.5.13b and Fig.5.13c respectively. From Fig.5.13a it is observed that C_1 increases up to a certain effective pressure, reaches a peak and then decreases. C_2 has the same trend (Fig.5.13b) as C_1. However C_3 continuously decreases with effective pressure (Fig.5.13c), initially at a faster rate up to the pressure level where C_1 and C_2 reaches the peak and then also decreases but a slower rate.

Plots of C_1, C_2 and C_3 in linear, semi-log and log-log scale for all tests are provided in Appendix.B.

64

Table 5.1 : Values of model parameters C_1, C_2 and C_3 from consolidation tests for specimens with 100 kPa pre-consolidation pressure.

Test desig-nation	Press-ure (kPa)	C_1	C_2	C_3	Test desig-nation	Press-ure (kPa)	C_1	C_2	C_3
P100T01	12.5	0.016	0.850	0.904	P100T05	12.5	0.005	0.100	0.829
	25.0	0.006	0.070	0.896		50.0	0.030	1.050	0.784
	50.0	0.008	0.200	0.884		200.0	0.180	2.500	0.587
	100.0	0.055	1.300	0.820		800.0	0.180	1.800	0.371
	200.0	0.080	1.750	0.732	P100T06	12.5	0.015	0.100	0.747
	400.0	0.090	1.500	0.634		50.0	0.055	1.700	0.685
	800.0	0.080	1.800	0.545		200.0	0.155	2.500	0.453
	1600.0	0.080	1.500	0.458		800.0	0.145	1.800	0.280
P100T02	12.5	0.014	0.500	0.851	P100T07	25.0	0.017	0.300	0.764
	25.0	0.016	1.050	0.832		100.0	0.055	1.700	0.695
	50.0	0.035	1.500	0.792		400.0	0.170	2.500	0.457
	100.0	0.058	1.700	0.729		800.0	0.075	1.650	0.373
	200.0	0.067	1.750	0.656	P100T08	25.0	0.015	0.250	0.809
	400.0	0.084	2.000	0.566		100.0	0.083	1.800	0.717
	800.0	0.078	2.000	0.479		400.0	0.181	2.200	0.501
P100T03	50.0	0.023	0.350	0.856		800.0	0.075	1.900	0.419
	100.0	0.042	0.700	0.806	P100T09	25.0	0.020	0.300	0.835
	200.0	0.086	1.400	0.703		50.0	0.029	0.900	0.802
	400.0	0.090	1.800	0.600		100.0	0.061	1.800	0.731
	800.0	0.080	1.400	0.512		200.0	0.070	2.900	0.654
	1600.0	0.105	1.450	0.400		400.0	0.091	2.000	0.554
P100T04	25.0	0.016	0.170	0.837		800.0	0.086	1.700	0.459
	50.0	0.014	0.350	0.818					
	100.0	0.051	1.200	0.756					
	200.0	0.080	2.200	0.661					
	400.0	0.091	2.200	0.557					
	800.0	0.085	1.450	0.463					
	1600.0	0.080	1.450	0.370					

Table 5.2 : Values of model parameters C_1, C_2 and C_3 from consolidation tests for specimens with 50 kPa pre-consolidation pressure.

Test designation	Pressure (kPa)	C_1	C_2	C_3	Test designation	Pressure (kPa)	C_1	C_2	C_3
P50T01	12.5	0.011	0.100	1.013	P50T06	50.0	0.090	3.000	0.807
	25.0	0.020	1.050	0.984		100.0	0.080	2.500	0.725
	50.0	0.075	1.400	0.902		208.4	0.093	2.200	0.626
	100.0	0.058	1.200	0.837		400.0	0.095	2.700	0.526
	200.0	0.115	2.000	0.710		800.1	0.087	2.000	0.427
	400.0	0.105	2.500	0.596	P50T07	25.0	0.015	0.125	0.936
	800.1	0.090	1.800	0.500		50.0	0.016	0.400	0.914
P50T02	12.5	0.023	0.700	1.056		100.0	0.052	1.600	0.853
	25.0	0.035	1.700	1.019		200.0	0.097	2.500	0.741
	50.0	0.080	3.000	0.935		400.0	0.105	3.000	0.617
	100.0	0.090	2.300	0.840		800.1	0.084	2.200	0.523
	200.0	0.095	2.500	0.734	P50T08	50.0	0.027	0.400	0.811
	400.0	0.105	2.500	0.629		100.0	0.057	2.700	0.742
	800.1	0.060	0.600	0.562		200.0	0.080	3.000	0.654
P50T03	12.5	0.015	0.300	0.919		400.0	0.088	2.500	0.558
	50.0	0.090	1.000	0.804		800.1	0.090	2.600	0.460
	200.0	0.180	1.700	0.582	P50T09	12.5	0.020	0.200	0.903
	800.1	0.180	1.600	0.361		50.0	0.080	1.600	0.798
P50T04	25.0	0.038	0.500	0.961		200.0	0.180	5.000	0.589
	64.0	0.094	2.200	0.857		800.1	0.165	2.400	0.387
	100.0	0.055	3.000	0.795					
	200.0	0.090	2.000	0.699					
	400.0	0.090	2.000	0.602					
	800.1	0.082	1.500	0.511					
P50T05	25.0	0.029	0.400	0.893					
	50.0	0.050	2.300	0.840					
	100.0	0.085	2.500	0.750					
	200.0	0.085	2.500	0.655					
	400.0	0.090	2.500	0.557					
	800.1	0.090	1.500	0.468					
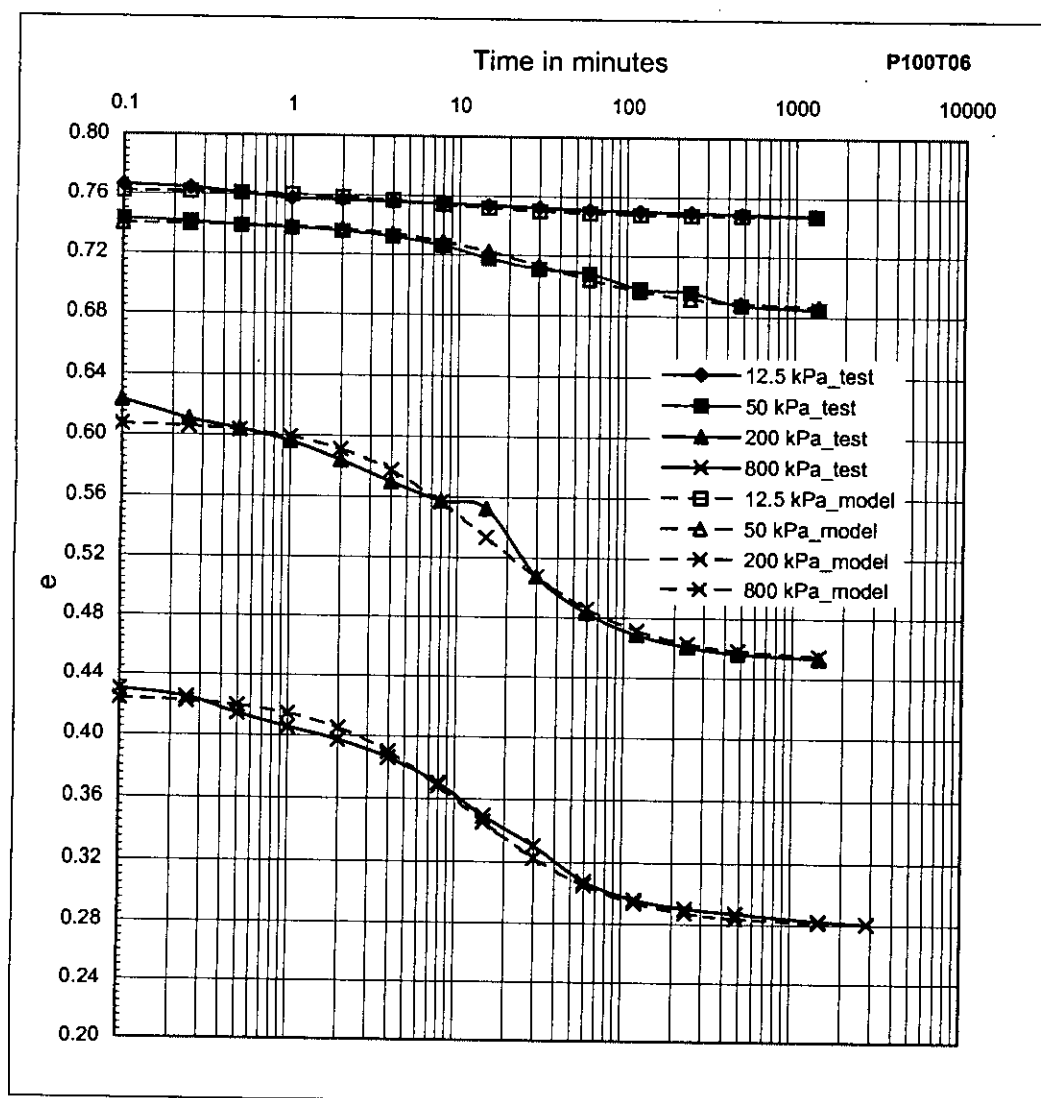
Fig.5.9 Typical comparison of e~log(t) relations between test data and that obtained using the model (method a, article 5.5)
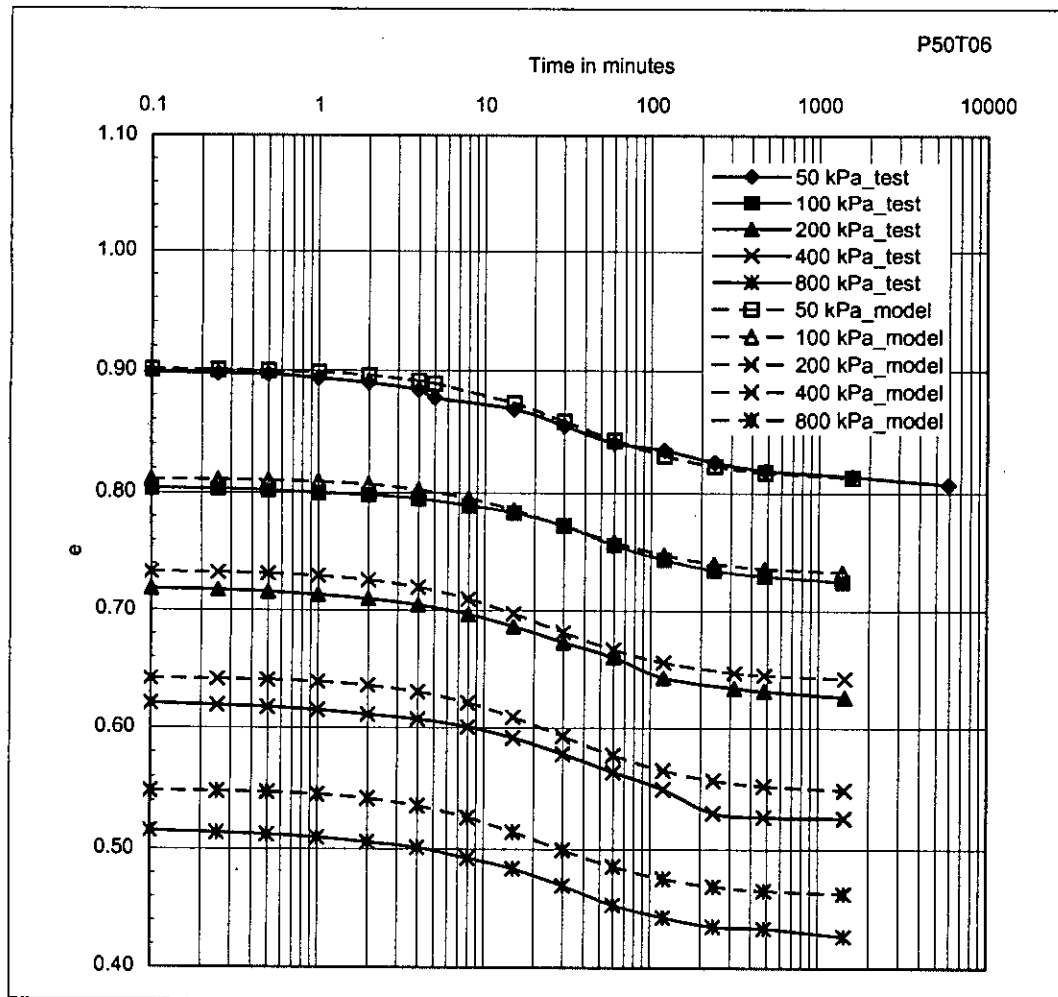
Model-comp_method_a_100

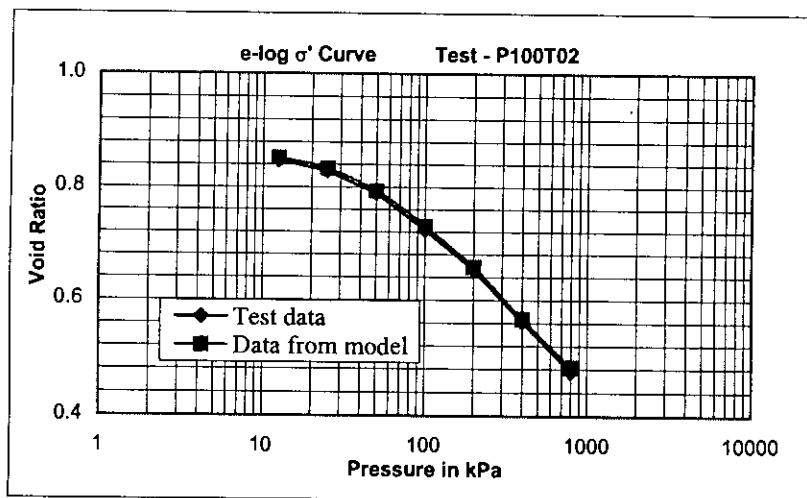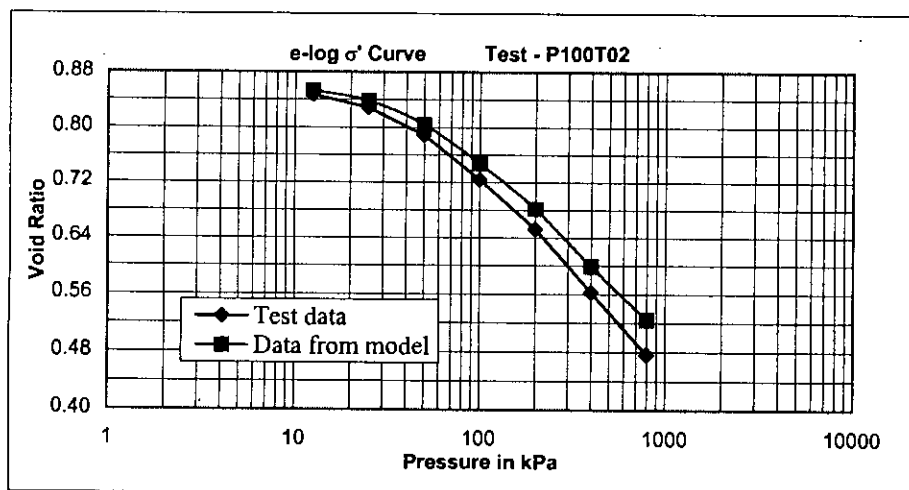Fig.5.10 Typical comparison of e~log(t) relations between test data and that obtained using the model (method b, article 5.5)

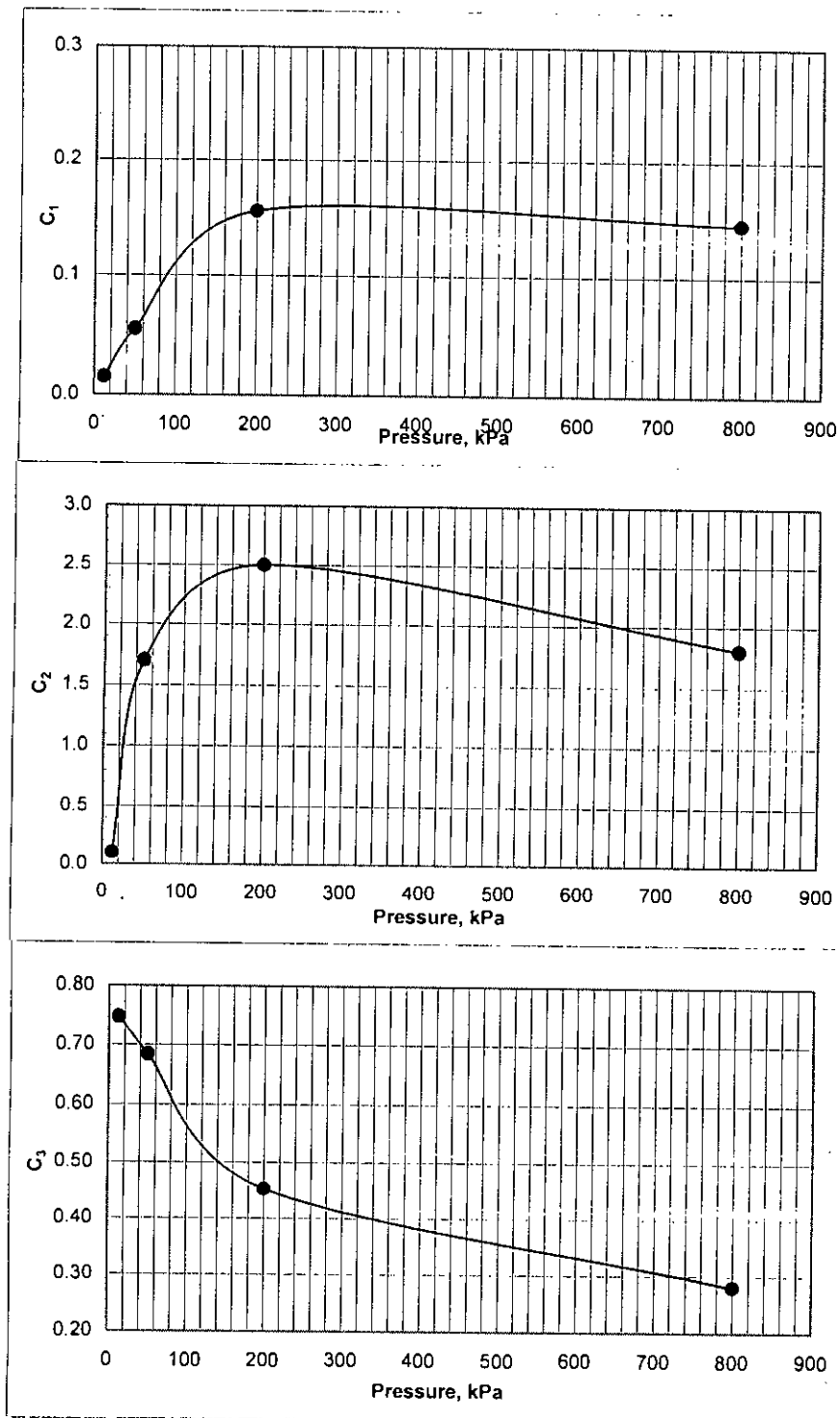Fig.5.11 Typical comparson of e~log(σ') relations between test data and that obtained using the model (method a, article 5.5)

Fig.5.12 Typical comparison of e~log(σ') relations between test data and that obtained using the model for tests (method b, article 5.5)

69

Fig. 5.13 Typical variation of model parameters (a) parameter C1
(b) parameter C2 (c)parameter C3.

Chapter 6

CONCLUSIONS AND RECOMMENDATIONS
FOR FUTURE RESEARCH

6.1 Conclusions

A model has been proposed that can represent the one-dimensional consolidation characteristics of a clay soil. One-dimensional consolidation tests were performed on reconstituted Dhaka clay to verify the model.

The outcome of the research may be summerised as follows:

(1) The mathematical model proposed is $e = 1/(1/C_1+t/C_2)+C_3$, (equation 5.4) which has three parameters C_1, C_2 and C_3.

(2) The significance and role of the parameters is demonstrated through experimental verification using Dhaka clay.

(3) Dependency of the model parameters on pressure level has been demonstrated.

(4) The effect of stress-increment ratio (2 and 4 used in the tests) appeared to have little influence on the model parameters. As such it may be suggested that stress increment ratios of 4 instead of 2 may be used in consolidation tests. However, this requires further investigation with various types of soils.

(5) Two approaches have been described (article 5.5) for the numerical implementation of the model. The effectiveness of these methods in reproducing the e~time and e~σ' relationships, (and therefore determination of parameters such as C_c, c_v) are demonstrated by comparing plots from test data and that generated using the model.

(6) The stress increment ratios employed in the consolidation tests performed, showed no significant effect of on e~log(σ') relations. Any such effect, even if exists, appears to be masked by the usual variations (due to sample disturbance, inhomogeneity etc.) in identical tests on specimens even from the same soil cake.

(7) Values of C_c and C_v are not found to depend on the stress increment ratio employed in the test.

(8) Casagrande's method for prediction of pre-consolidation is verified. Estimated pre-consolidation pressure by Casagrande's method varied from the actual pre-consolidation pressure within a range of 80% to 120%.

71

6.2 Recommendations for future research

This research work aimed to establish a mathematical model to represent the one-dimensional consolidation behaviour of clays. Following are the recommendations for future research works.

(1) The magnitude and nature of variation of the model parameters for different natural soils need to be studied.

(2) Ageing may have significant effect on the consolidation characteristics of clay deposits and it may be investigated using reconstituted and natural soil of different ages.

(3) The proposed model may be implemented numerically by finite element method. The results of settlements and rates of settlements may be compared with field observations.

(4) The model did not consider the effect of secondary consolidation. It may be modified to incorporate the effects of secondary consolidation.

Appendix-A
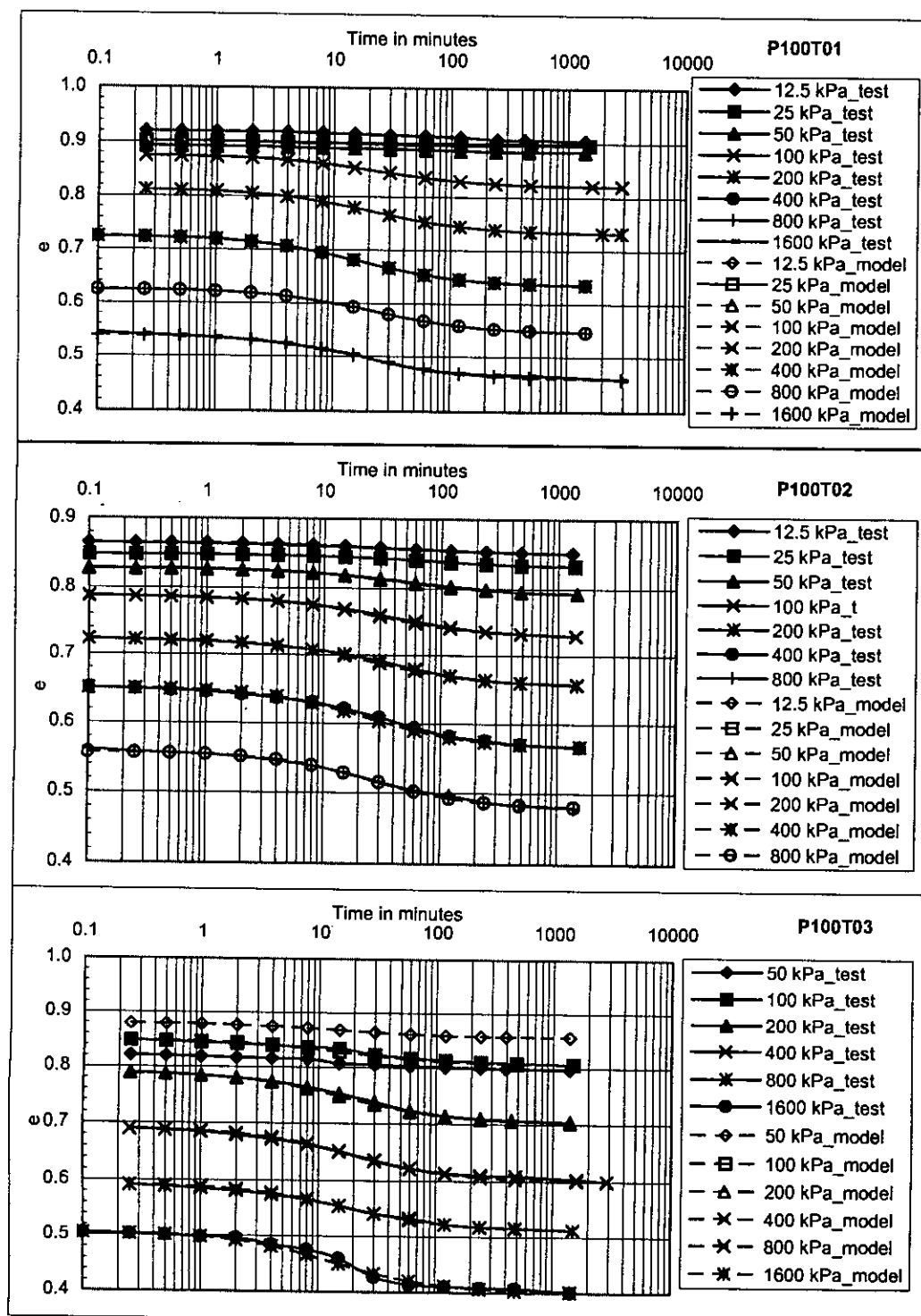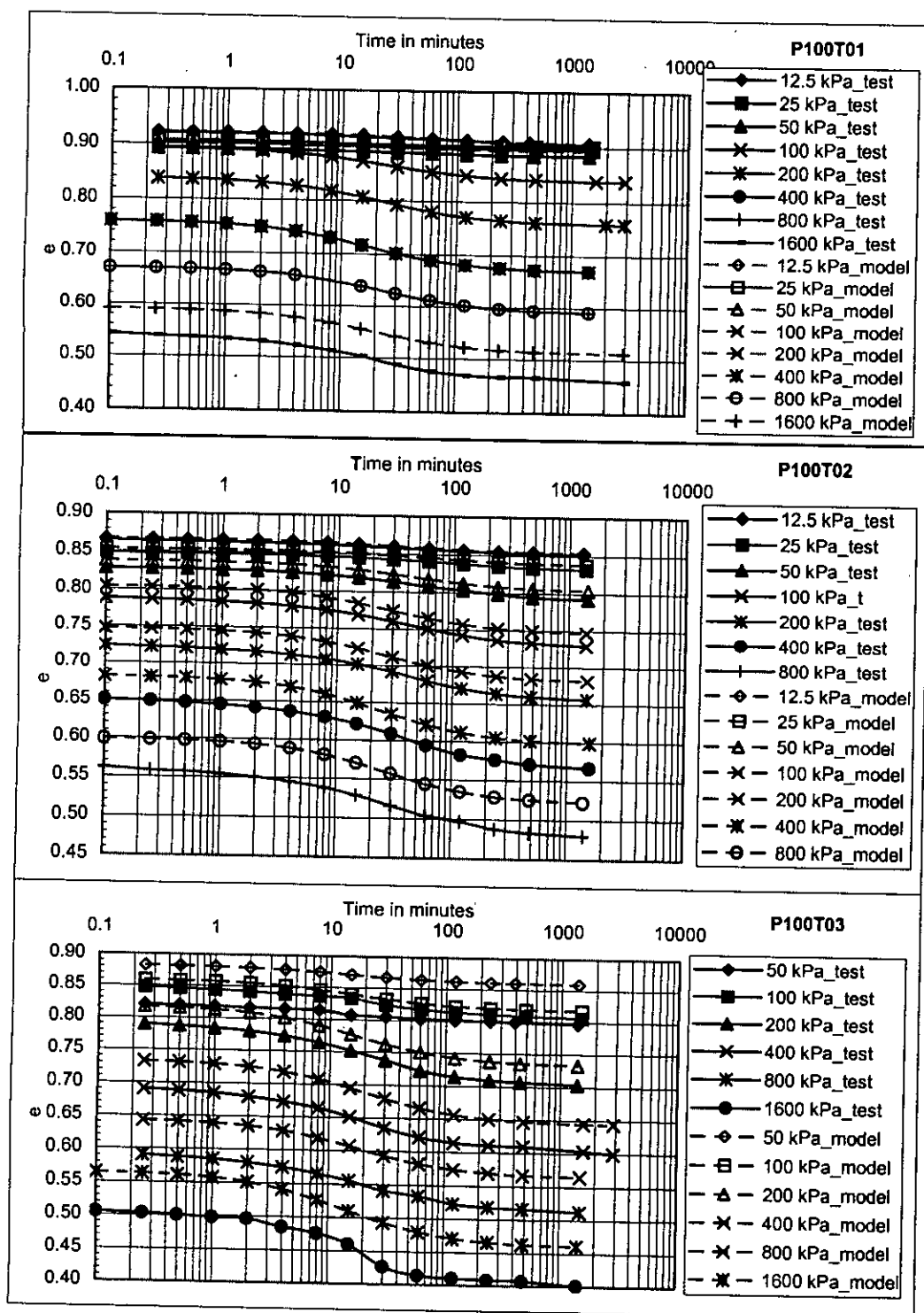
Fig.A.1 Figure comparing e~log(t) relations between test data and that obtained using the model for tests P100T01, P100T02, P100T03 (method a, article 5.5)
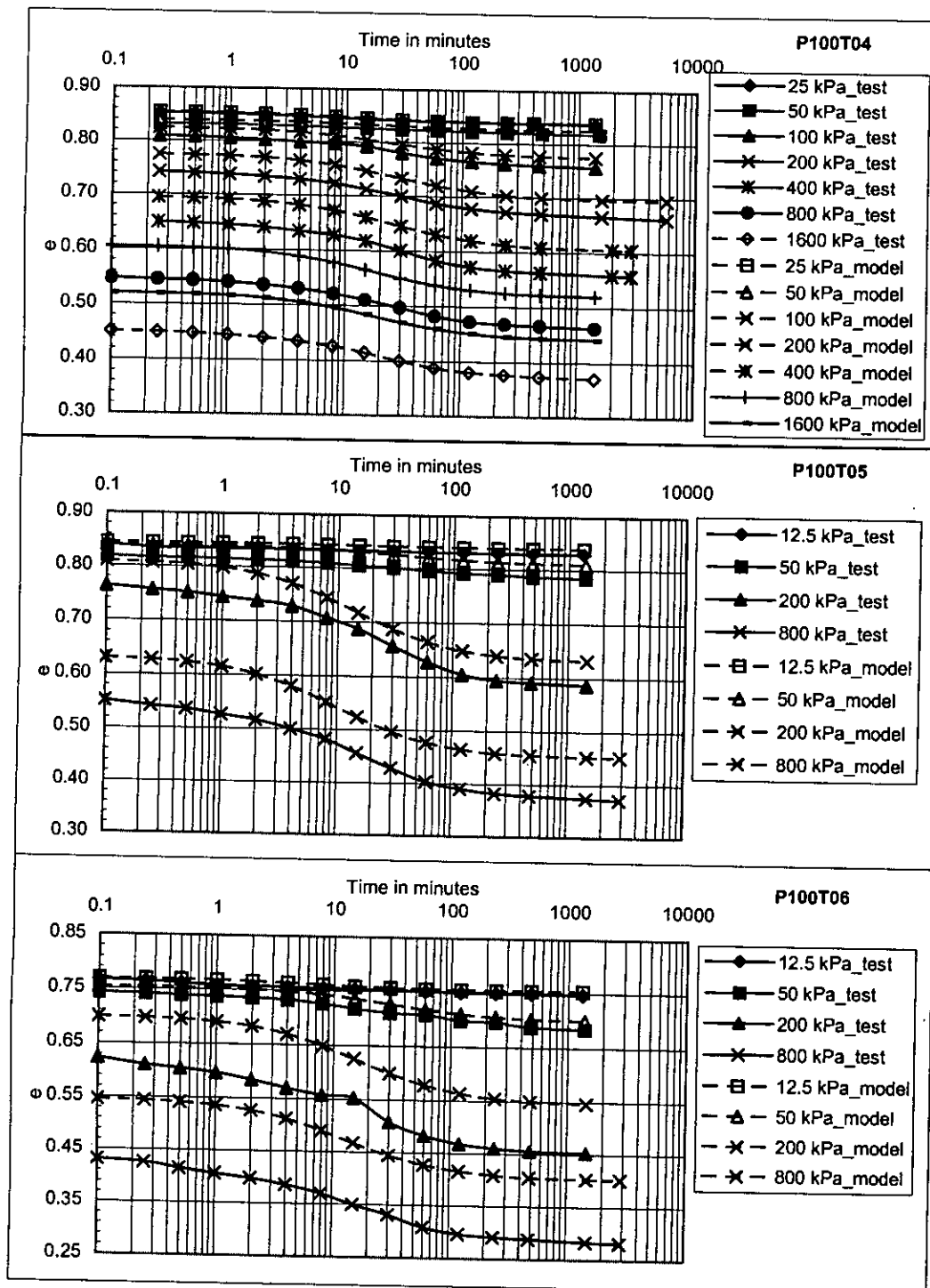
74

Fig.A.2 Figure comparing e~log(t) relations between test data and that obtained using the model for tests P100T04, P100T05, P100T06 (method a, article 5.5)
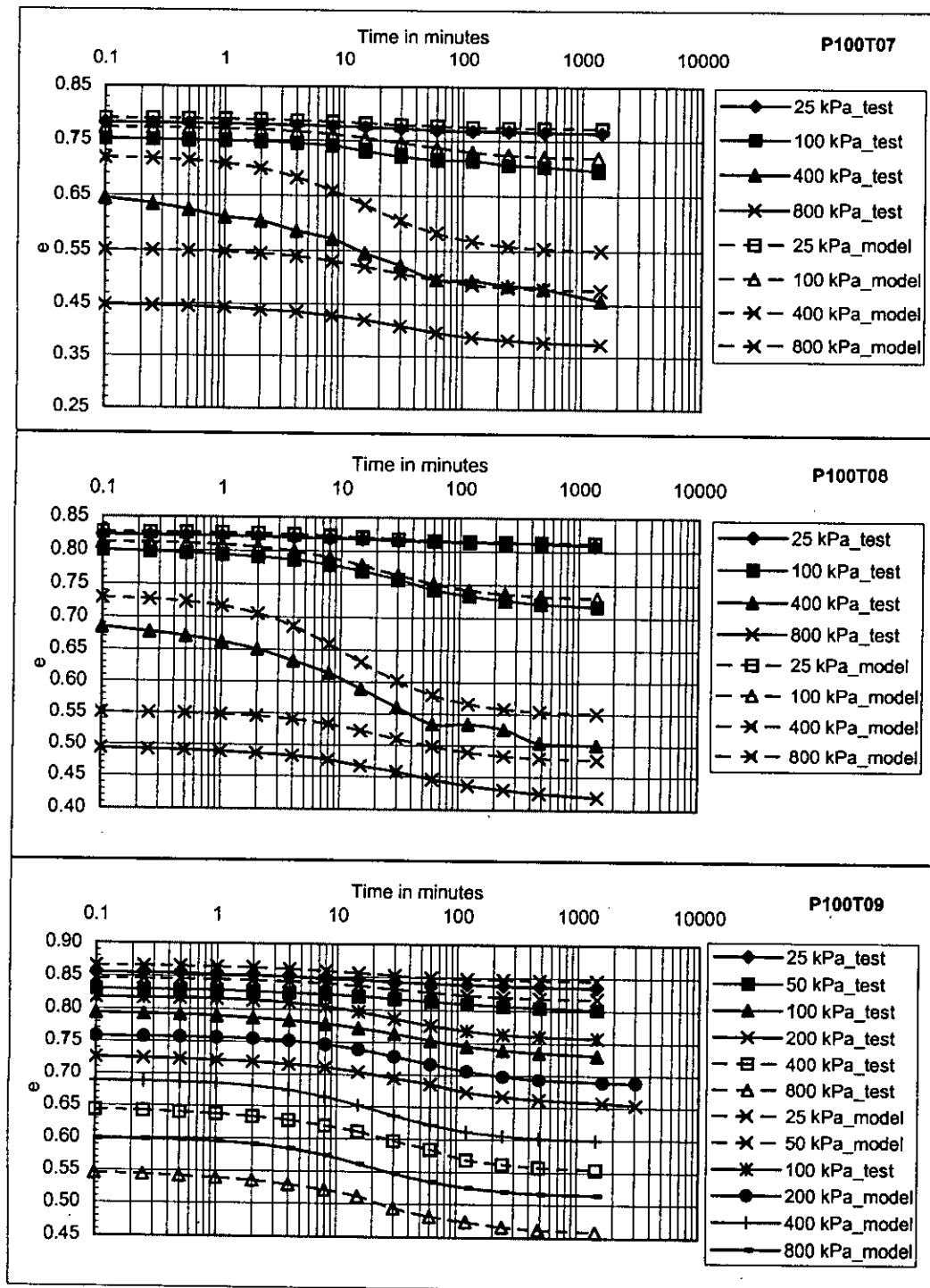
Model-comp_method_a_100

Fig.A.3 Figure comparing e~log(t) relations between test data and that obtained using
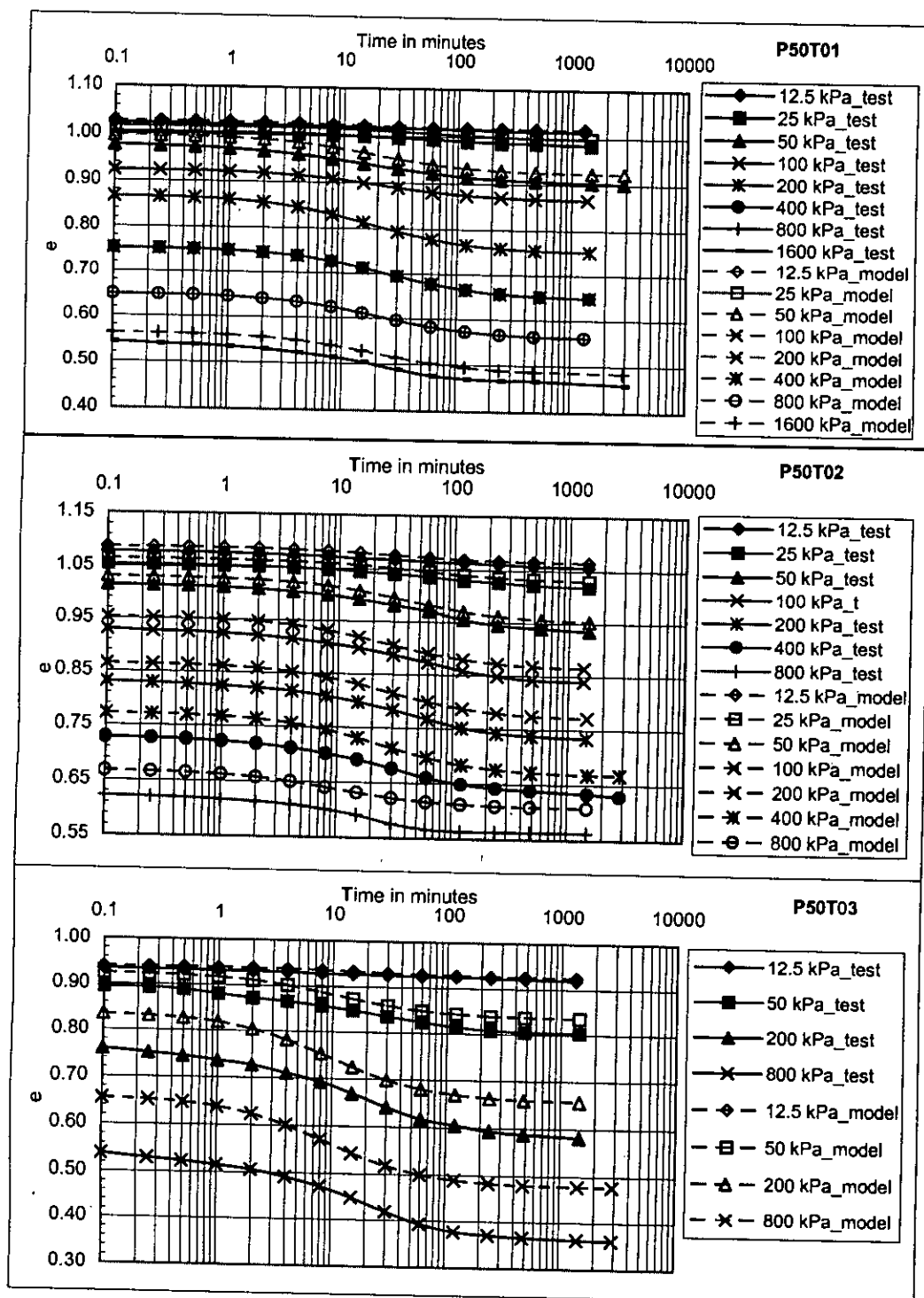the model for tests P100T07, P100T08, P100T09 (method a, article 5.5)

Model-comp_method_a_100

Fig.A.4 Figure comparing e~log(t) relations between test data and that obtained using the model for tests P50T01, P50T02, P50T03 (method a, article 5.5)

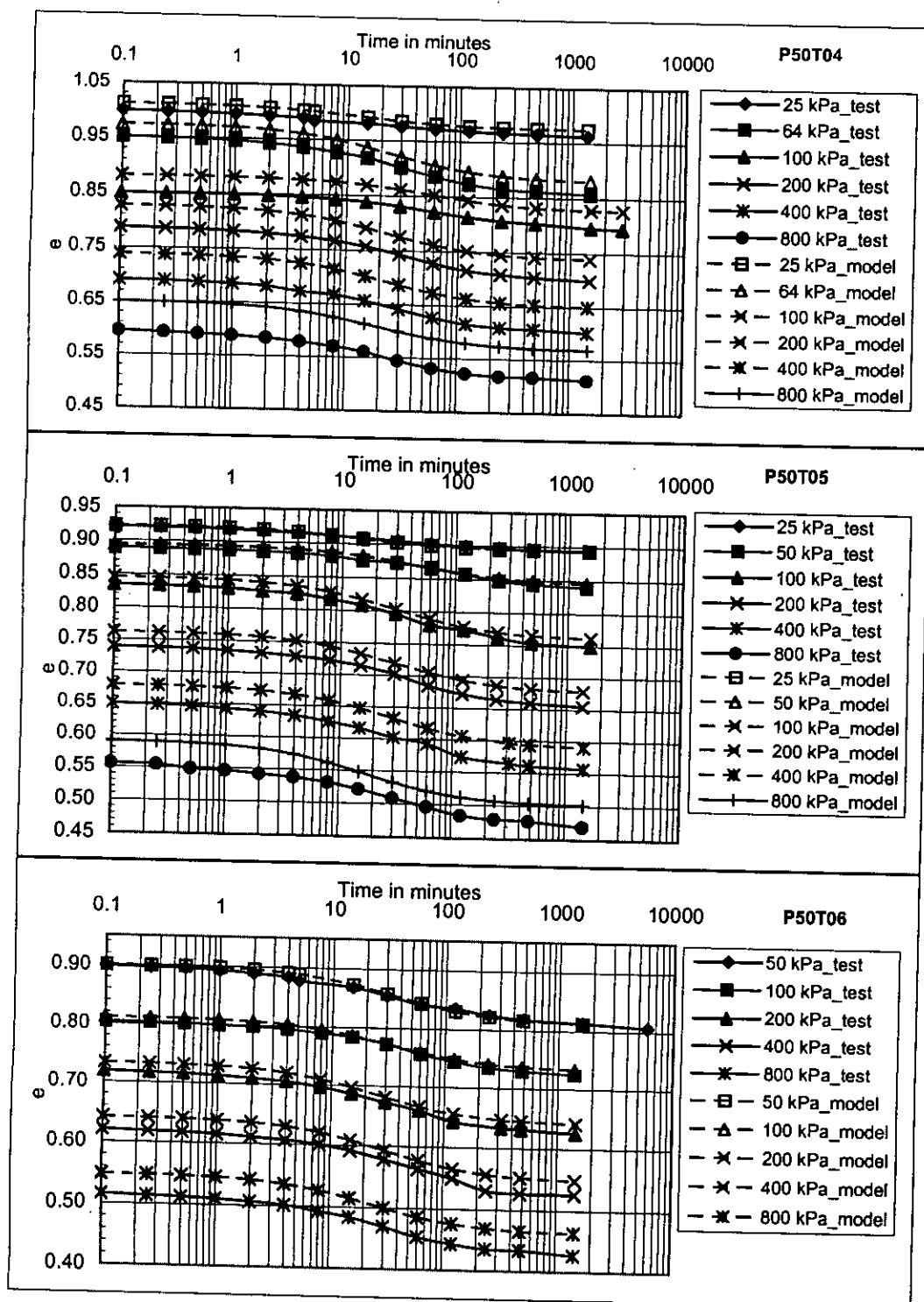Model-comp_method_a_50
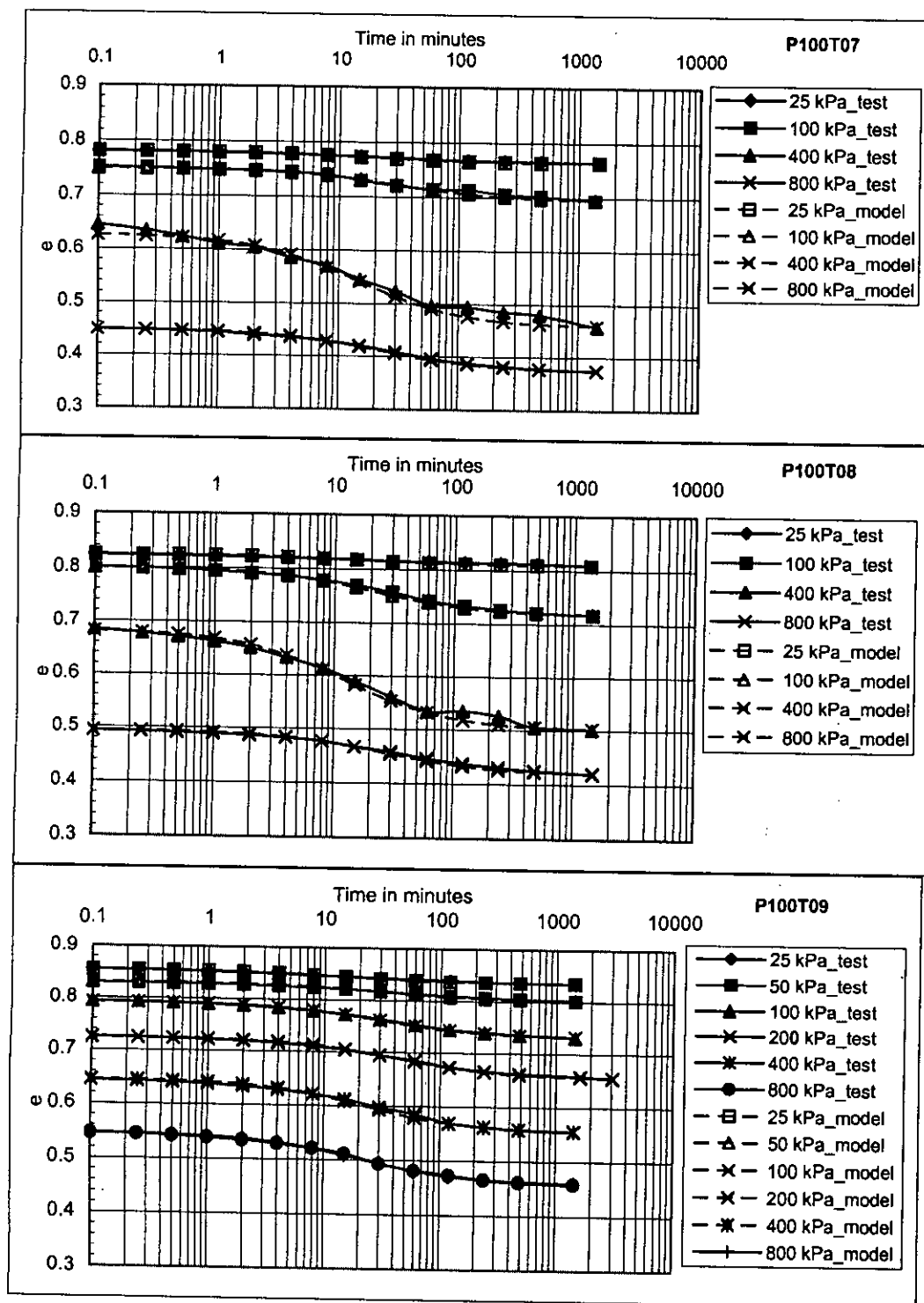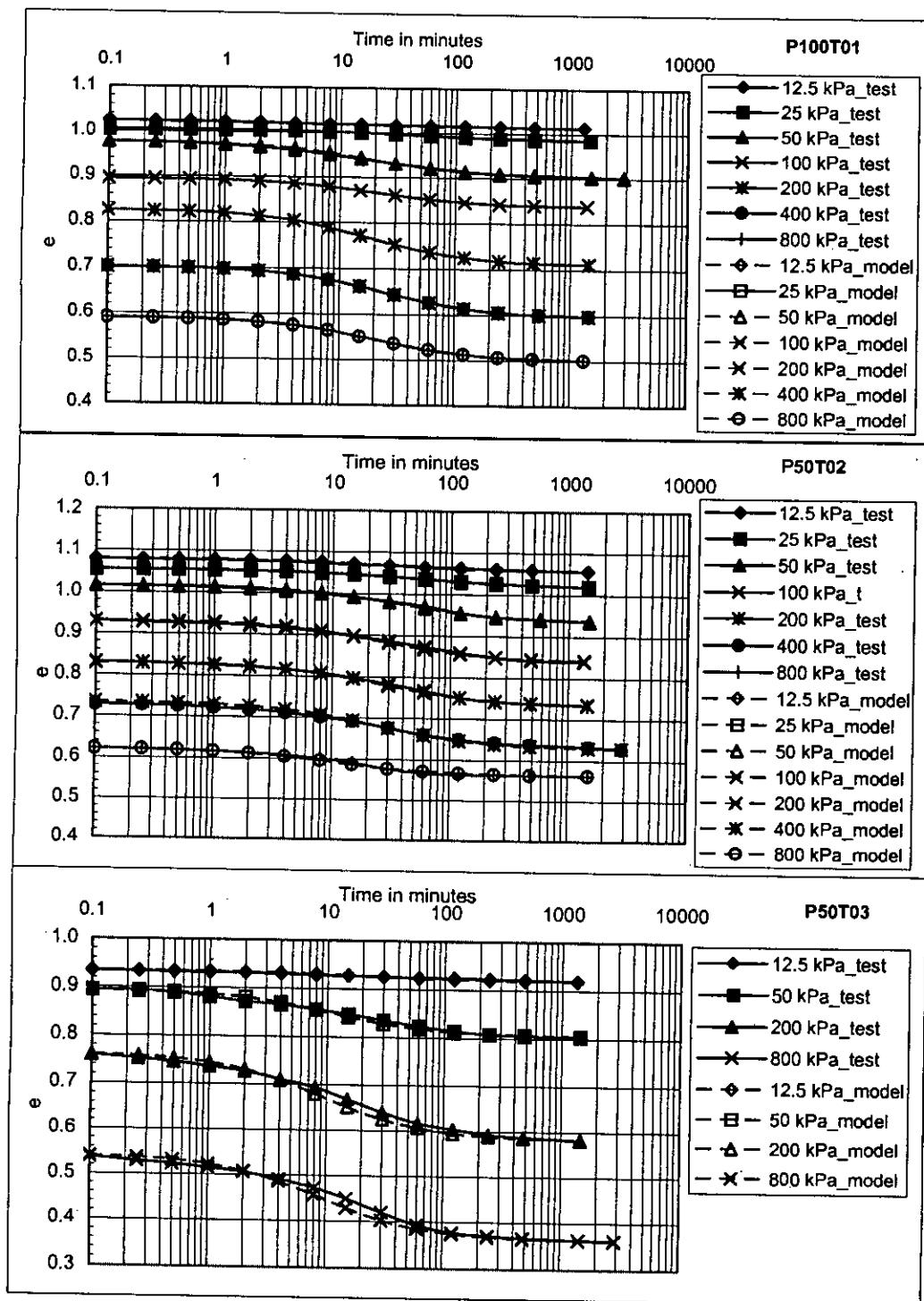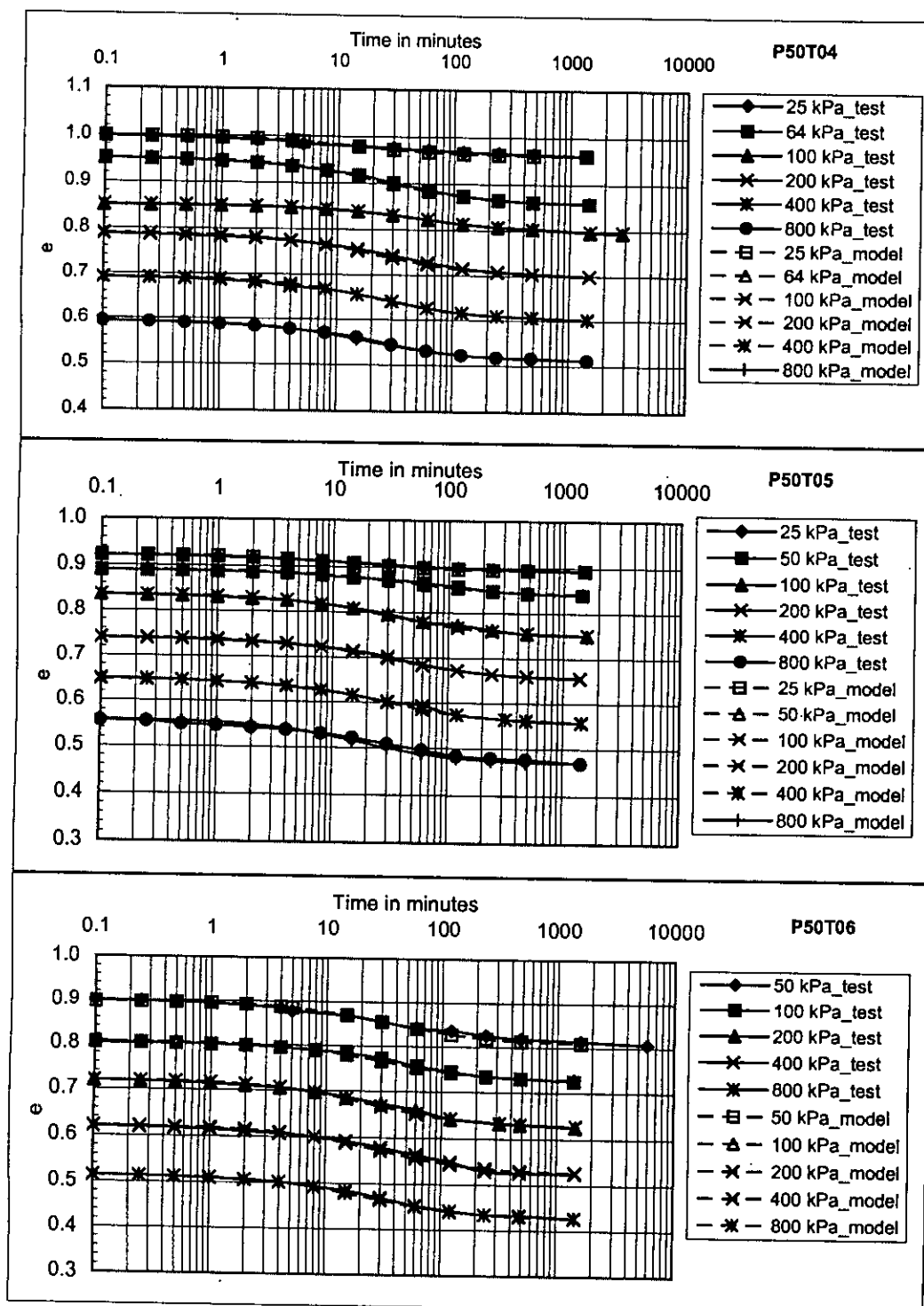
Fig.A.5 Figure comparing e~log(t) relations between test data and that obtained using the model for tests P50T04, P50T05, P50T06 (method a, article 5.5)
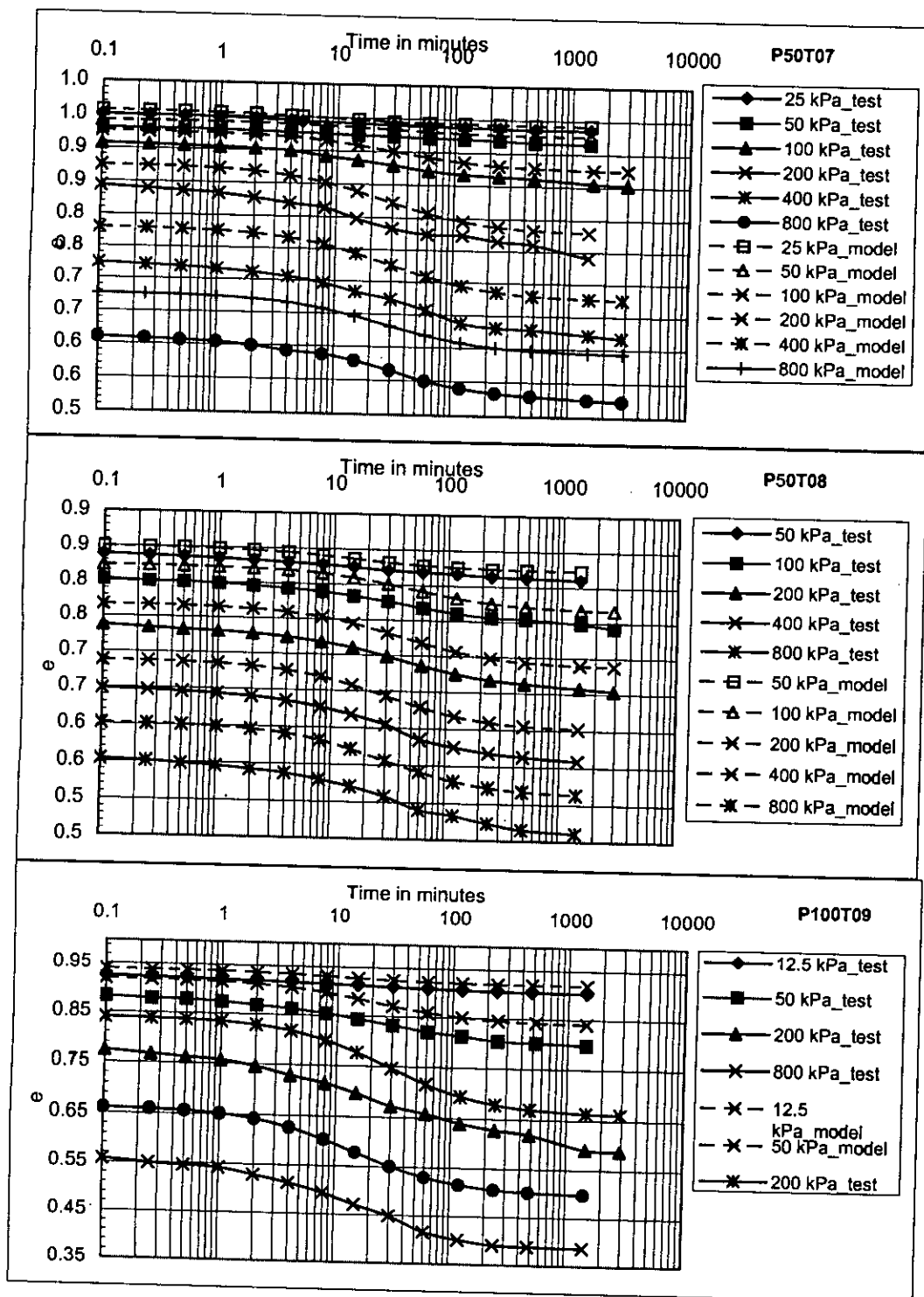
Fig.A.6 Figure comparing e~log(t) relations between test data and that obtained using the model for tests P50T07, P50T08, P50T09 (method a, article 5.5)
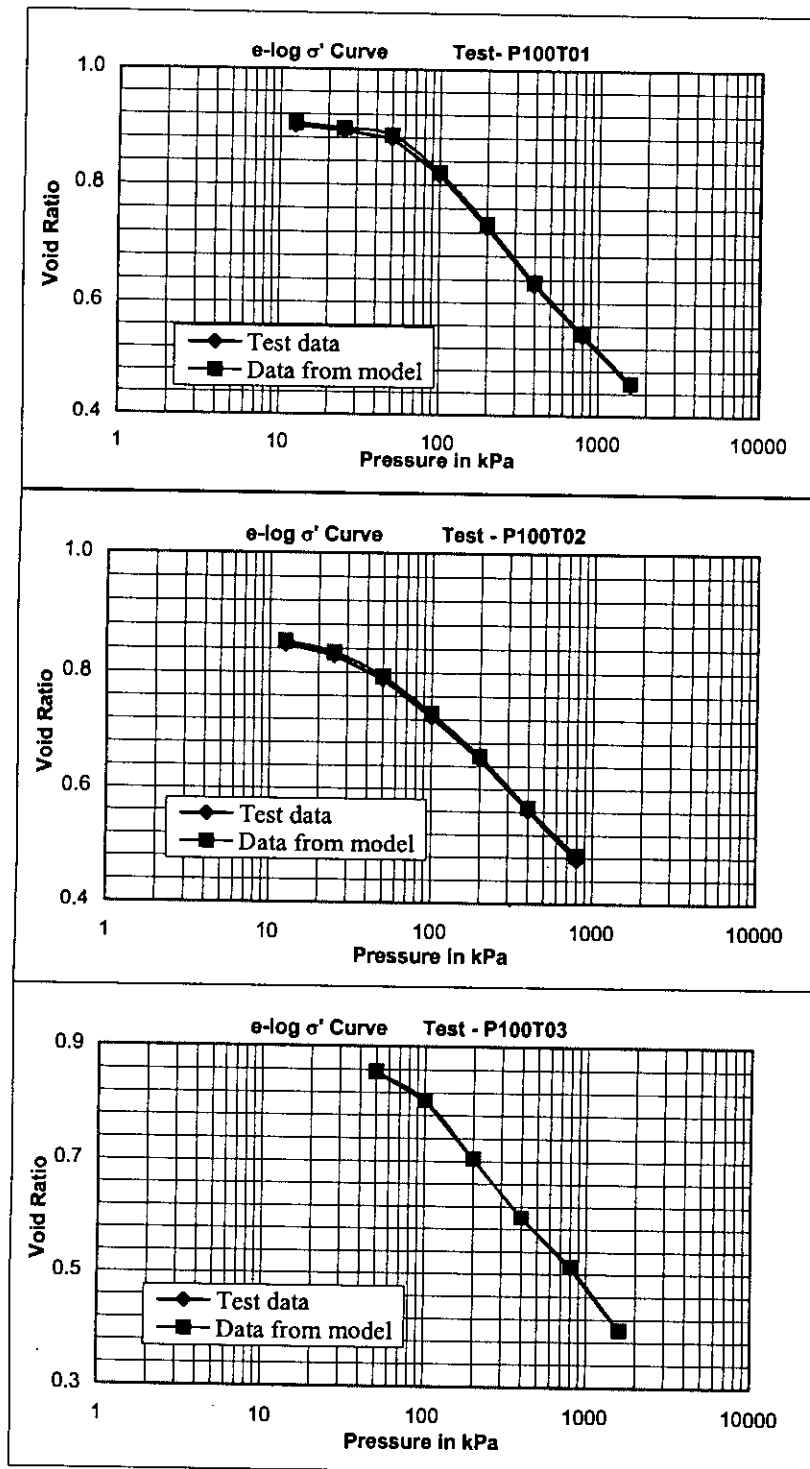
Fig.A.7 Figure comparing e~log(t) relations between test data and that obtained using the model for tests P100T01, P100T02, P100T03 (method b, article 5.5)

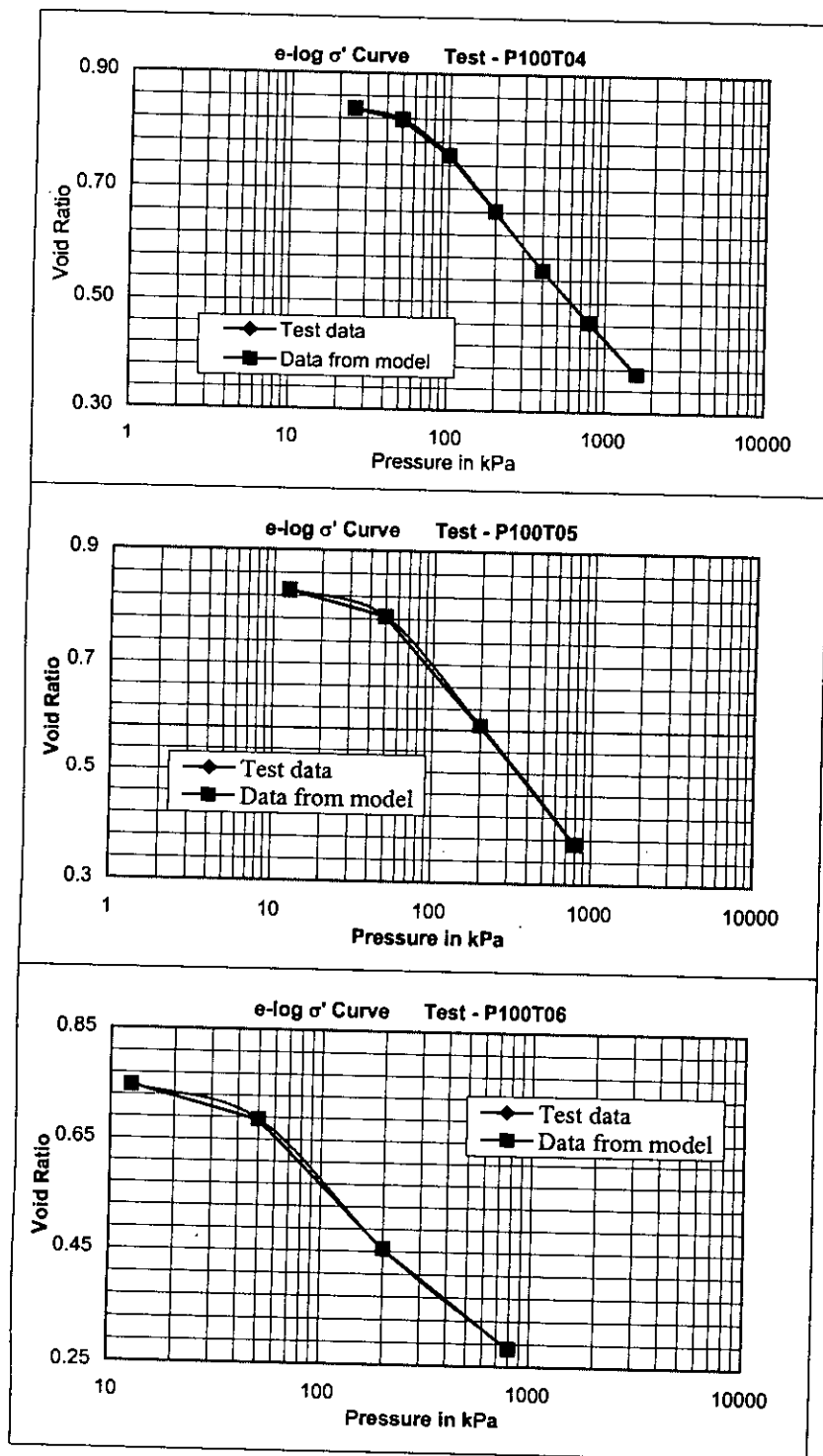Fig.A.8 Figure comparing e~log(t) relations between test data and that obtained using the model for tests P100T04, P100T05, P100T06 (method b, article 5.5)

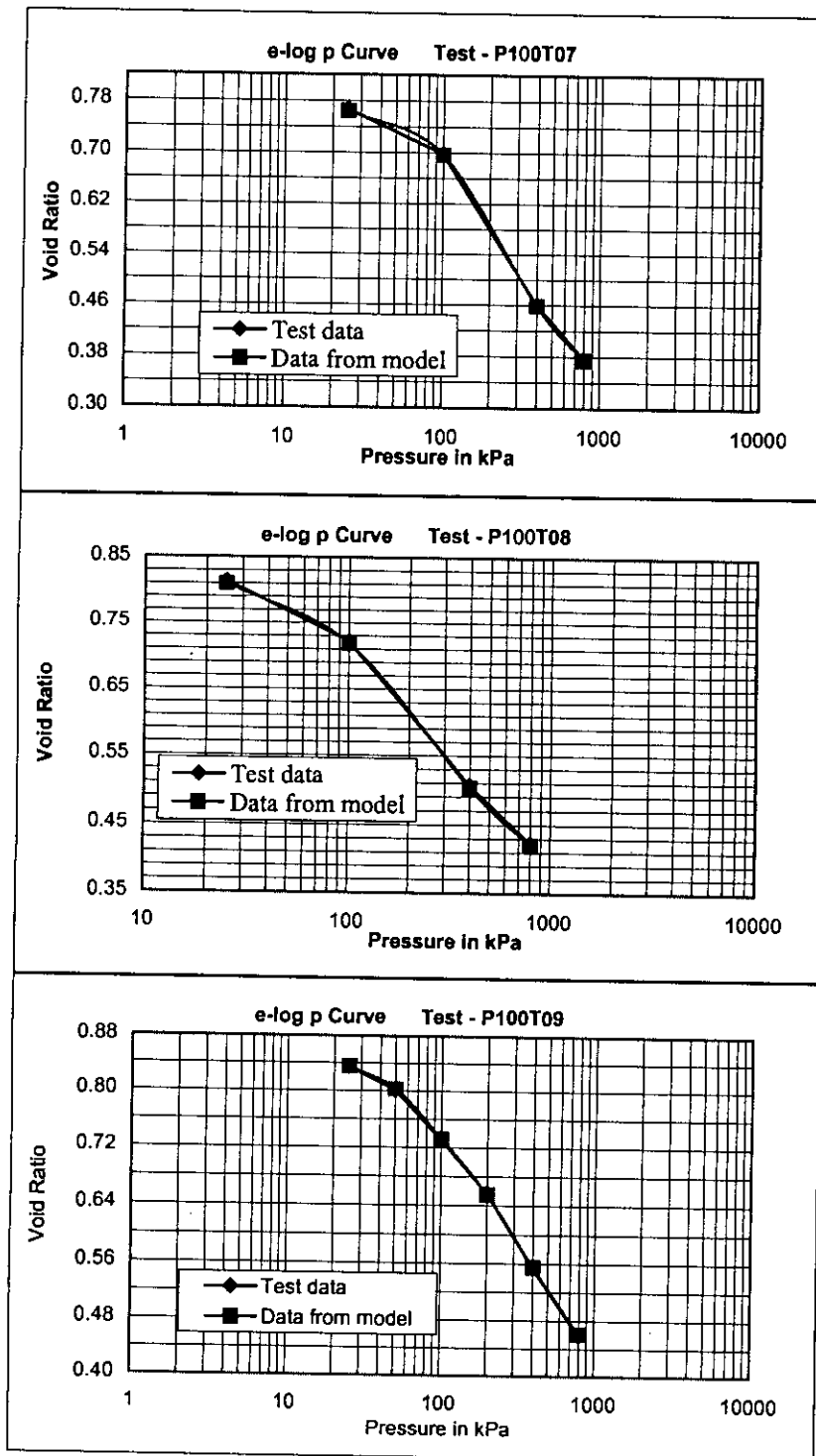Fig.A.9 Figure comparing e~log(t) relations between test data and that obtained using
the model for tests P100T07, P100T08, P100T09 (method b, article 5.5)

Model-comp_method_b_100

Fig.A.10 Figure comparing e~log(t) relations between test data and that obtained using the model for tests P50T01, P50T02, P50T03 (method b, article 5.5)

Model-comp_method_b_50

Fig.A.11 Figure comparing e~log(t) relations between test data and that obtained using the model for tests P50T04, P50T05, P50T06 (method b, article 5.5)
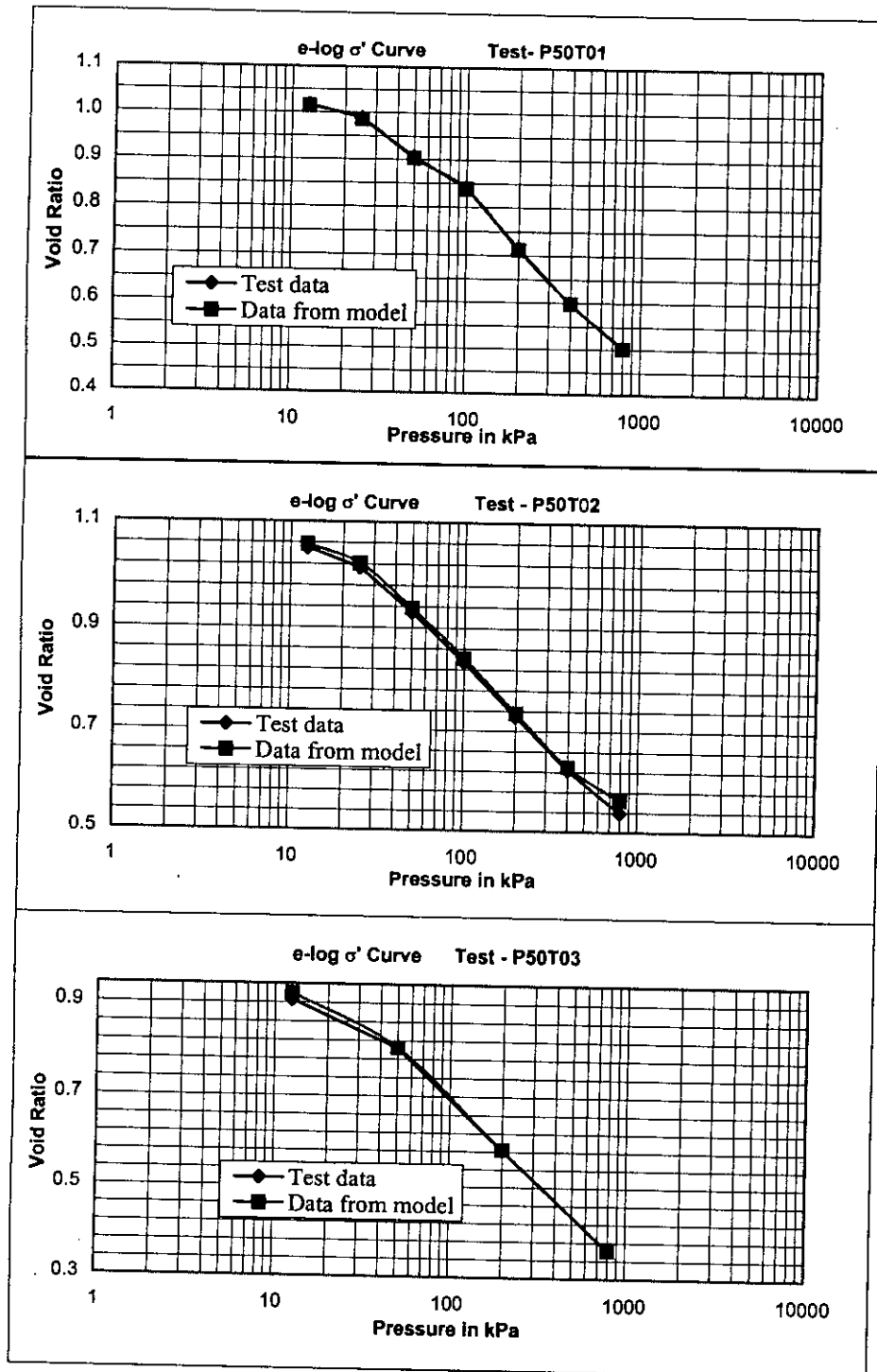
Model-comp_method_b_50

Fig.A.12 Figure comparing e~log(t) relations between test data and that obtained using the model for tests P50T7, P50T08, P50T09 (method b, article 5.5)

Model-comp_method_b_50
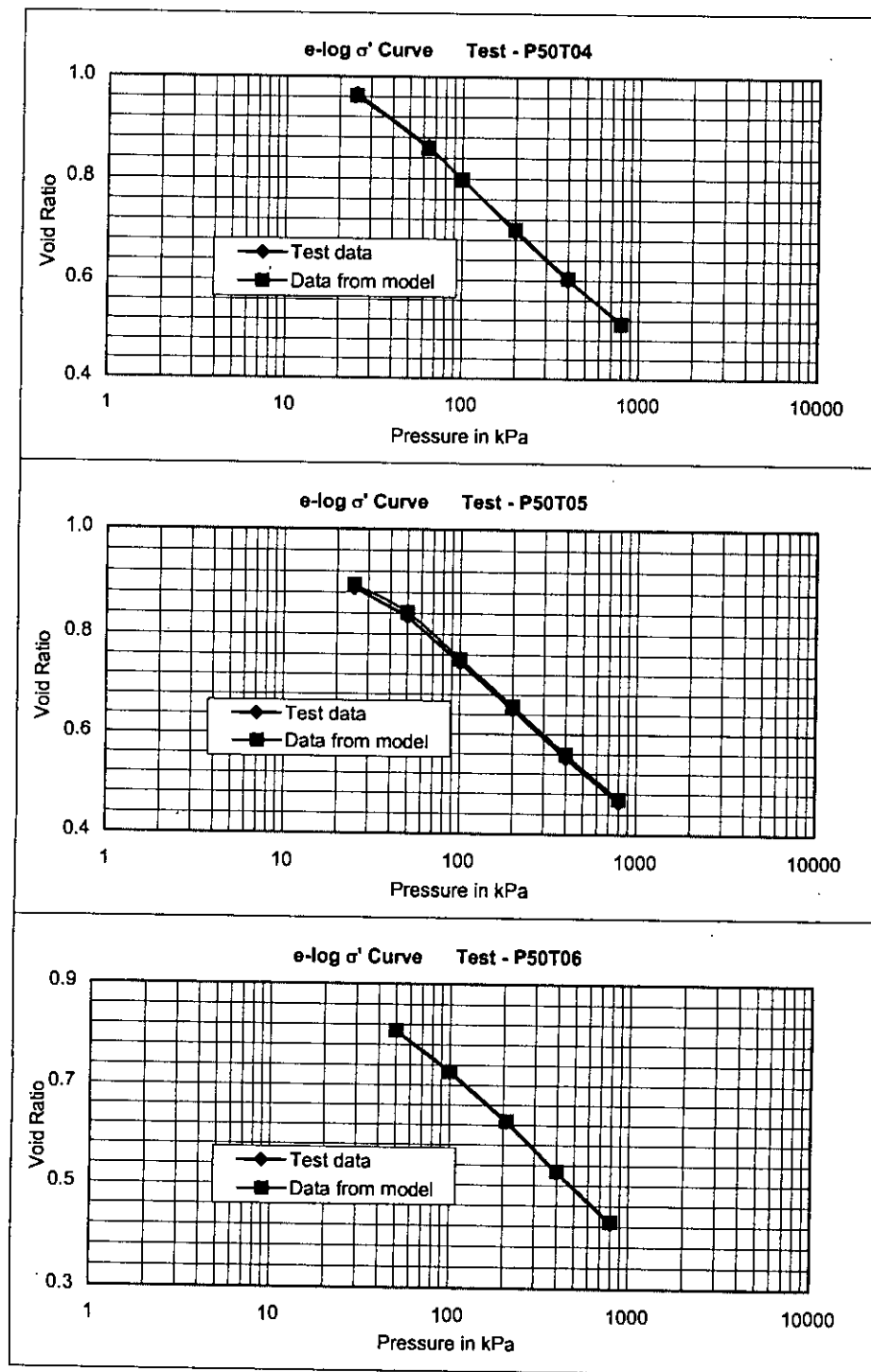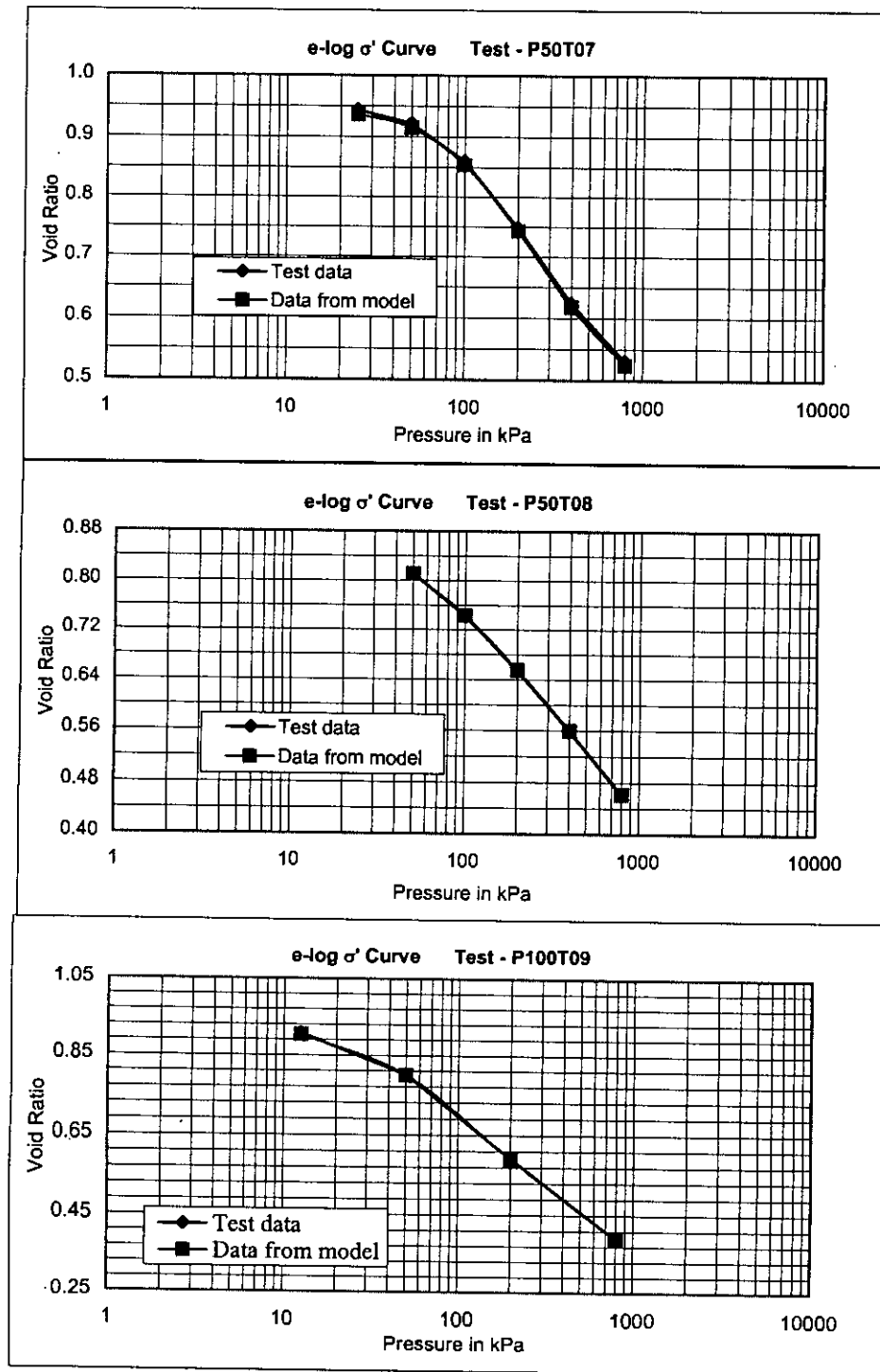
Fig.A.13 Figure comparing e~log(σ') relations between test data and
that obtained using the model for tests P100T01, P100T02
P100T03 (method a, article 5.5)

Model-comp_method_a_100

Fig.A.14 Figure comparing e~log(σ') relations between test data and
that obtained using the model for tests P100T04, P100T05
P100T06 (method a, article 5.5)

Fig.A.15 Figure comparing e~log(σ') relations between test data and
that obtained using the model for tests P100T07, P100T08
P100T09 (method a, article 5.5)

Fig.A.16 Figure comparing e~log(σ') relations between test data and that
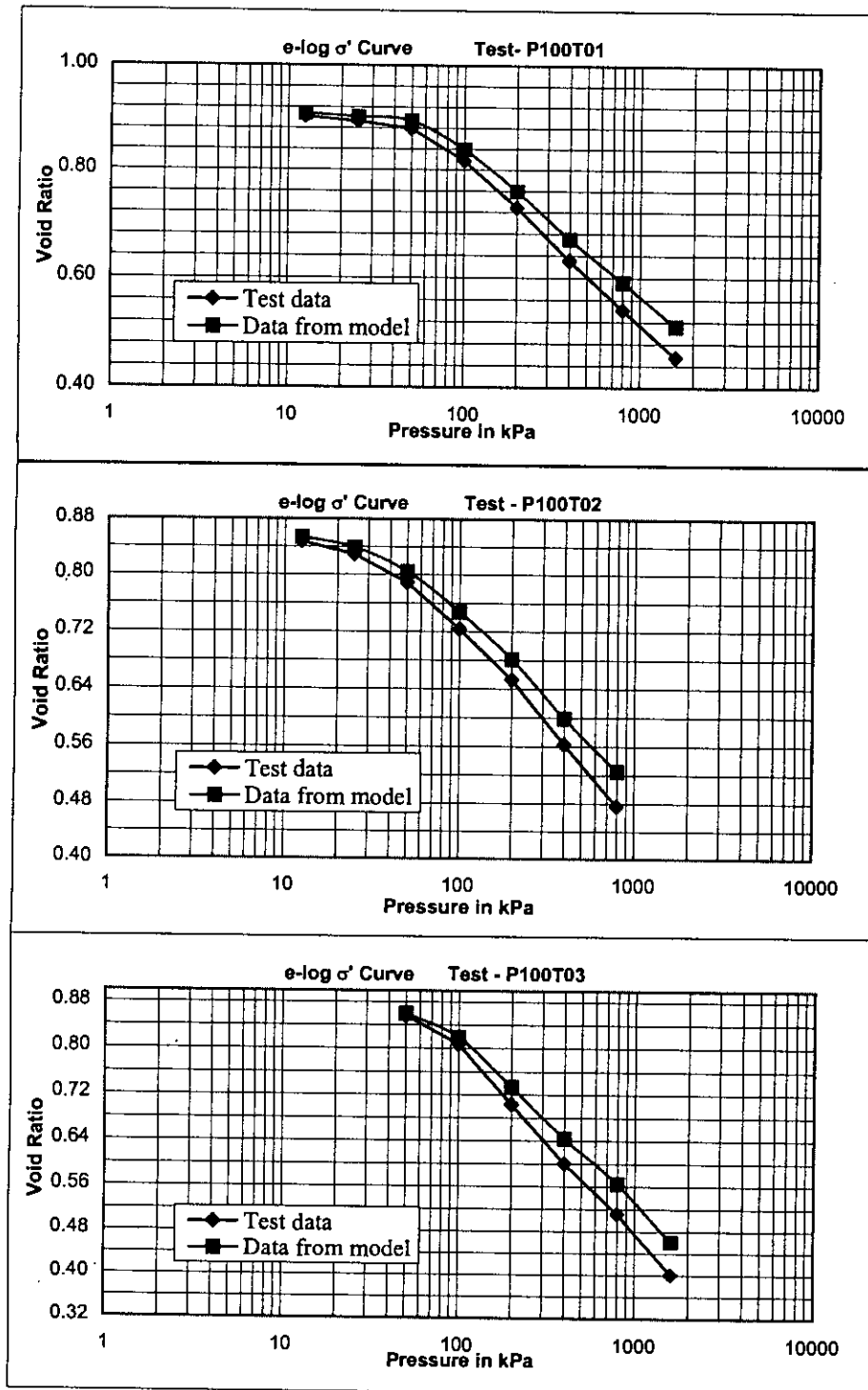obtained using the model for tests P50T01, P50T02, P50T03
(method a, article 5.5)

Model-comp_method_a_50
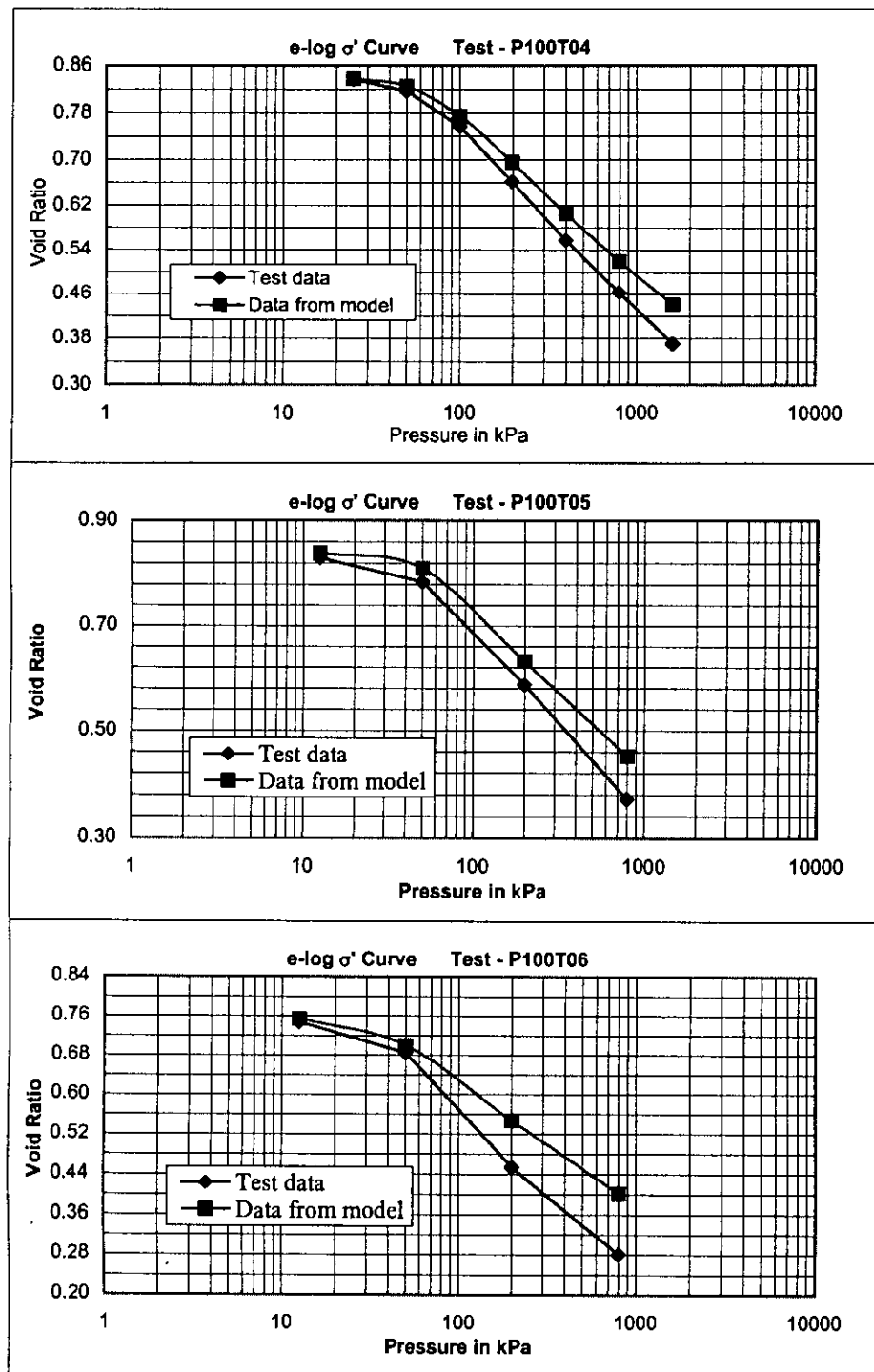
Fig.A.17 Figure comparing e~log(σ') relations between test data and that
obtained using the model for tests P50T04, P50T05, P50T06
(method a, article 5.5)

Model-comp_method_a_50

Fig.A.18 Figure comparing e~log(σ') relations between test data and that
obtained using the model for tests P50T07, P50T08, P50T09
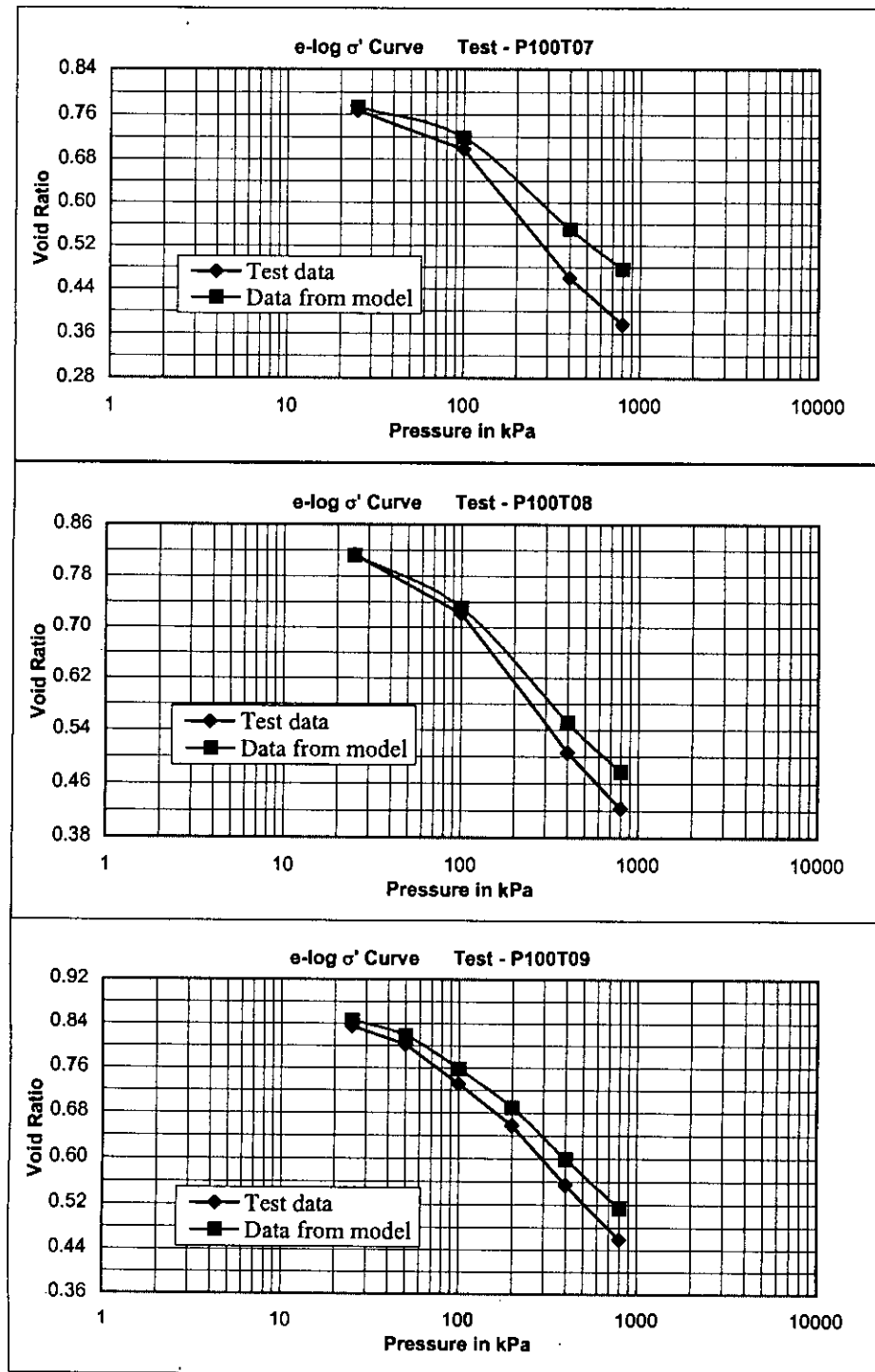(method a, article 5.5)

Model-comp_method_a_50

Fig.A.19 Figure comparing e~log(σ') relations between test data and that
obtained using the model for tests P100T01, P100T02, P100T03
(method b, article 5.5)

Model-comp_method_b_100

Fig.A.20 Figure comparing e~log(σ') relations between test data and that
obtained using the model for tests P100T04, P100T05, P100T06
(method b, article 5.5)

Fig.A.21 Figure comparing e~log(σ') relations between test data and that
obtained using the model for tests P100T07, P100T08, P100T09
(method b, article 5.5)

94
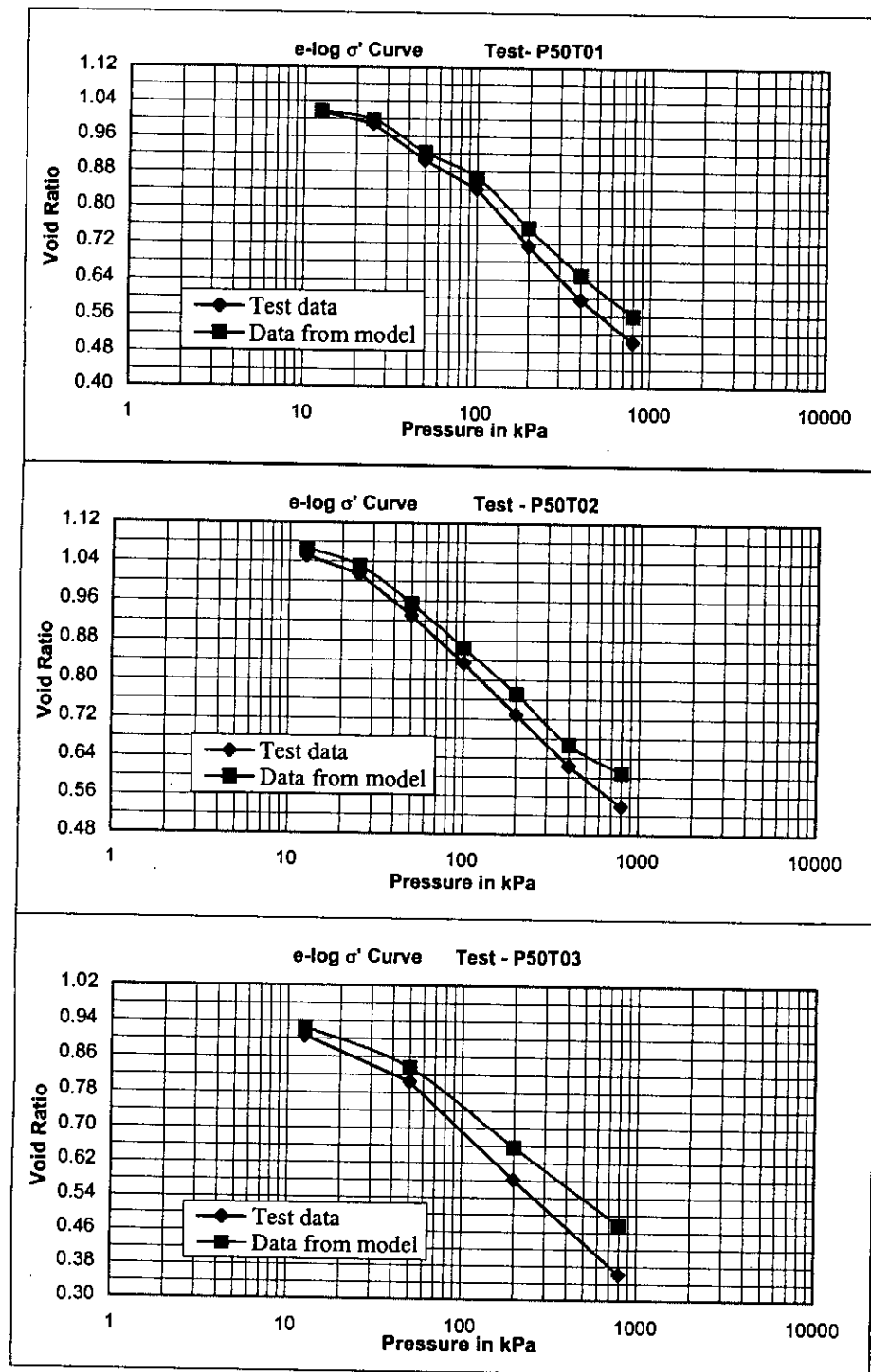
Fig.A.22 Figure comparing e~log(σ') relations between test data and that
obtained using the model for tests P50T01, P50T02, P50T03
(method b, article 5.5)

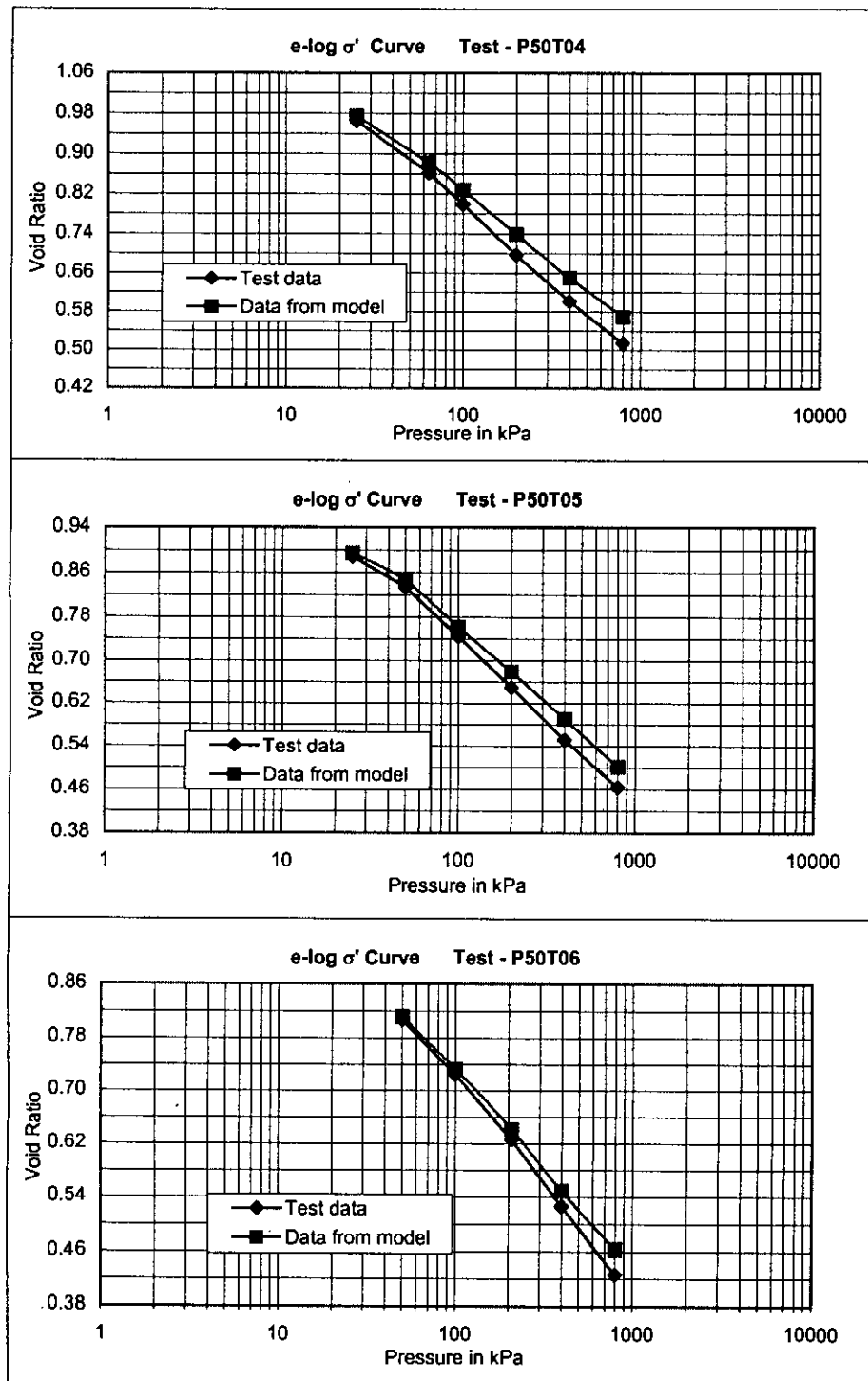Fig.A.23 Figure comparing e~log(σ') relations between test data and that
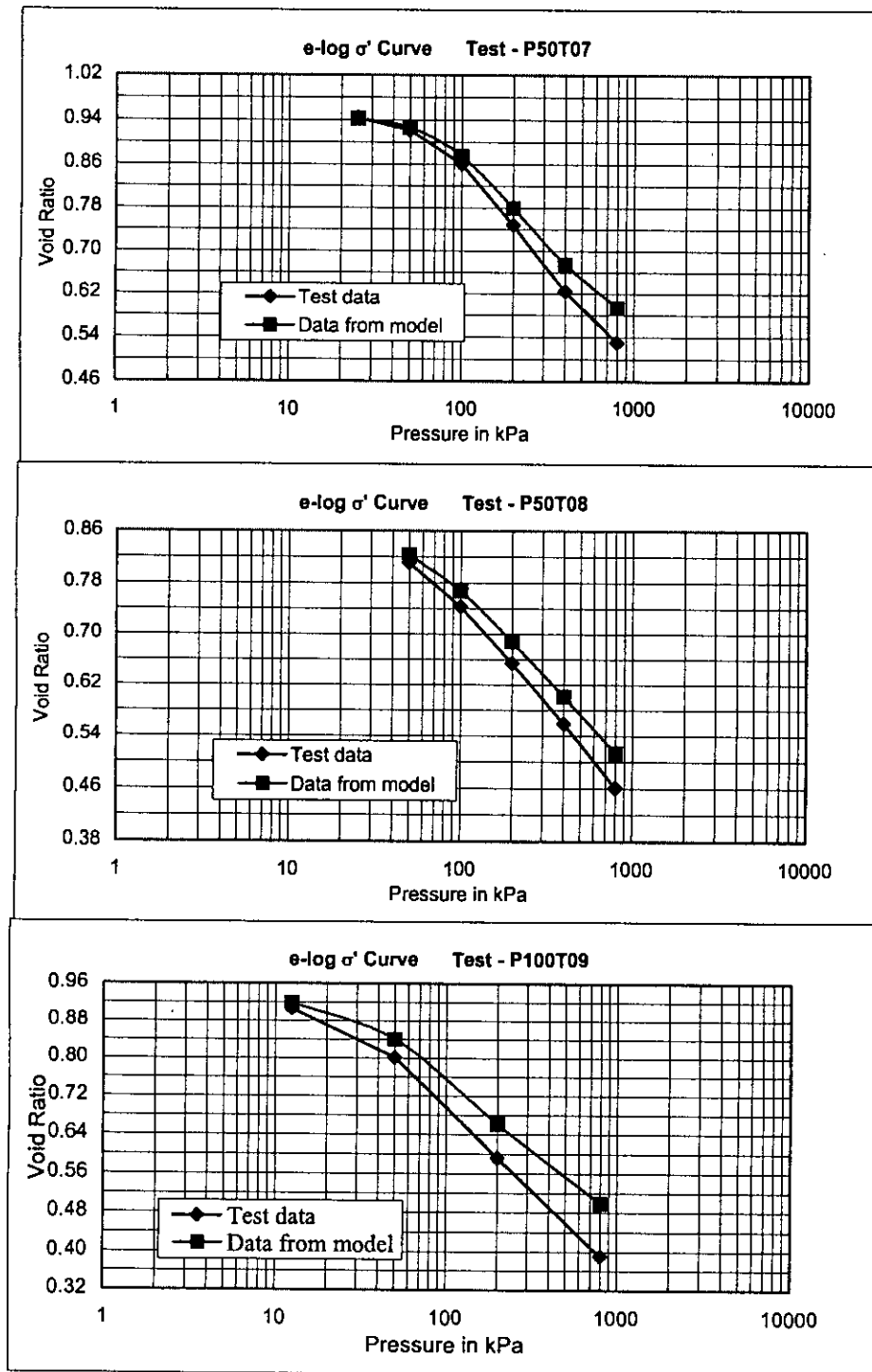obtained using the model for tests P50T04, P50T05, P50T06
(method b, article 5.5)

Fig.A.24 Figure comparing e~log(σ') relations between test data and that
obtained using the model for tests P50T07, P50T08, P50T09
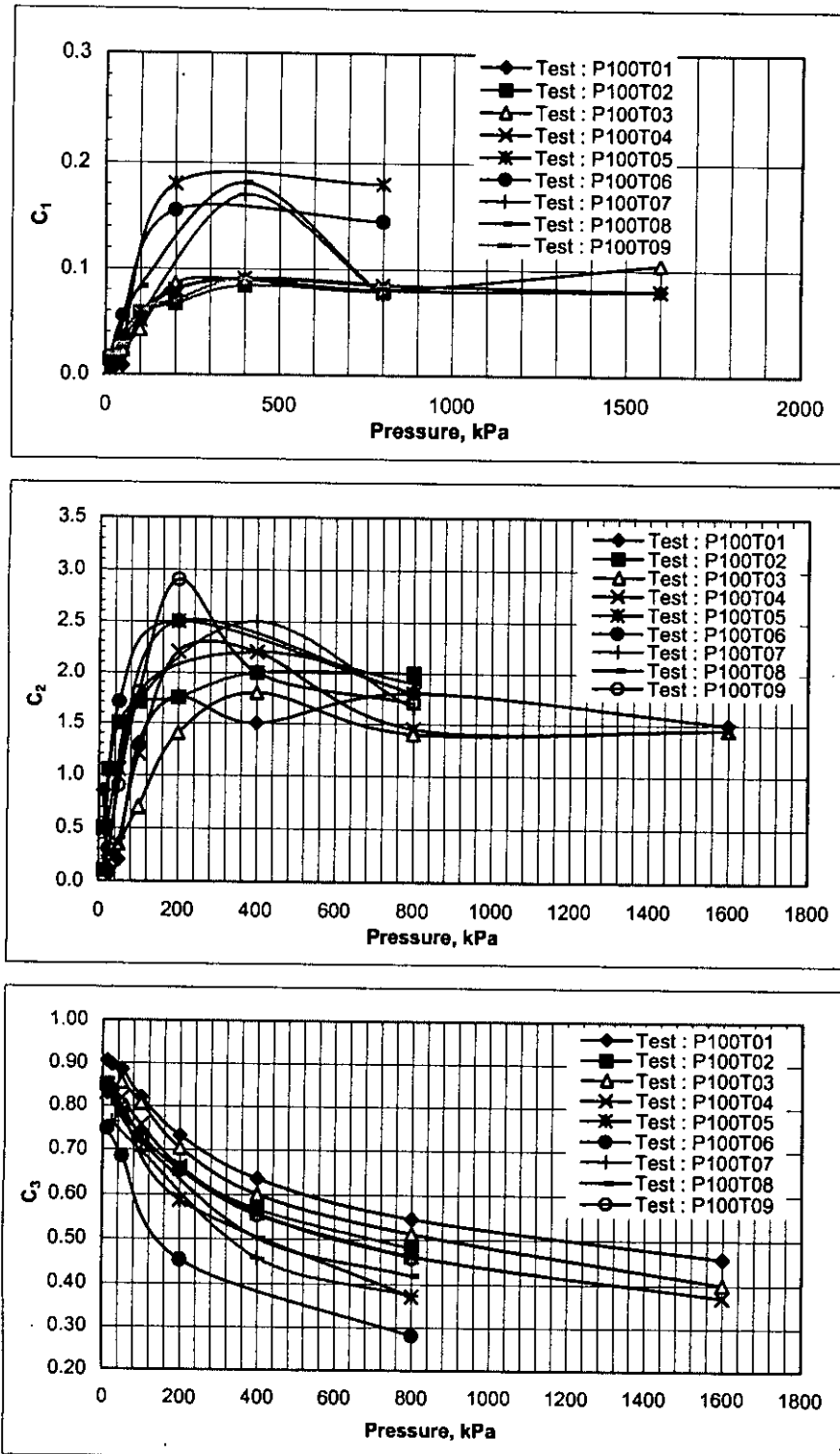(method b, article 5.5)

Appendix-B

Fig.B.1　Variation of parameter C_1, C_2 and C_3 with pressure (both in arithmatic scale) for specimens with $\sigma'_0 = 100$ kPa.
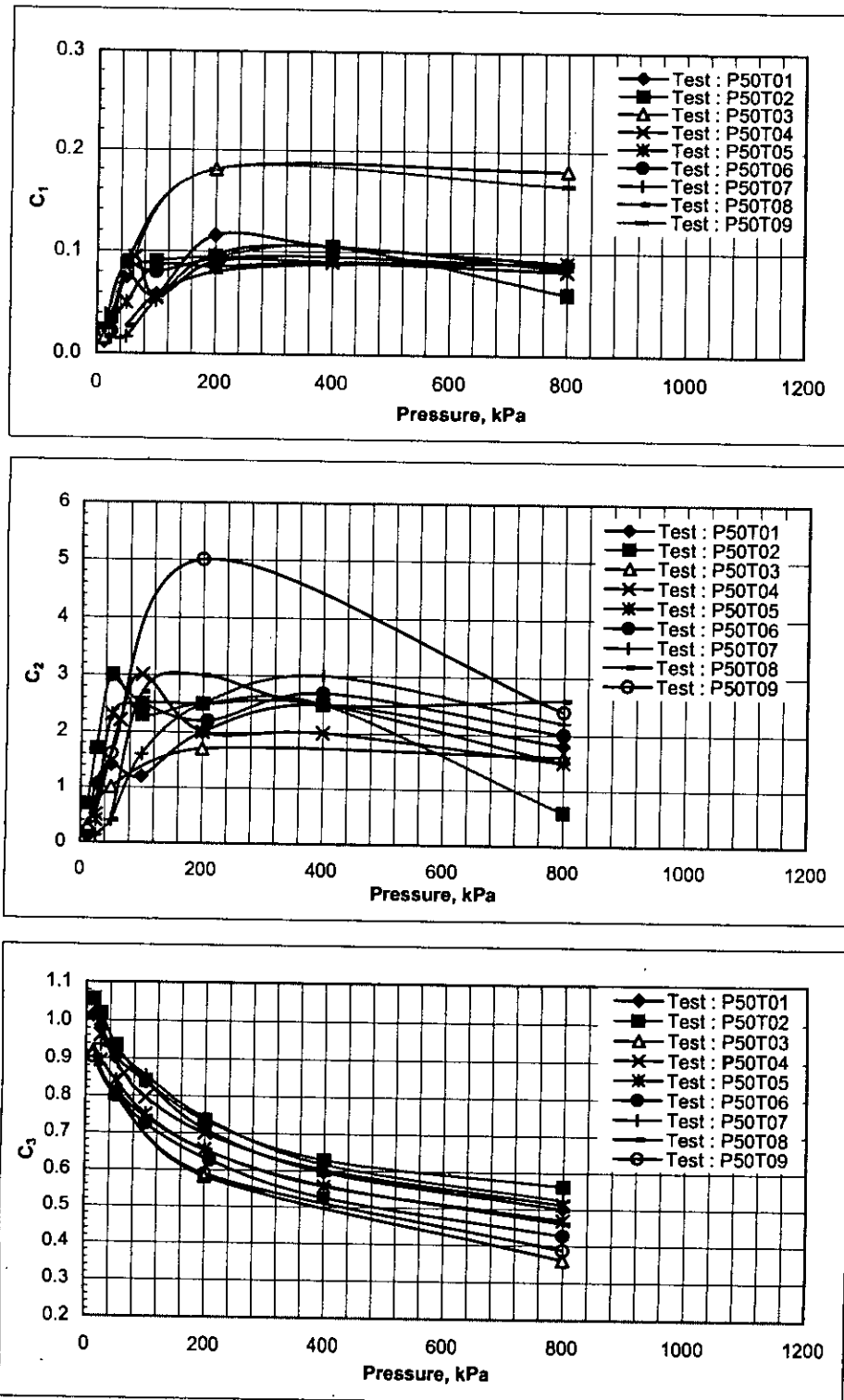
Fig.B.2   Variation of parameter C_1, C_2 and C_3 with pressure (both in arithmatic scale) for specimens with σ'_0=50 kPa.

Fig.B.3 Variation of parameter C_1, C_2 and C_3 with pressure (parameter in arithmetic scale, pressure in log scale) for specimens with $\sigma'_0=100$ kPa.

combined_data_p100
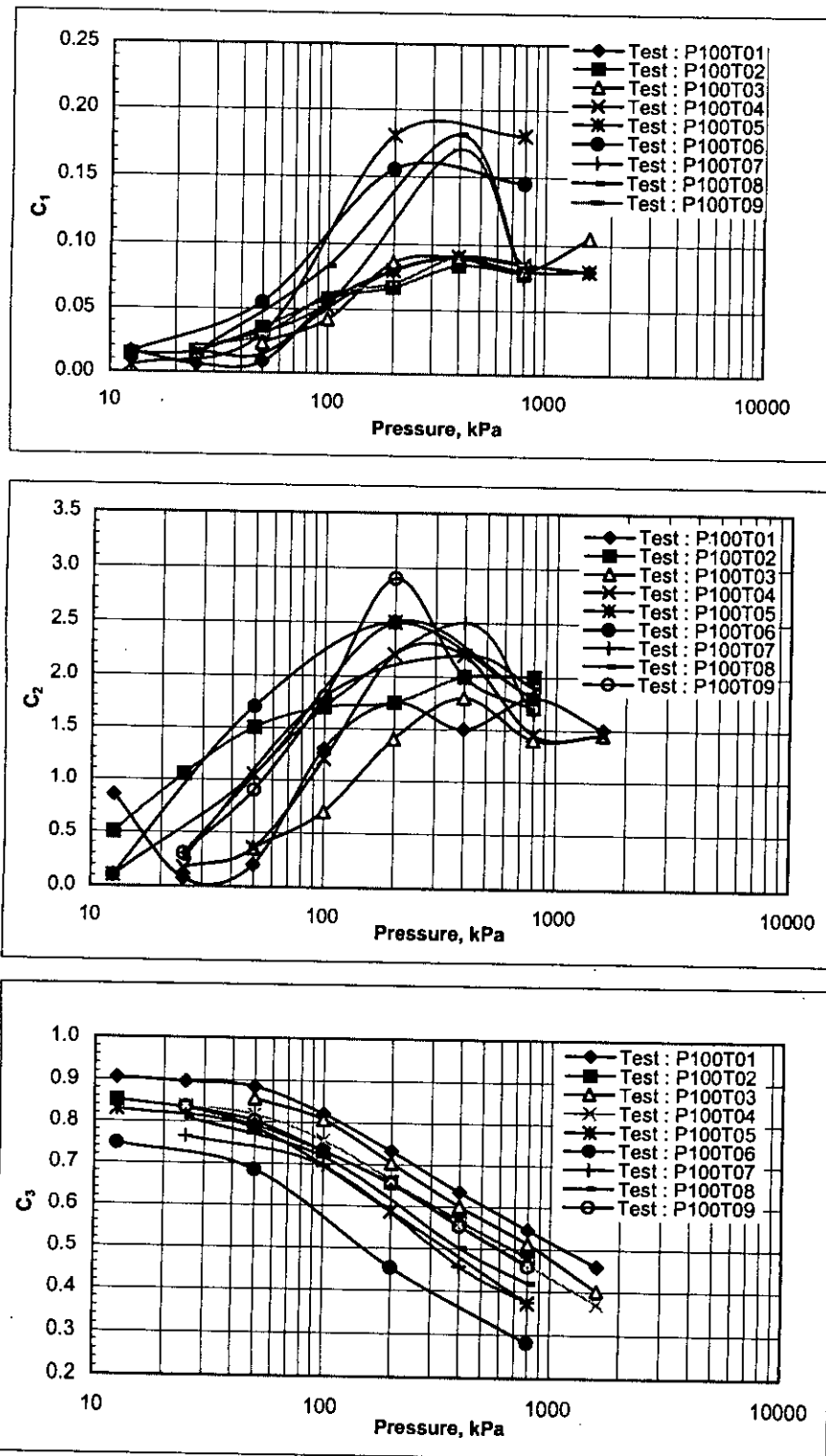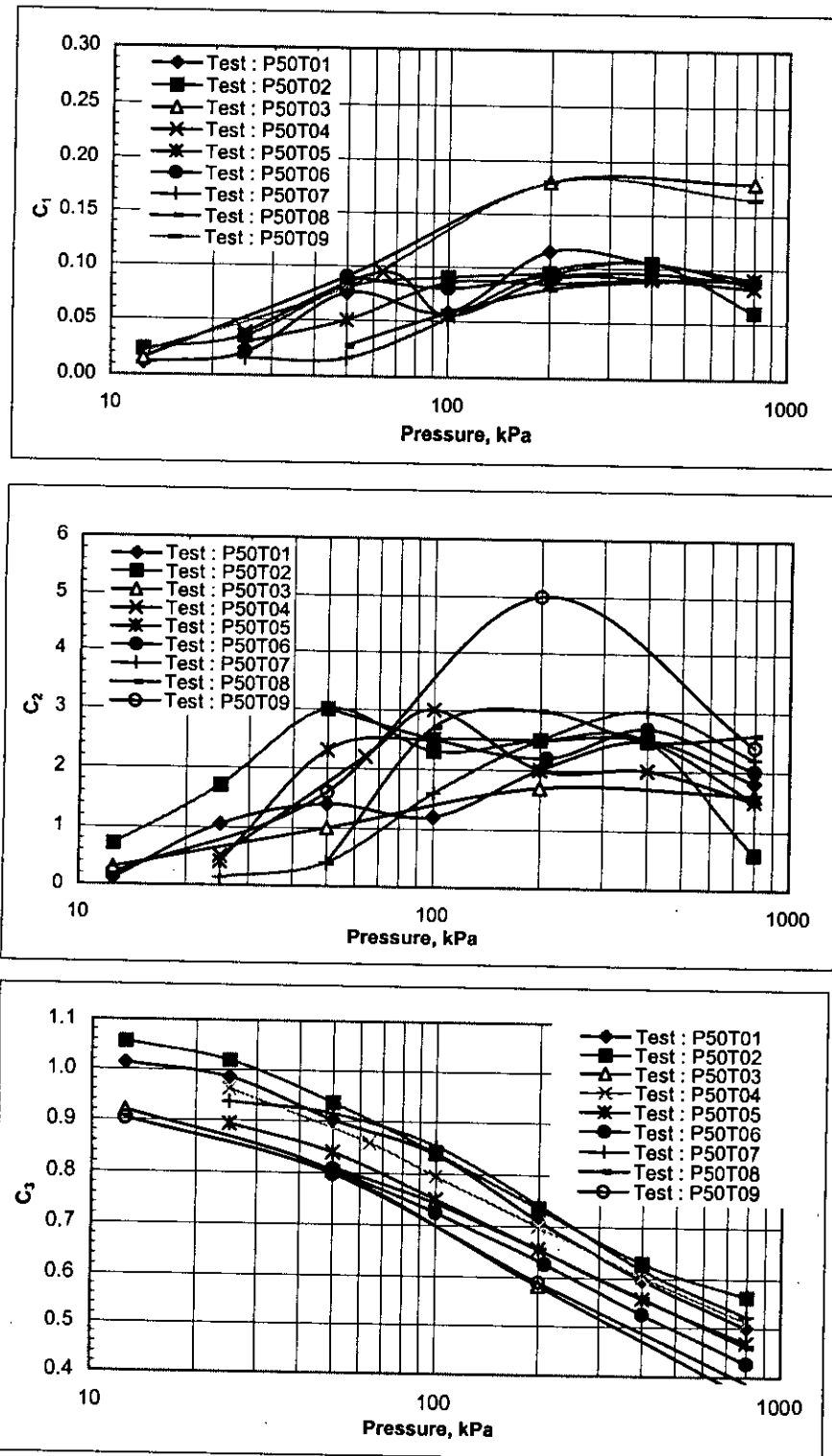
Fig.B.4   Variation of parameter C_1, C_2 and C_3 with pressure (parameter in arithmetic scale, pressure in log scale) for specimens with σ'_0=50 kPa.

102
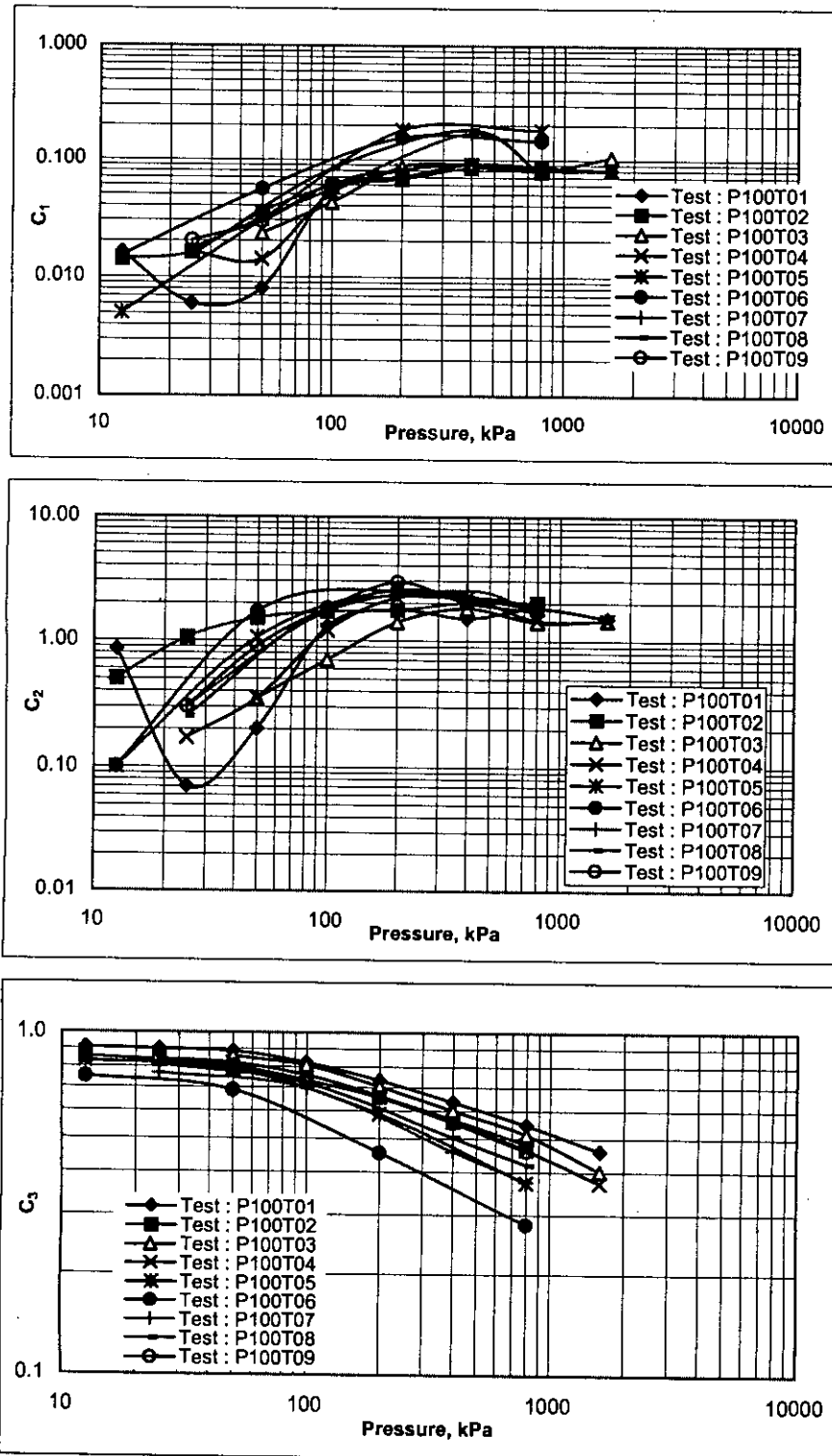
Fig.B.5   Variation of parameter C_1, C_2 and C_3 with pressure (both in log scale) for specimens with σ'_0=100 kPa.
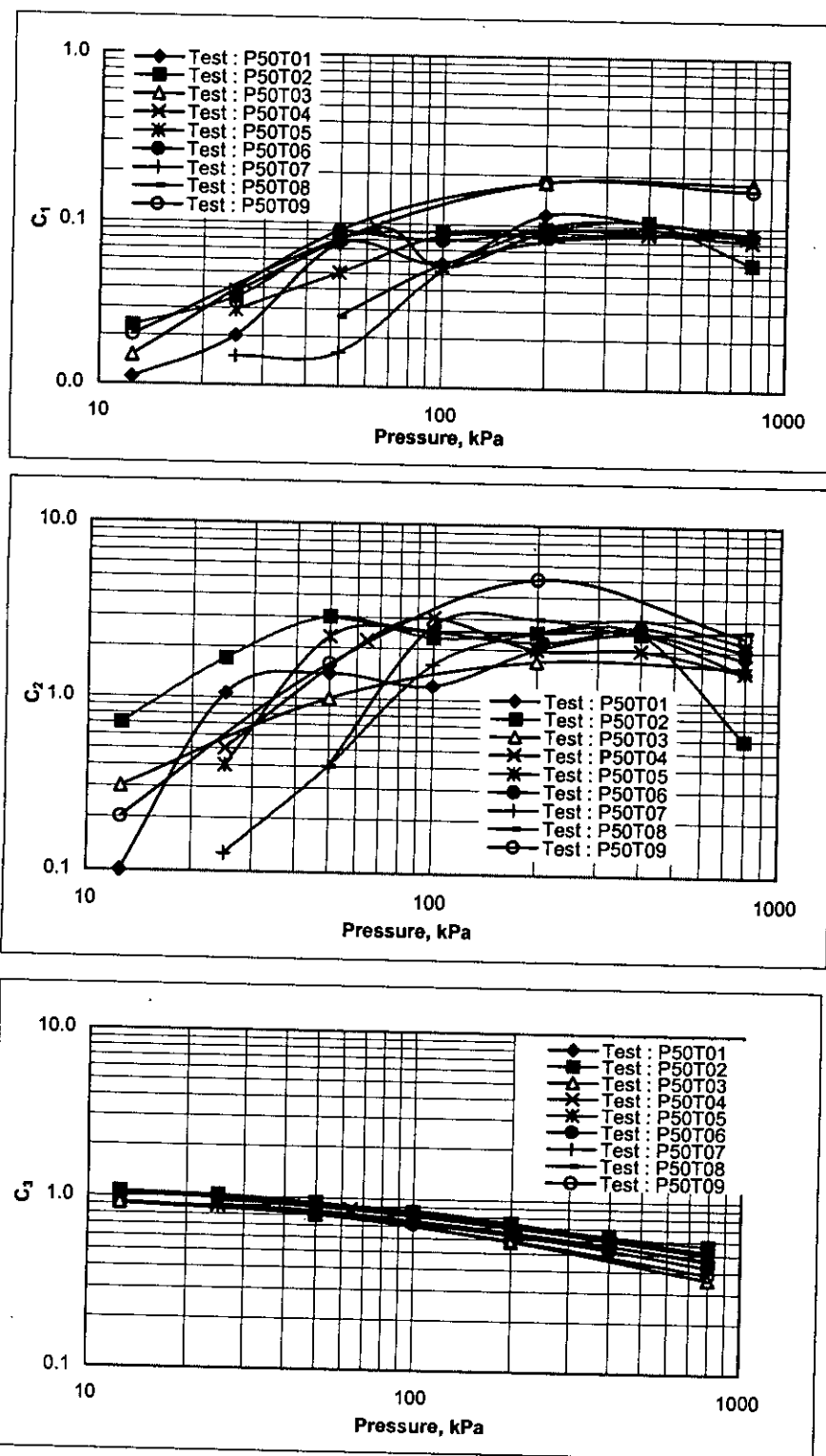
combined_data_p100

Fig.B.6 Variation of parameter C_1, C_2 and C_3 with pressure (both in log scale) for specimens with σ'_0=50 kPa.

104

REFERENCES

ASTM (1986) Annual Book of ASTM standards: Part 19, American Society for Testing Materials.

Azzouz,A.S., Krizek R.J. and Corotis, R.B.(1976) Regression analysis of soil compressibility, Soils and foundation, Vol.16, No.2,pp.19-29.

Balasubramaniam, A.S. and Brenner, R.P. (1981) Soft clay engineering, William Brand and R.P.Brenner editors, Chapter 7, pp.481-566, Elsevier Scientific Publishing Company.

Barnes, G.E. (1995) Soil Mechanics, principles and practice, Macmillan.

Bowels, J.E.(1984) Physical and Engineering properties of soils, 2nd edition, McGraw-Hill book company.

Casagrande, A. (1936) The determination of the preconsolidation load and its practical significance, Proceedings, 1st International Conference on Soil Mechanics and Foundaton Engineering, Harvard, pp.60-64.

Casagrande, A., and Fadum, R.E. (1940) Notes on soil testing for engineering purpose, Harvard University Graduate School of Engineering, Publication no.8.

Crawford, C. B. (1964) Interpretation of consolidation tests, Journal of Soil Mechanics and Foundation Division, ASCE, vol.90, SM5.

Das,B.M.(1983)Advanced Soil Mechanics, McGraw-Hill International Edns.

Farooqu (1995) Effctes of sampling disturbance on engineering behaviour of coastal soils from Chittagong, M.Sc. Thesis, CE Dept., BUET.

Head, K.H. (1982) Manual of soil laboratory testing, Vol.2 : Permeability, shear strength and compressibility tests, Pentech Press, London.

Hopper, R.J. (1992) The effects and implications of sampling clay soils, Ph.D. thesis, University of Surrey, England.

Jardine, R.J. (1985) Investigations of pile soil behaviour with special reference to foundations of offshore structures, Ph.D. thesis, Imperial College, University of London.

Lamb, T.W. and Whitman, R.V. (1979) Soil mechanics (SI version), Wiley, New York.

Leonards, G.A. (1962) Foundation Engineering, Mcgraw-Hill Book Co., New York.

Leonards, G.A. and Altschaeffl, A.G. (1964) Compressibility of clay, Journal of Soil Mechanics and Foundation Division, ASCE, vol.90, SM5, pp.133-156.

Nacci,V.A., Wang,M.C. and Demars, K.R. (1975) Engineering behaviour of calcareous soils, Proc. Civil Engg.Oceans III, ASCE, vol.1, pp.380-400.

Schmertmann, J.H.(1953) Estimating the true consolidation behaviour of clay from laboratory test results, Proceedings, ASCE, Vol.1979.

Schmertmann, J.H. (1955) The undisturbed consolidation behaviour of clay, Transactions, ASCE, No.120, Paper 2775, pp.1201-1227.

Siddique, A.(1990) A numerical and experimental study of sampling disturbance, Ph.D. theses, University of Surrey, England.

Singh, A. (1992) Modern geotechnical engineering, 3rd edn., CBS publishers.

Taylor, D.W. (1942) Research on consolidation of clays, Massachusetts Institute of Technology, publication no.82.

Terzaghi, K. (1925) Erdbaumechanik auj Boden-physicalischen Grundlagen, Deuticke, Vienna.

Terzaghi, K. (1943) Theoretical Soil Mechanics", Wiley, New York.

Terzaghi, K. and R.B.Peck (1967) Soil Mechanics in Engineering Practice, 2nd edn., Wiley, New York.

Wagener,A.A. (1957) The use of the Unified Soil Classification system by the Bureau of Reclamation, Proceedings, 4th international Conference, SMFE, London, Vol.1, pp.125-134.

Whitlow, R (1995) Basic Soil Mechanics, 3rd edition, Longman.